

NPS ARCHIVE
1959
PALMIERI, J.

SHEAR DISTRIBUTION
AND IT'S RELATION TO
BULKHEAD STIFFENER SELECTION

JOHN JOSEPH PALMIERI
AND
VINCENT JAMES ARGIRO

LIBRARY
U.S. NAVAL POSTGRADUATE SCHOOL
MONTEREY, CALIFORNIA

SHEAR DISTRIBUTION AND ITS RELATION TO
BULKHEAD STIFFENER SELECTION

by

JOHN JOSEPH PALMIERI

and

VINCENT JAMES ARGIRO

SUBMITTED IN PARTIAL FULFILLMENT OF THE
REQUIREMENTS FOR THE DEGREE OF NAVAL ENGINEER

and

FOR THE DEGREE OF MASTER OF SCIENCE IN
NAVAL ARCHITECTURE AND MARINE ENGINEERING

at the

MASSACHUSETTS INSTITUTE OF TECHNOLOGY

MAY, 1959

SHEAR DISTRIBUTION AND ITS RELATION TO
BULKHEAD STIFFENER SELECTION

by

JOHN JOSEPH PALMIERI

and

VINCENT JAMES ARGIRO

Submitted to the Department of Naval Architecture and Marine Engineering on May 25, 1959 in partial fulfillment of the requirements for the Master of Science Degree in Naval Architecture and Marine Engineering and the Professional Degree, Naval Engineer.

ABSTRACT

This thesis is a continuation of a series (ref. 2, 3, 4, 5 and 6) having, as a general objective, the collection and analysis of data which may be used to improve the design of ship transverse bulkheads. The previous investigations involved photoelastic studies of the vertical shear stress distributions along the clamped sides of edge-loaded plates of aspect ratios 1:1, 2:1, 3:1 and 5:1 for various conditions of vertical stiffening and bottom support. This thesis summarizes the experimental data in a consistent, non-dimensional form. The data are corrected where possible, and are then analyzed to determine the effects of aspect ratio, stiffening and bottom support. Various theoretical approaches to the problem are discussed.

Non-dimensional plots of the variation in vertical shear stress along the clamped sides of the plates are presented. In addition, curves illustrating the effect of aspect ratio, stiffening and bottom support are included.

For all types of loading aspect ratio has a greater effect than degree of stiffening. Only in the case of concentrated load with bottom support is the curve of vertical shear stress significantly different from a parabola. In the uniform load cases the vertical stiffeners act as columns to transmit load into the bottom

support. The load into the bottom is apparently a function of plate and panel aspect ratios.

It is recommended that further experimental work be conducted with uniform load cases. The possibility of arriving at an analytical solution warrants further investigation.

Thesis Supervisor: J. Harvey Evans

Title: Associate Professor of
Naval Architecture

ACKNOWLEDGEMENT

The authors wish to express their appreciation to Professor J. Harvey Evans of the Department of Naval Architecture and Marine Engineering who acted as thesis supervisor and directed us in the field of ship bulkhead research.

TABLE OF CONTENTS

	Page
Title Page	i
Abstract	ii
Acknowledgement	iv
Table of Contents	v
List of Figures	vi
List of Tables	x
Notation	xii
I Introduction	1
II Procedure	5
III Results	10
IV Discussion of Results	42
V Conclusions	53
VI Recommendations	56
VII Appendices	
A - Supplementary Introduction	59
B - Details of Procedure	67
C - Summary of Data and Calculations	89
D - Sample Calculations	116
E - Literature Citations	118

LIST OF FIGURES

- Figure I Plot of τ_{xy}/τ_m for AR 2:1, concentrated load, with two degrees of stiffening, supported and unsupported.
- Figure II Plot of τ_{xy}/τ_m for AR 3:1, concentrated load, with two degrees of stiffening, supported.
- Figure III Plot of τ_{xy}/τ_m for AR 5:1, concentrated load, with two degrees of stiffening, supported and unsupported.
- Figure IV Plot of τ_{xy}/τ_m for unstiffened case with concentrated load, unsupported.
- Figure V Plot of τ_{xy}/τ_m for unstiffened case with concentrated load, theoretical results.
- Figure VI Plot of τ_{xy}/τ_m for unstiffened case with concentrated load, supported.
- Figure VII Plot of τ_{xy}/τ_m for one stiffener case with concentrated load, supported and unsupported.
- Figure VIII Plot of % load transmitted into bottom support vs. aspect ratio for concentrated load cases.
- Figure IX Plot of % load transmitted into bottom support/Aspect ratio vs. panel width/panel depth, for concentrated load cases.
- Figure X Plot of τ_{xy}/τ_m for AR 1:1, uniform load, with four degrees of stiffening, unsupported.
- Figure XI Plot of τ_{xy}/τ_m for AR 1:1, uniform load, with four degrees of stiffening, supported.
- Figure XII Plot of τ_{xy}/τ_m for AR 2:1, uniform load, with four degrees of stiffening, unsupported.

- Figure XIII Plot of τ_{xy}/τ_m for AR 2:1, uniform load, with four degrees of stiffening, supported
- Figure XIV Plot of τ_{xy}/τ_m for AR 3:1, uniform load, with four degrees of stiffening, unsupported
- Figure XV Plot of τ_{xy}/τ_m for AR 3:1, uniform load, with four degrees of stiffening, supported
- Figure XVI Plot of τ_{xy}/τ_m for AR 5:1, uniform load, with four degrees of stiffening, unsupported
- Figure XVII Plot of τ_{xy}/τ_m for AR 5:1, uniform load, with four degrees of stiffening, supported
- Figure XVIII Plot of τ_{xy}/τ_m for unstiffened case with uniform load, unsupported
- Figure XIX Plot of τ_{xy}/τ_m for unstiffened case with uniform load, supported
- Figure XX Plot of τ_{xy}/τ_m for one stiffener case with uniform load, unsupported
- Figure XXI Plot of τ_{xy}/τ_m for one stiffener case with uniform load, supported
- Figure XXII Plot of τ_{xy}/τ_m for two stiffener case with uniform load, unsupported
- Figure XXIII Plot of τ_{xy}/τ_m for two stiffener case with uniform load, supported
- Figure XXIV Plot of τ_{xy}/τ_m for three stiffener case with uniform load, unsupported
- Figure XXV Plot of τ_{xy}/τ_m for three stiffener case with uniform load, supported
- Figure XXVI Plot of location and magnitude of $\left[\tau_{xy}/\tau_m\right]_{\max}$ by method of least squares for uniform load,

supported and unsupported

- Figure XXVII Plot of % reduction in $[\tau_{xy}/\tau_m]$ max due to bottom support/Aspect ratio vs panel width/panel depth
- Figure XXVIII Plot of % load transmitted into bottom support vs panel width/panel depth for uniform load
- Figure XXIX Plot of % load transmitted into bottom support/Aspect ratio vs panel width/panel depth for uniform load.
- Figure XXX Plot of magnitude of $[\tau_{xy}/\tau_m]$ max for the uniform load, unsupported, uncorrected condition.
- Figure XXXI Plot of magnitude of $[\tau_{xy}/\tau_m]$ max for the uniform load, unsupported, corrected condition.
- Figure XXXII Plot of location of $[\tau_{xy}/\tau_m]$ max for the uniform load, unsupported condition
- Figure XXXIII Plot of magnitude of $[\tau_{xy}/\tau_m]$ max for the uniform load, supported condition
- Figure XXXIV Plot of location of $[\tau_{xy}/\tau_m]$ max for the uniform load, supported condition
- Figure XXXV Plot of faired correction to τ_{xy}/τ_m for AR 3:1, uniform load, unstiffened and unsupported
- Figure XXXVI Plot of load correction to τ_{xy}/τ_m for AR 3:1, uniform load, two stiffeners, and unsupported
- Figure XXXVII Plot of correction to τ_{xy}/τ_m for AR 2:1, uniform load, unstiffened and unsupported
- Figure XXXVIII Stresses in a semi-infinite plate
- Figure XXXIX Side supported rectangular beam
- Figure XL Superposition of radial and elementary bending stress systems in a side supported beam

Figure XLI Approximate superposition of radial and elementary bending stress systems in a side supported beam.

LIST OF TABLES

Table I	Characteristics of Experimental Models	
	<u>Concentrated Load Condition</u>	
Table II	Aspect Ratio 1:1	Theoretical Calculation
Table III	Aspect Ratio 2:1	Theoretical Calculation
Table IV	Aspect Ratio 2:1 Bottom Unsupported	Unstiffened
Table V	Aspect Ratio 2:1 Bottom Supported	Unstiffened
Table VI	Aspect Ratio 2:1 Bottom Supported	Centerline Stiffener
Table VII	Aspect Ratio 3:1	Theoretical Calculation
Table VIII	Aspect Ratio 3:1 Bottom Supported	Unstiffened
Table IX	Aspect Ratio 3:1 Bottom Supported	Centerline Stiffener
Table X	Aspect Ratio 5:1	Theoretical Calculation
Table XI	Aspect Ratio 5:1 Unstiffened	Bottom Unsupported Centerline Stiffener
Table XII	Aspect Ratio 5:1 Unstiffened	Bottom Supported Centerline Stiffener
	<u>Uniform Load Condition</u>	
Table XIII	Aspect Ratio 1:1 Bottom Supported and	Unstiffened Unsupported
Table XIV	Aspect Ratio 1:1 Bottom Supported and	Centerline Stiffener Unsupported
Table XV	Aspect Ratio 1:1 Bottom Supported and	Two Stiffeners Unsupported
Table XVI	Aspect Ratio 1:1 Bottom Supported and	Three Stiffeners Unsupported
Table XVII	Aspect Ratio 2:1 Bottom Supported and	Unstiffened Unsupported
Table XVIII	Aspect Ratio 2:1 Bottom Supported and	Centerline Stiffener Unsupported

Table XIX	Aspect Ratio 2:1 Bottom Supported and	Two Stiffeners Unsupported
Table XX	Aspect Ratio 2:1 Bottom Supported and	Three Stiffeners Unsupported
Table XXI	Aspect Ratio 3:1 Bottom Supported and	Unstiffened Unsupported
Table XXII	Aspect Ratio 3:1 Bottom Supported and	Centerline Stiffener Unsupported
Table XXIII	Aspect Ratio 3:1 Bottom Supported and	Two Stiffeners Unsupported
Table XXIV	Aspect Ratio 3:1 Bottom Supported and	Three Stiffeners Unsupported
Table XXV	Aspect Ratio 5:1 Bottom Supported and	Unstiffened Unsupported
Table XXVI	Aspect Ratio 5:1 Bottom Supported and	Centerline Stiffener Unsupported
Table XXVII	Aspect Ratio 5:1 Bottom Supported and	Two Stiffeners Unsupported
Table XXVIII	Aspect Ratio 5:1 Bottom Supported and	Three Stiffeners Unsupported
Table XXIX	Summary of Data for Calculation of Theoretical Shear Stress Distribution - Aspect Ratio 2:1	

NOTATION

a	Distance between stiffeners and/or supports measured in the x-direction, also called panel width
b	Depth of beam in the y-direction
F	Fringe constant of the material (pounds per inch per order)
h	Thickness of beam
L	Span of beam between supports
l	One-half span of beam
n	Order of interference
P	Concentrated load (pounds)
w	Uniform load (pounds per inch)
y	Vertical distance from top edge of beam to any point on the beam
AR	Plate aspect ratio (L/b)
a/b	Panel aspect ratio
τ_m	Average vertical shear stress over a boundary assuming side support only (pounds per square inch)
τ_{xy}	Shear stress in the plane perpendicular to the x-axis and in the y-direction, also called vertical shear stress (pounds per square inch)
θ	Direction of the principal stresses from the x- and y-axes clockwise (degrees)
#	Pounds

Subscripts

c	Corrected value
f	Faired value
β	Value due to bending stress
ρ	Value due to radial compressive stress

I. INTRODUCTION

The transverse bulkheads of a ship's structure are in reality short, deep beams*. The Bernoulli-Euler elementary beam theory does not generally apply to short, deep beams due to the simplifying assumptions made in its development. This elementary theory represents an essentially true solution for sections far from loads and supports, but such sections do not exist in short span beams. Expressions for stress distribution developed from elasticity theory require the solution of certain partial differential equations with given boundary conditions. Only in the case of simple boundaries can these equations be treated in a rigorous manner.

The boundary conditions which exist in the transverse bulkhead of a ship are subject to question. It may be stated that in the actual case, the rigidity of side connections lies somewhere between the condition of fully supported in shear but unrestrained against rotation, and the fully clamped condition, while the degree of bottom support is somewhere between the unsupported and fully supported conditions. From an analysis of the ship structure it is logical to assume greater rigidity in the side connections than in the bottom.

In the absence of an analytical solution, and in order to gain some insight into this problem, a number of investigators have conducted studies using photoelastic methods to determine the stress distribution along the sides of a transverse bulkhead (ref. 2, 3, 4, 5, 6). These investigations have included a number of aspect ratios (1:1, 2:1, 3:1, 5:1), various degrees of

* P.H. Kaar has defined a deep beam as "any beam in which the height-to-span ratio is great enough to cause non-linearity in the elastic flexural stresses over the beam depth" (ref. 1).

stiffening, and the conditions of bottom supported and unsupported for both the concentrated load and uniform load cases. In all cases the sides of the models were clamped approximating the true conditions, based on the assumption of greater rigidity in the side connections previously mentioned. The technique of photo-elastic analysis is widely accepted. This, coupled with the knowledge that extrapolation from model to full scale structure is possible without serious error (ref. 7), provides the engineer with a valuable tool to gain information which may be used to develop design procedures.

Design criteria for the transverse bulkheads of a ship have been evolved and used successfully for many years. The usual procedure is to design the bulkhead to withstand both the hydrostatic load that would be imposed if the adjacent compartment were flooded to the waterline and the load imposed in transmitting the deck loadings along its upper boundary into the framework of the ship. At present, the Bureau of Ships, in the design of transverse bulkheads for naval vessels, employs somewhat arbitrary criteria for the transmission of the latter type of loads into the ship framework. The Bureau of Ships specifies that "the vertical load which is considered to be distributed to the boundaries by shear, should be based upon a shear stress in the plating for one deck height (or where no deck is connected below the point of application of the load, then seven feet) of about one-half of the critical shear stress for the thickness of plating and the size of the panel in question". This assumption has never been substantiated. The shear stress along the side boundaries governs the size of the plating that will sustain the load. To achieve the

optimum design, which is the minimum weight structure consistent with the load to be supported, it is axiomatic that only that thickness of plating absolutely required be used. In order to determine this thickness it is essential that the shear stress distribution along the edge be known. The immediate purpose of the studies conducted by previous investigators in this field (ref. 2, 3, 4, 5, 6) has been the determination of this shear stress distribution. The long term objective of this series of theses is the verification of the bulkhead design criteria presently used, and where findings deem it necessary, the refinement or complete revision of these procedures.

In brief, the steps necessary to achieve this long term goal are:

1. The correlation of all previous experimental results and the presentation of these results on a common basis more suitable for comparative purposes.
2. Presentation of available analytical solutions.
3. Analysis of results to determine;
 - a. The effect of aspect ratio on shear distribution.
 - b. The effect of stiffeners on shear distribution.
 - c. The effect of bottom support on shear distribution.
 - d. The validity of the 10 percent reduction of load per deck assumption which is used by the Bureau of Ships in bulkhead design.
 - e. The validity of the assumption used by the Bureau of Ships that only the top seven feet

of a bulkhead are useful in the transmission of shear stress to the hull.

This paper contributes to this goal by making a complete analysis of the experimental results previously obtained and by presenting various analytical approaches pertinent to the problem which were found by a thorough survey of the literature.

II. PROCEDURE

References (2, 3, 4, 5, 6) are a series of photoelastic investigations to determine the vertical shear stress distributions over the clamped side edges of plates under various conditions of bottom support, edge loading and stiffening. The characteristics of the models examined are presented in Table I. From the experimentally determined values of vertical shear stress (τ_{xy}) over the clamped edges dimensionless curves have been plotted of this vertical shear stress versus percent of plate depth. The dimensionless value of shear stress plotted is (τ_{xy}/τ_m) where;

τ_{xy} = experimentally determined value of vertical shear stress

τ_m = average shear stress over the clamped edges assuming side support only

For the concentrated load cases;

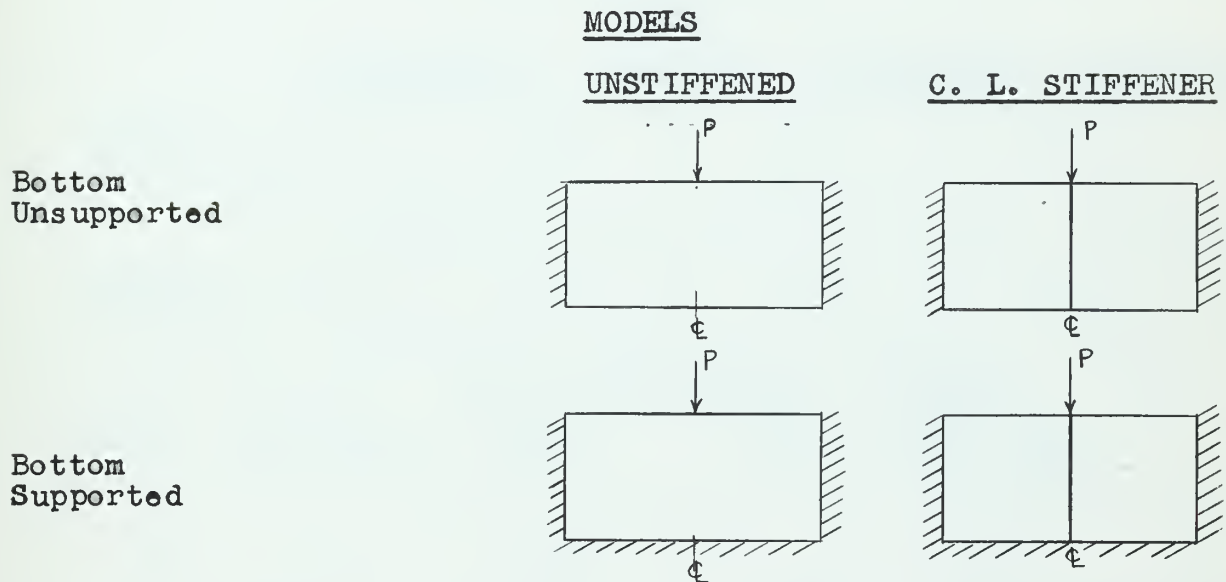
$$\tau_m = \frac{P}{2bh} \quad (1)$$

For the uniform load cases;

$$\tau_m = \frac{w}{2h} \cdot \frac{L}{b} = \frac{w}{2h} \cdot AR \quad (2)$$

In the cases of side support only an original experimental error was determined by integrating the areas under the (τ_{xy}/τ_m) curves with a planimeter and comparing them with the area under the curve ($\tau_{xy}/\tau_m = 1.0$). The probable causes of the errors are discussed in Appendix B. The original errors are presented in Table I. Because of small differences in plotting, many curves differ slightly from the values presented in the experimental theses. The errors given in Table I were obtained from plots twice the size of those presented in the Results.

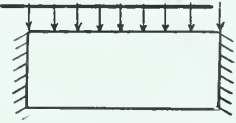
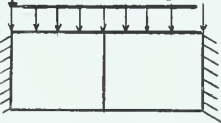
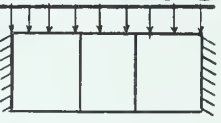

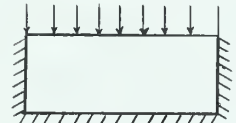
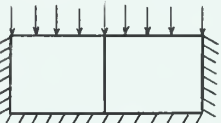
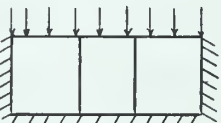
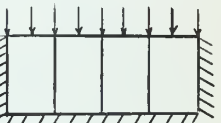
TABLE I
CHARACTERISTICS OF EXPERIMENTAL MODELS
A. CONCENTRATED LOAD



<u>Aspect Ratio</u>	<u>Bottom Condition</u>	<u>No. of Stiffeners</u>	<u>Experimental Error</u>	<u>Load Trans. Into Bottom</u>	<u>Reference</u>
2:1	Unsupported	0	-18.7%		(5)
5:1	Unsupported	0	-26.6%		(4)
5:1	Unsupported	1	+13.9%		(4)
2:1	Supported	0		58.1%	(5)
2:1	Supported	1		50.2%	(5)
3:1	Supported	0		80.2%	(4)
3:1	Supported	1		50.3%	(4)
5:1	Supported	0		70.7%	(4)
5:1	Supported	1		73.0%	(4)

TABLE I
CHARACTERISTICS OF EXPERIMENTAL MODELS

B. UNIFORM LOAD

		<u>MODELS</u>			
		<u>Unstiffened</u>	<u>1 Stiffener</u>	<u>2 Stiffeners</u>	<u>3 Stiffeners</u>
Bottom Unsupported					
					
		<u>BOTTOM UNSUPPORTED</u>		<u>BOTTOM SUPPORTED</u>	<u>Reference</u>
<u>Aspect Ratio</u>	<u>No. of Stiffeners</u>	<u>Experimental Error</u>	<u>Corrected Error</u>	<u>Lead Trans. Into Bottom</u>	
1:1	0	3.4%		9.1%	(2)
1:1	1	- 9.0%	1.0%	10.2%	(2)
1:1	2	1.3%		10.1%	(2)
1:1	3	-10.0%	- 3.0%	12.1%	(2)
2:1	0	-18.1%	- 2.0%	12.7%	(3)
2:1	1	2.0%		21.4%	(3)
2:1	2	3.1%		30.6%	(2)
2:1	3	-15.2%	0%	23.3%	(2)
3:1	0	19.5%	3.0%	17.9%	(3)
3:1	1	- 1.9%		25.3%	(3)
3:1	2	-25.8%	1.0%	34.0%	(2)
3:1	3	14.8%	-2.0%	28.3%	(3)
5:1	0	1.0%		22.4%	(3)
5:1	1	33.7%	-1.0%	23.9%	(3)
5:1	2	- 1.0%		48.8%	(2)
5:1	3	-10.1%	0%	22.1%	(2)

For the cases of side and bottom support it was not possible to determine an experimental error because the investigators did not measure the amount of load transmitted into the bottom support. They assumed that it was the difference between the load applied and the integrated value of side shear. Actually this difference also includes the experimental errors which because of their inconsistency are generally inseparable from the total. Table I presents the difference as a percent of the applied load under the heading of "load transmitted into the bottom". The quotations are used as a reminder that this percent includes an indeterminate error.

There were a sufficient number of consistent results for the bottom unsupported uniform load cases so that a method could be developed for making corrections to the experimental data. The details and justifications of these corrections are presented in Appendix B. Briefly, unless the shear distribution curves were irregular in shape the experimental error was assumed to be in the magnitude of the load applied. For all such cases in which the experimental error was $\geq \pm 5\%$ the magnitude of the load was corrected by applying the error to τ_m .

No corrections were made to the bottom unsupported concentrated load data. The data are generally insufficient and suffer from experimental problems that were less troublesome in the later experiments with uniform loading. The experimental errors determined herein were two to three times the values presented in the original theses.

An approximate theoretical solution of the vertical shear stress distribution over the clamped edge of a bottom unsupported,

unstiffened beam subjected to a concentrated load in the plane of the beam was developed. It is essentially the superposition of the stress system produced by a concentrated load acting on the edge of a semi-infinite plate over the elementary bending stress system of Bernoulli-Euler. This procedure only approximates the true boundary conditions. Its edge supports are not rigidly clamped against rotation and a radial tensile force system necessary to eliminate stresses over the bottom free boundary are replaced by a statically equivalent concentrated load. The same theoretical solution was used to determine what portion of the load will be transmitted into the bottom of a bottom supported beam. The solution is derived in Appendix B.

III. RESULTS

The results of this thesis are shown in the following figures:

- Figure I Plot of τ_{xy}/τ_m for AR 2:1, concentrated load, with two degrees of stiffening, supported and unsupported.
- Figure II Plot of τ_{xy}/τ_m for AR 3:1, concentrated load, with two degrees of stiffening, supported.
- Figure III Plot of τ_{xy}/τ_m for AR 5:1, concentrated load, with two degrees of stiffening, supported and unsupported.
- Figure IV Plot of τ_{xy}/τ_m for unstiffened case with concentrated load, unsupported.
- Figure V Plot of τ_{xy}/τ_m for unstiffened case with concentrated load, theoretical results.
- Figure VI Plot of τ_{xy}/τ_m for unstiffened case with concentrated load, supported.
- Figure VII Plot of τ_{xy}/τ_m for one stiffener case with concentrated load, supported and unsupported.
- Figure VIII Plot of % load transmitted into bottom support vs. aspect ratio for concentrated load cases.
- Figure IX Plot of % load transmitted into bottom support/Aspect ratio vs. panel width/panel depth, for concentrated load cases.
- Figure X Plot of τ_{xy}/τ_m for AR 1:1, uniform load, with four degrees of stiffening, unsupported.
- Figure XI Plot of τ_{xy}/τ_m for AR 1:1, uniform load, with four degrees of stiffening, supported.
- Figure XII Plot of τ_{xy}/τ_m for AR 2:1, uniform load, with four degrees of stiffening, unsupported.

- Figure XIII Plot of τ_{xy}/τ_m for AR 2:1, uniform load, with four degrees of stiffening, supported
- Figure XIV Plot of τ_{xy}/τ_m for AR 3:1, uniform load, with four degrees of stiffening, unsupported
- Figure XV Plot of τ_{xy}/τ_m for AR 3:1, uniform load, with four degrees of stiffening, supported
- Figure XVI Plot of τ_{xy}/τ_m for AR 5:1, uniform load, with four degrees of stiffening, unsupported
- Figure XVII Plot of τ_{xy}/τ_m for AR 5:1, uniform load, with four degrees of stiffening, supported
- Figure XVIII Plot of τ_{xy}/τ_m for unstiffened case with uniform load, unsupported
- Figure XIX Plot of τ_{xy}/τ_m for unstiffened case with uniform load, supported
- Figure XX Plot of τ_{xy}/τ_m for one stiffener case with uniform load, unsupported
- Figure XXI Plot of τ_{xy}/τ_m for one stiffener case with uniform load, supported
- Figure XXII Plot of τ_{xy}/τ_m for two stiffener case with uniform load, unsupported
- Figure XXIII Plot of τ_{xy}/τ_m for two stiffener case with uniform load, supported
- Figure XXIV Plot of τ_{xy}/τ_m for three stiffener case with uniform load, unsupported
- Figure XXV Plot of τ_{xy}/τ_m for three stiffener case with uniform load, supported
- Figure XXVI Plot of location and magnitude of $\left[\tau_{xy}/\tau_m\right]_{\max}$ by method of least squares for uniform load,

supported and unsupported

Figure XXVII Plot of % reduction in $\left[\tau_{xy}/\tau_m\right]_{\max}$ due to bottom support/Aspect ratio vs panel width/panel depth

Figure XXVIII Plot of % load transmitted into bottom support vs panel width/panel depth for uniform load

Figure XXIX Plot of % load transmitted into bottom support/Aspect ratio vs panel width/panel depth for uniform load.

AR 2:1 CONCENTRATED LOAD
TWO DEGREES OF STIFFENING,
SUPPORTED AND UNSUPPORTED

FIGURE 1

V.J.A
4/15/59

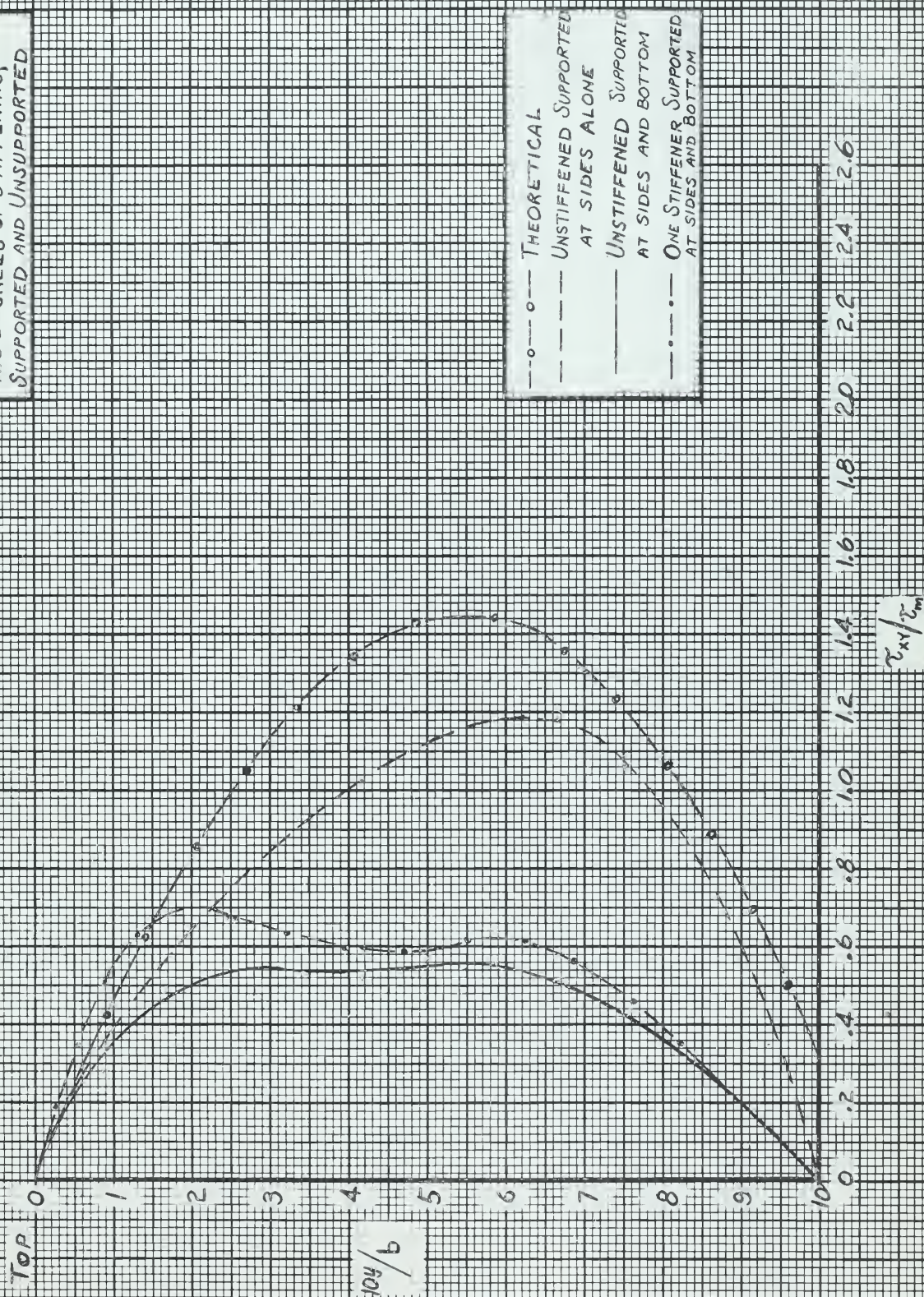
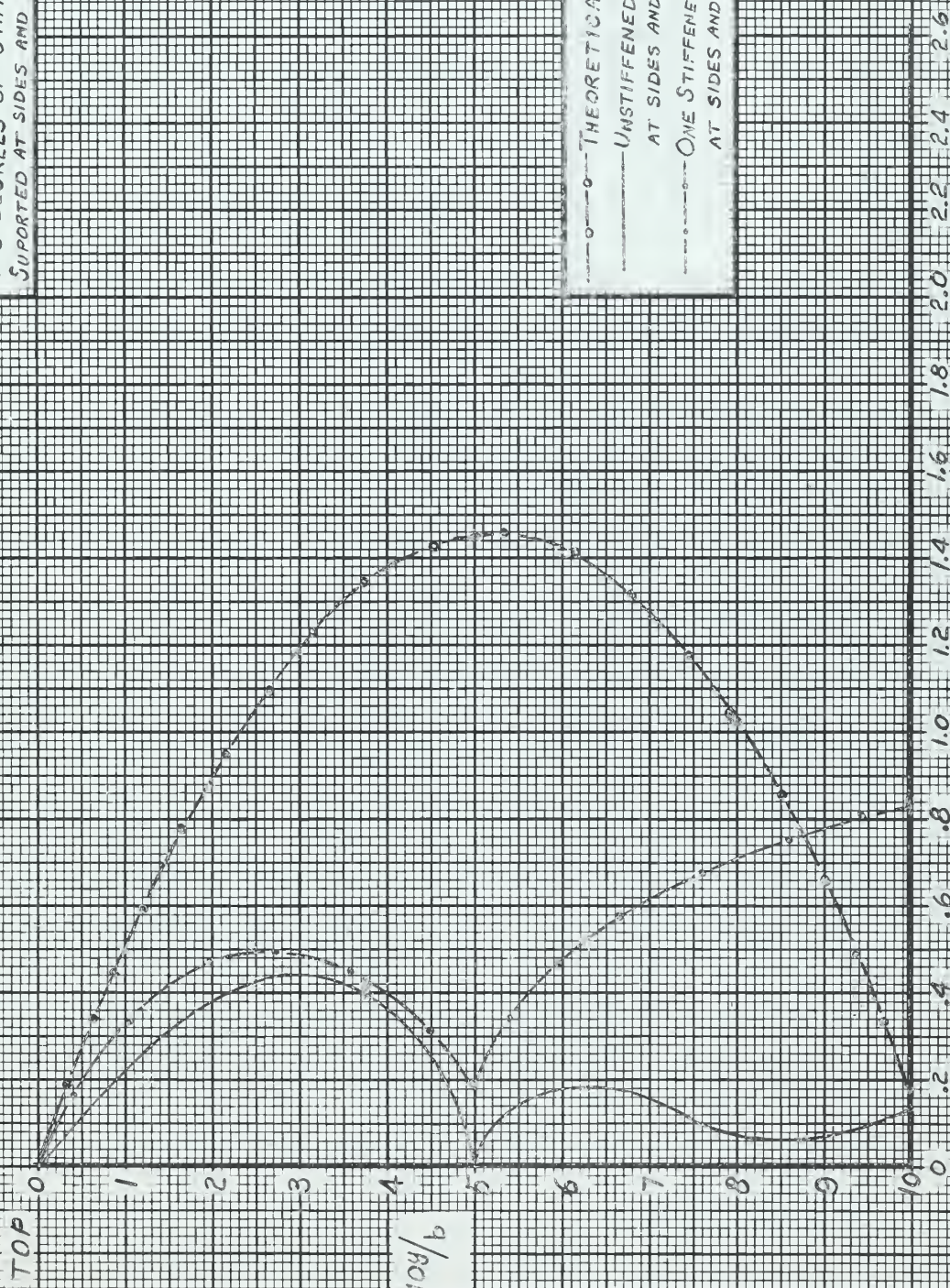


FIGURE II

V.J.A.
4/15/59

AR 3:1 CONCENTRATED LOAD
TWO DEGREES OF STIFFENING,
SUPPORTED AT SIDES AND BOTTOM

THEORETICAL
UNSTIFFENED, SUPPORTED
AT SIDES AND BOTTOM
ONE STIFFENER, SUPPORTED
AT SIDES AND BOTTOM



V.J. 4/15/59

FIGURE III

AR 5:1 CONCENTRATED LOAD
TWO DEGREES OF STIFFENING,
SUPPORTED AND UNSUPPORTED

- THEORETICAL
- UNSTIFFENED SUPPORTED AT SIDES ALONE
- UNSTIFFENED SUPPORTED AT SIDES AND BOTTOM
- ONE STIFFENER SUPPORTED AT SIDES ALONE
- ONE STIFFENER SUPPORTED AT SIDES AND BOTTOM

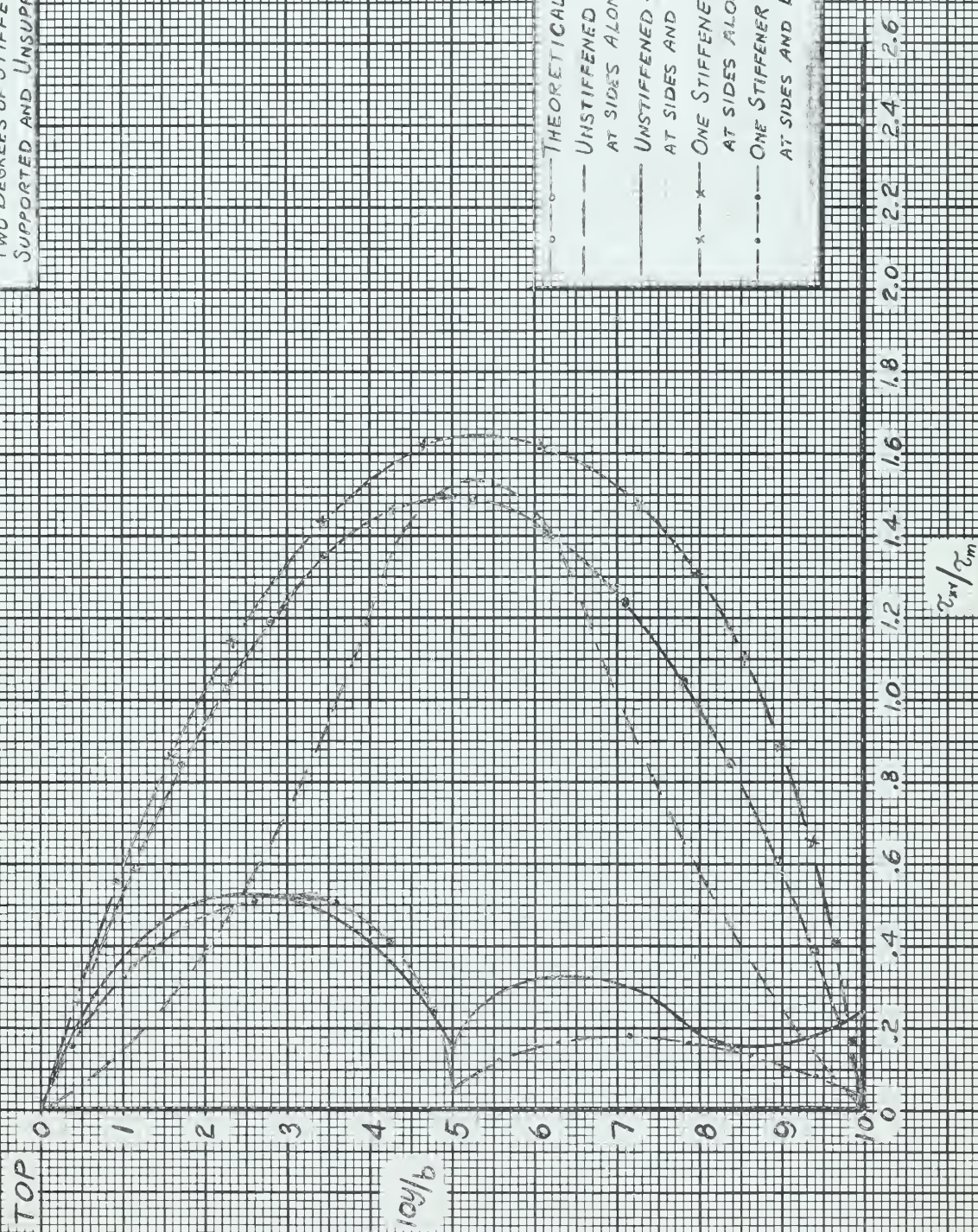
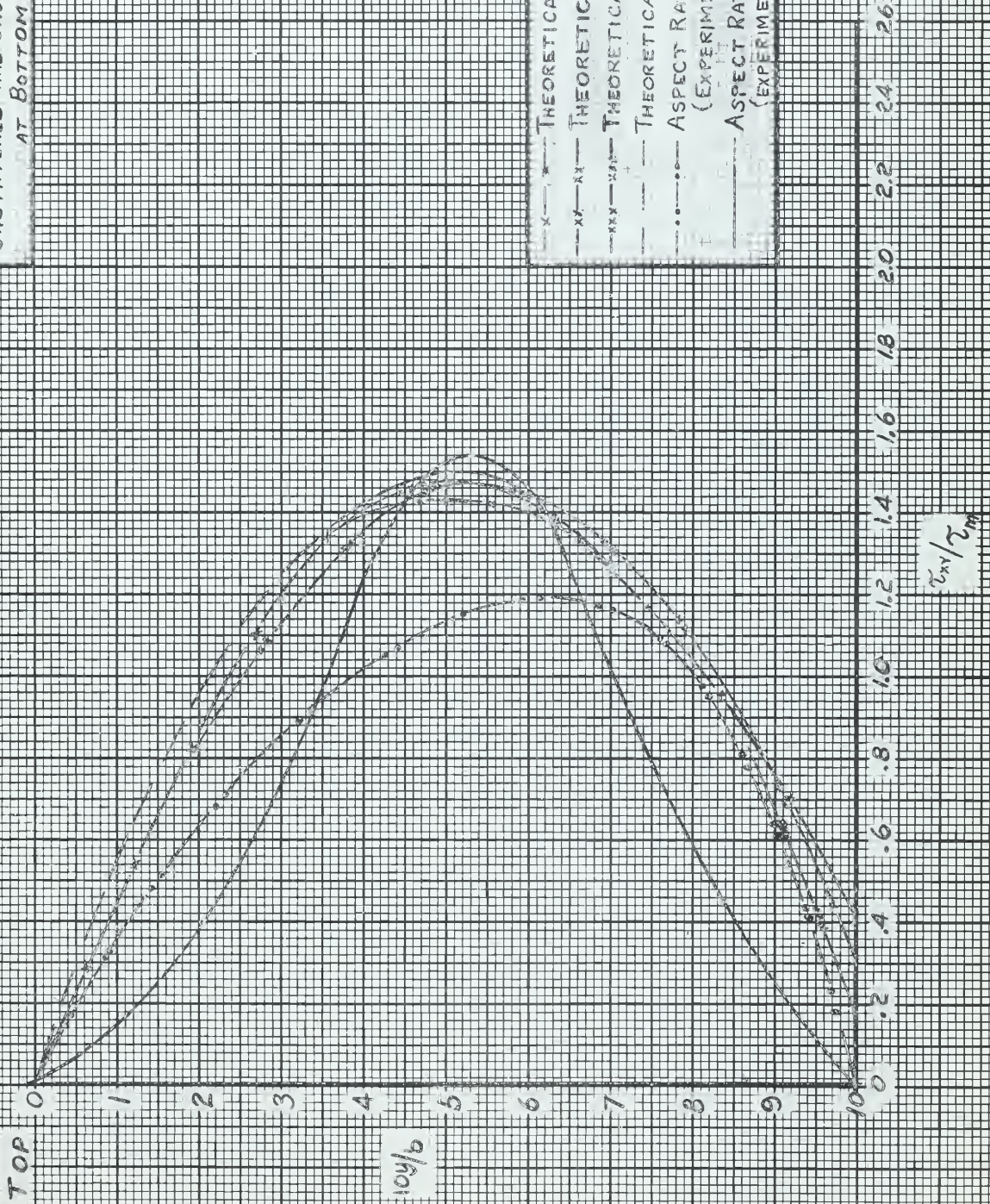


FIGURE IV

V.J.A.
4/15/59

CONCENTRATED LOAD
UNSTIFFENED AND UNSUPPORTED
AT BOTTOM

THEORETICAL AR 1:1
THEORETICAL AR 2:1
THEORETICAL AR 3:1
THEORETICAL AR 5:1
ASPECT RATIO 2:1
(EXPERIMENTAL)
ASPECT RATIO 5:1
(EXPERIMENTAL)



CONCENTRATED LOAD
THEORETICAL RESULTS

- x---x--- THEORETICAL AR 1:1
- x--- THEORETICAL AR 2:1
- - -x- - - THEORETICAL AR 3:1
- x--- THEORETICAL AR 5:1

FIGURE V

V.J.A.
4/16/59

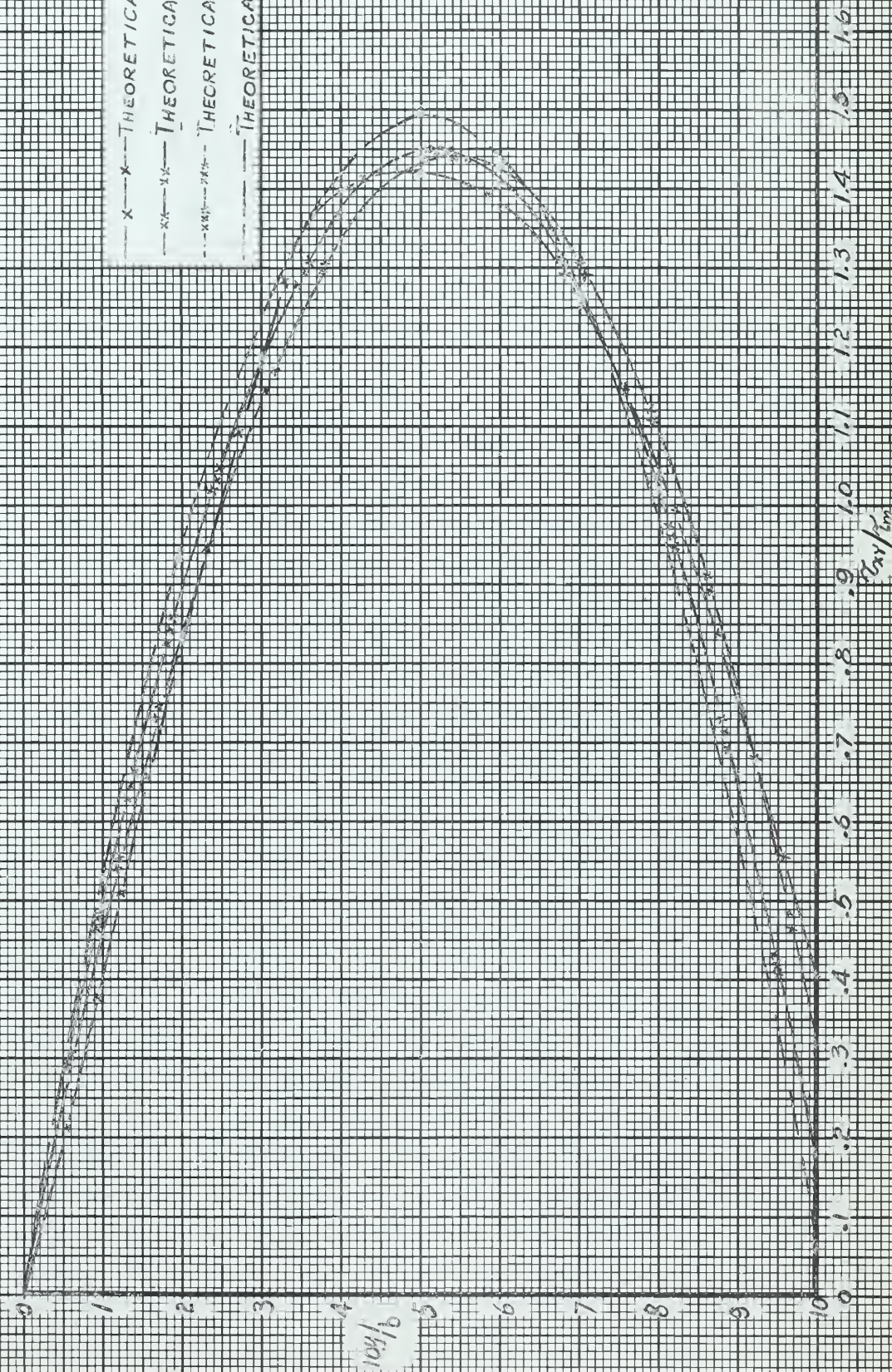
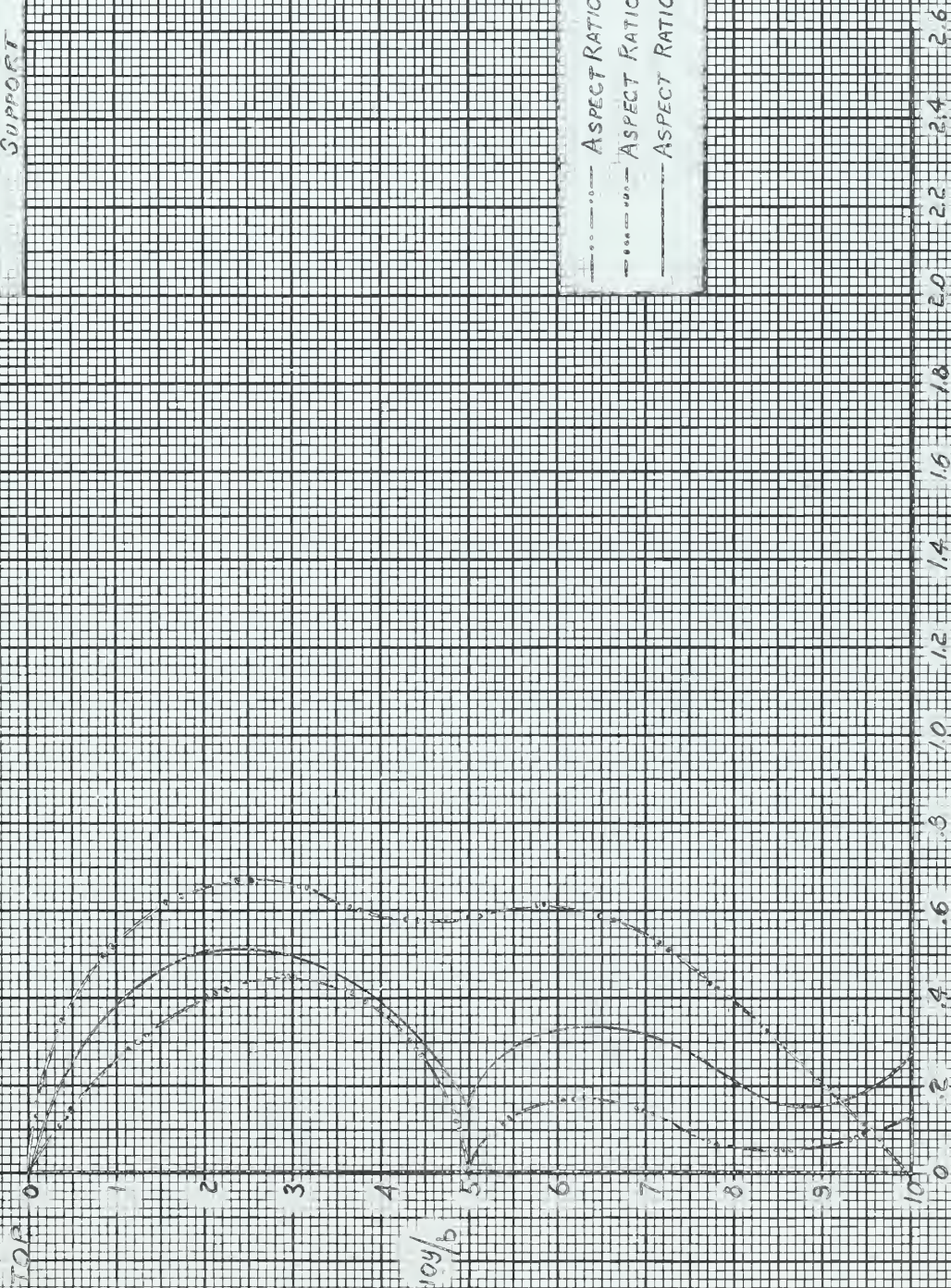


FIGURE VI

V.J.A
4/4/50

CONCENTRATED LOAD
UNSTIFFENED WITH BOTTOM
SUPPORT

ASPECT RATIO 2:1
ASPECT RATIO 3:1
ASPECT RATIO 5:1



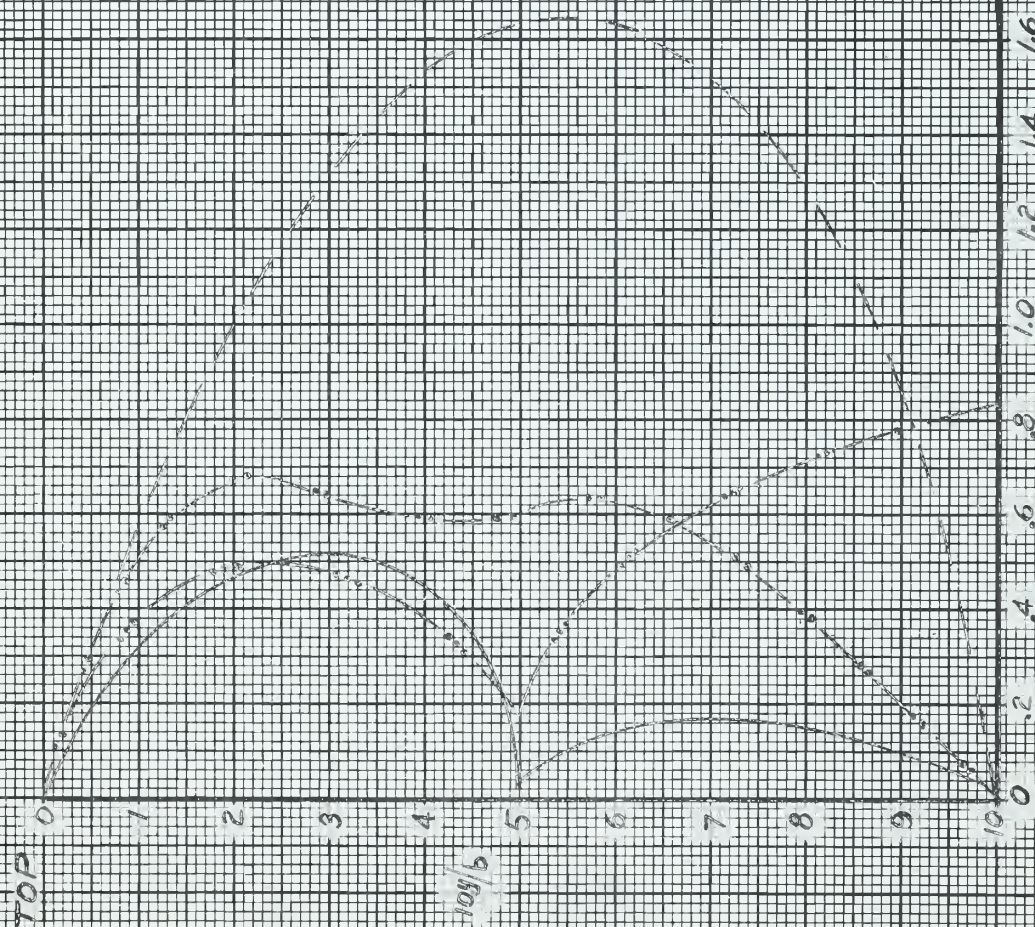
x/x_m

FIGURE VII

V.J.A.
4/6/59

CONCENTRATED LOAD
ONE STIFFENER SUPPORTED
AND UNSUPPORTED

AR 2:1 SUPPORTED AT
SIDES AND BOTTOM
AR 3:1 SUPPORTED AT
SIDES AND BOTTOM
AR 5:1 SUPPORTED AT
SIDES AND BOTTOM
AR 5:1 SUPPORTED AT
SIDES ALONE



σ_{xx}/σ_{00}

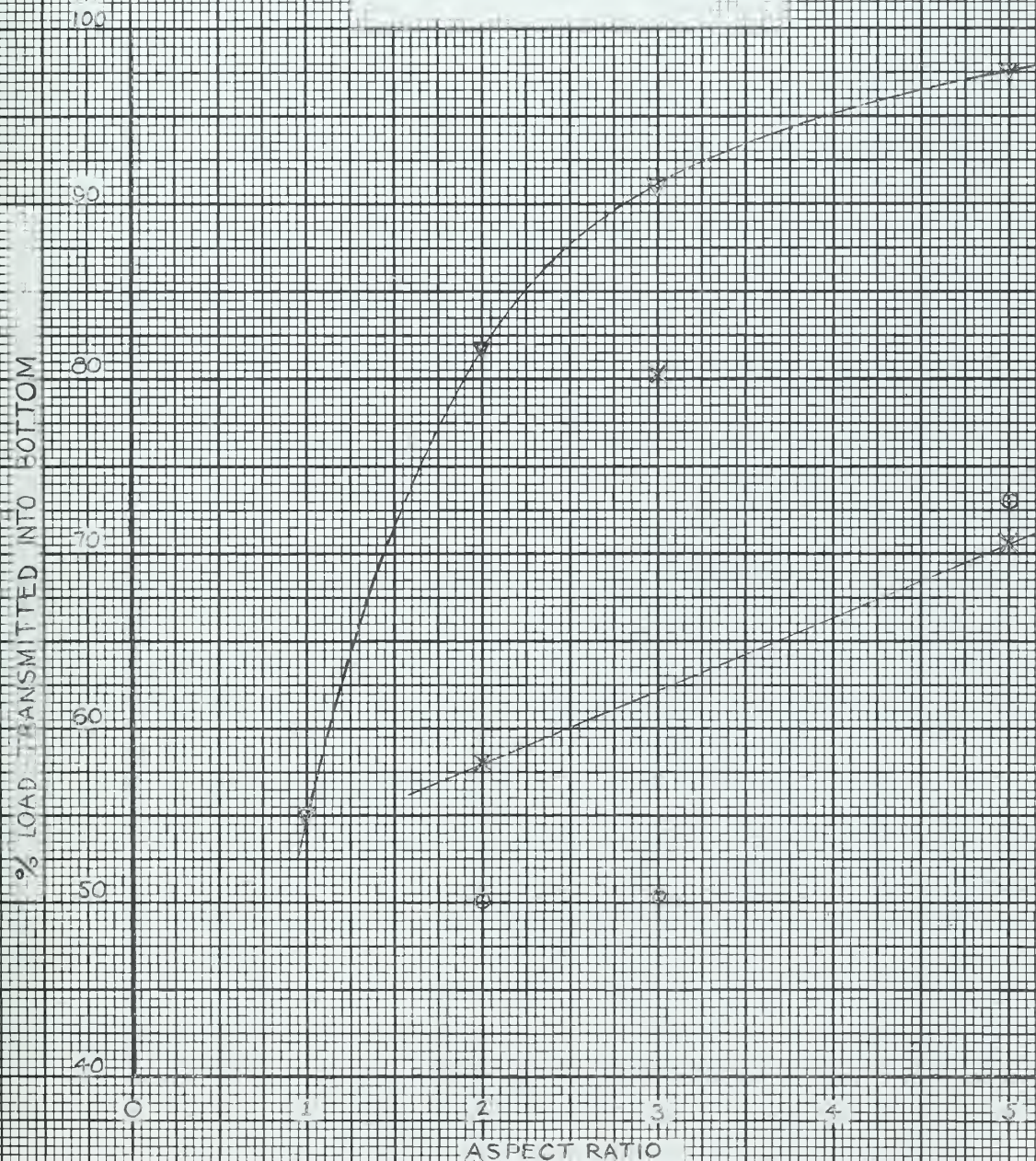
FIGURE VII

% LOAD TRANSMITTED INTO BOTTOM VS

ASPECT RATIO

CONCENTRATED LOAD AT C

- X UNSTIFFENED
- STIFFENED
- ▽ CONCENTRATED LOAD EFFECT ON BOTTOM OF UNSTIFFENED SEMI-INFINITE PLATE



JJP
4-3-59

FIGURE IX

% LOAD TRANSMITTED INTO BOTTOM / ASPECT RATIO VS.

PANEL WIDTH

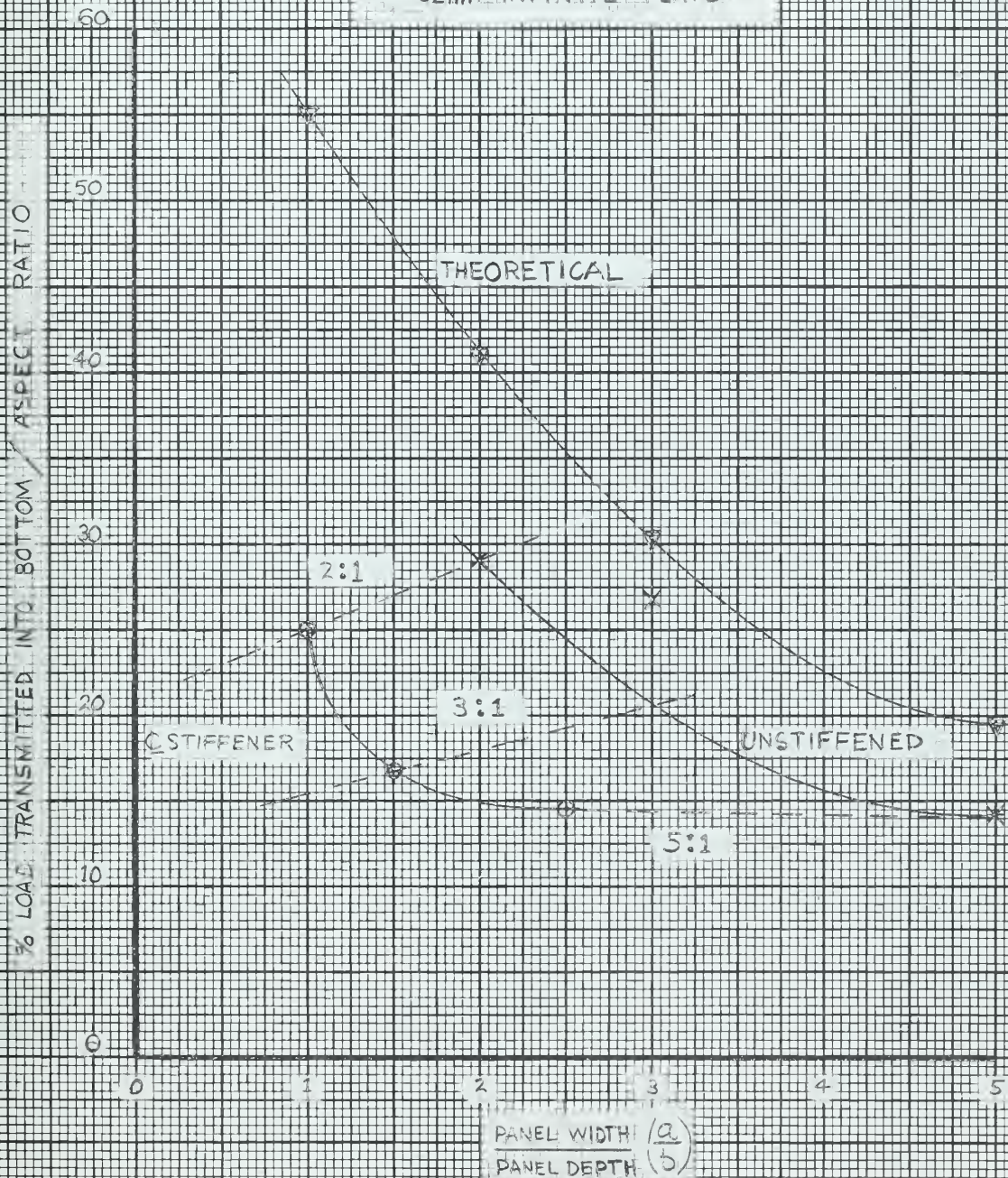
PANEL DEPTH

CONCENTRATED LOAD AT $\frac{a}{2}$

X UNSTIFFENED

O STIFFENER

▽ CONCENTRATED LOAD EFFECT
ON BOTTOM OF UNSTIFFENED
SEMI-INFINITE PLATE

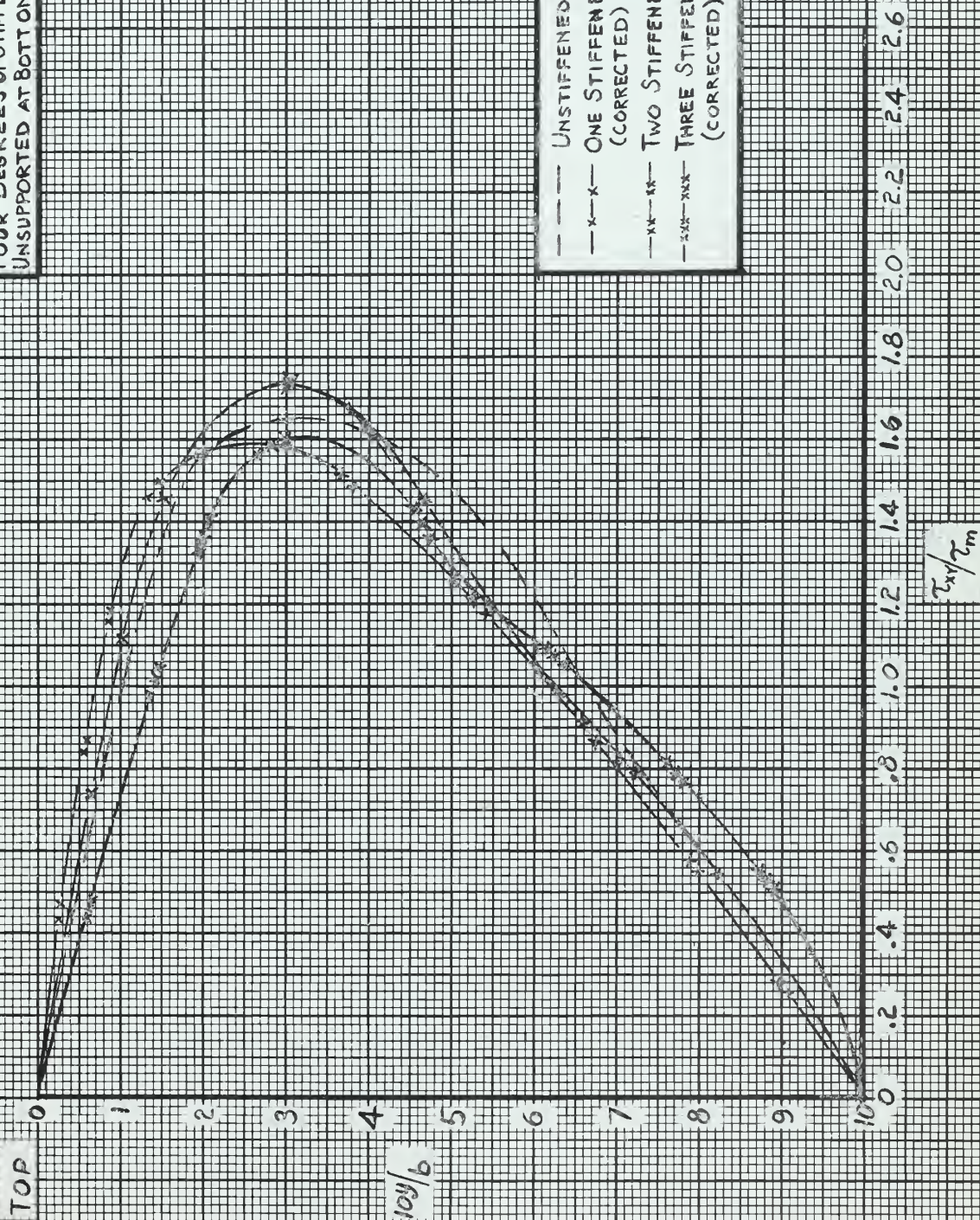


VJ.A
4/7/59

FIGURE X

AR 11: UNIFORM LOAD
FOUR DEGREES OF STIFFENING
UNSUPPORTED AT BOTTOM

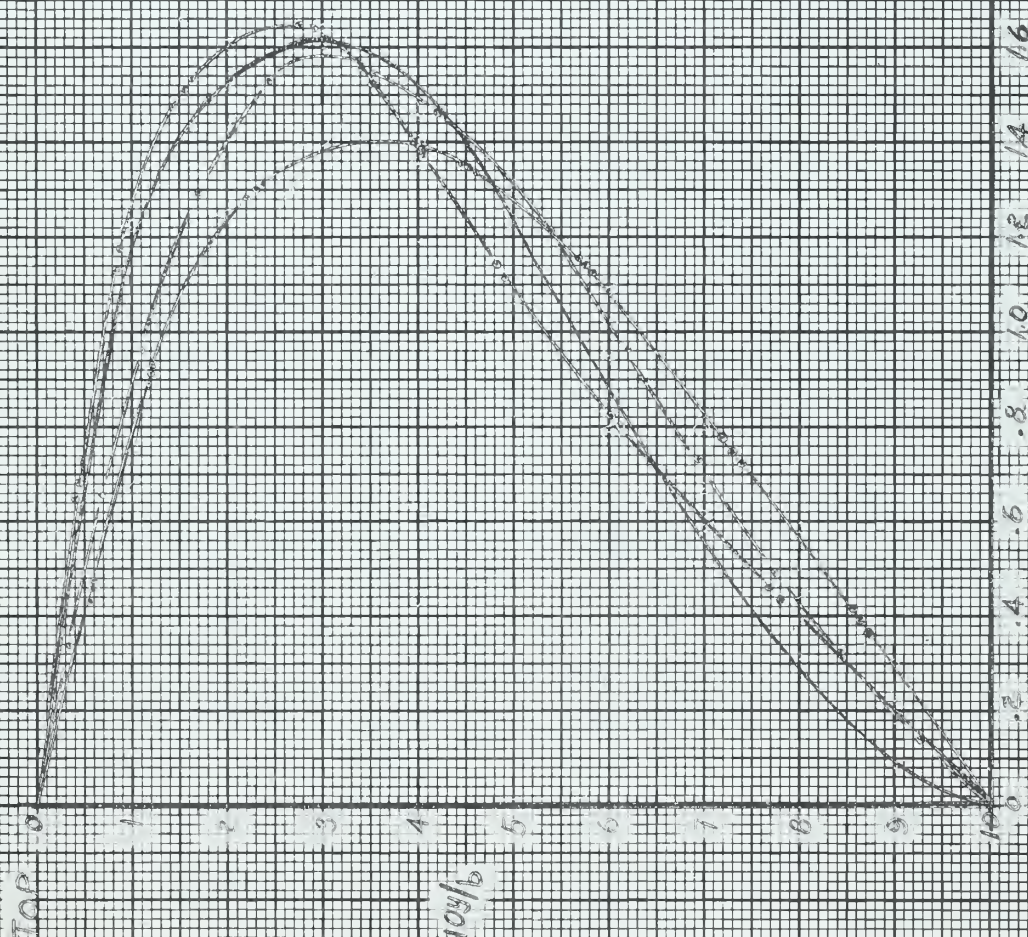
--- UNSTIFFENED
-x-x- ONE STIFFENER
(CORRECTED)
-xx-xx- TWO STIFFENERS
-xxx-xxx- THREE STIFFENERS
(CORRECTED)



AR 1:1 UNIFORM LOAD
FOUR DEGREES OF STIFFENING
SUPPORTED AT SIDE AND BOTTOM

FIGURE XI

— UNSTIFFENED
- - - ONE STIFFENER
... TWO STIFFENERS
--- THREE STIFFENERS



$\frac{w}{l}$

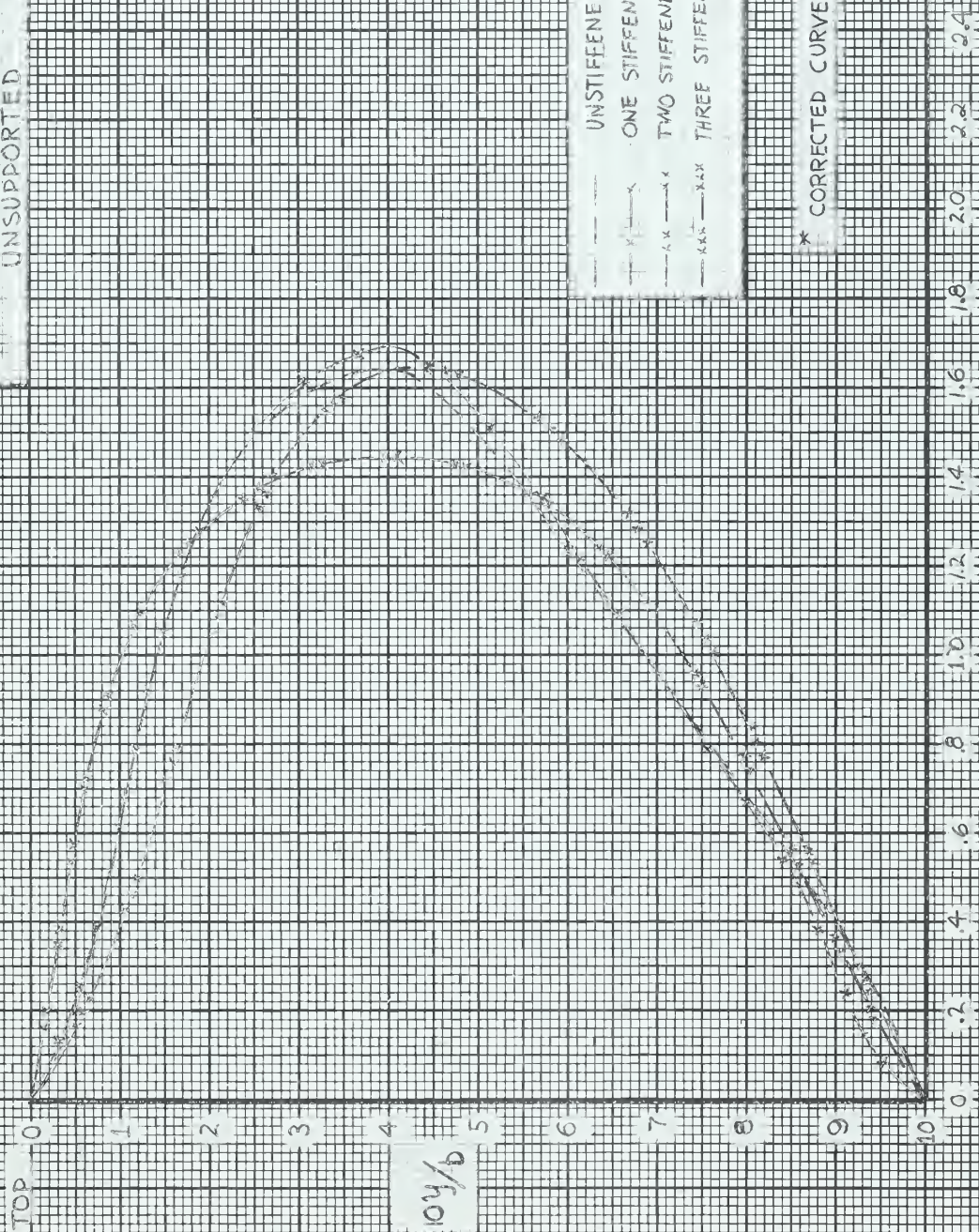
V.10
4/7/59

FIGURE XII

AR 2:1 UNIFORM LOAD
FOUR DEGREES OF STIFFENING
UNSUPPORTED

UNSTIFFENED*
ONE STIFFENER
TWO STIFFENERS
THREE STIFFENERS

* CORRECTED CURVES



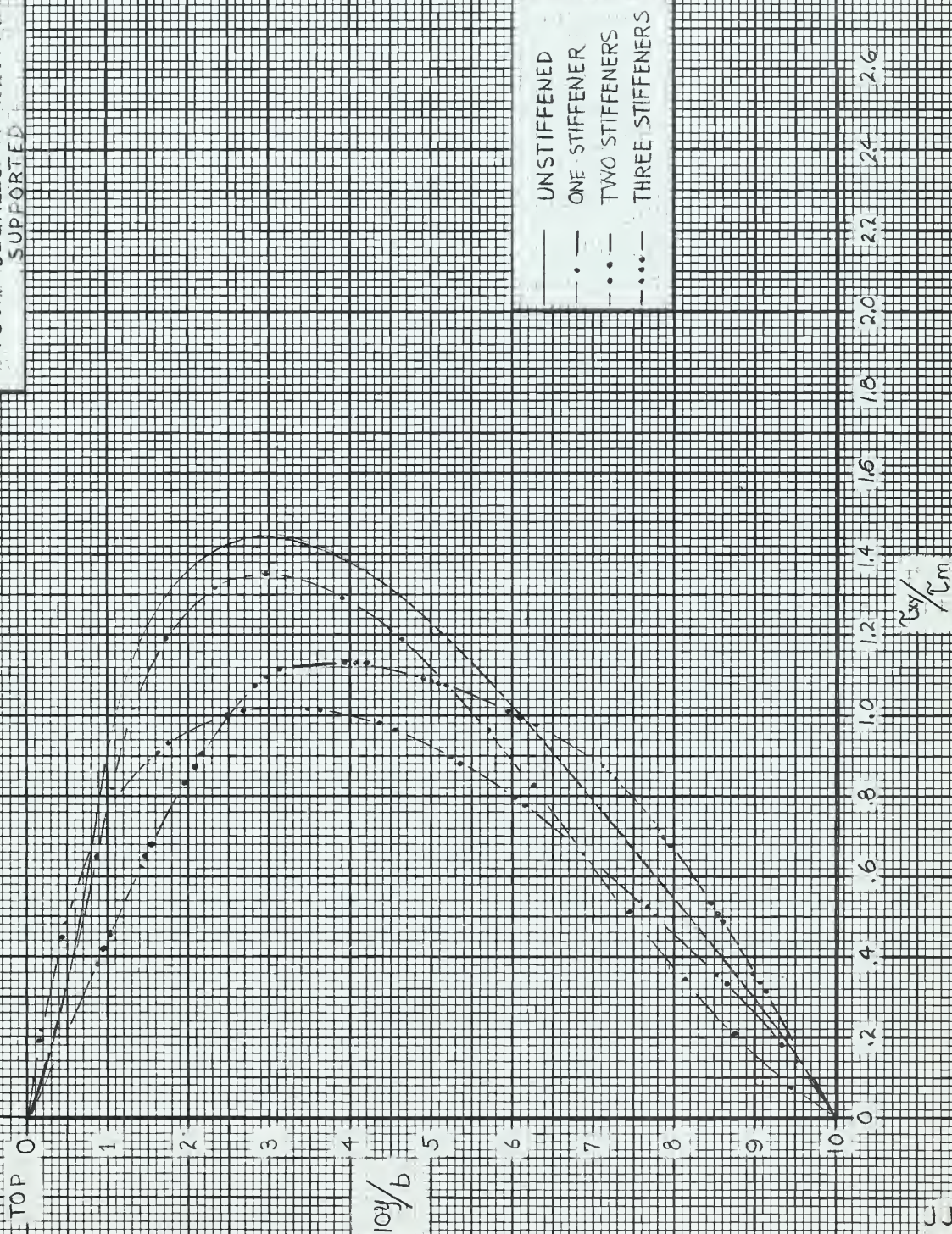
x/l

$10y/b$

JJP
4-6-59

FIGURE XIII

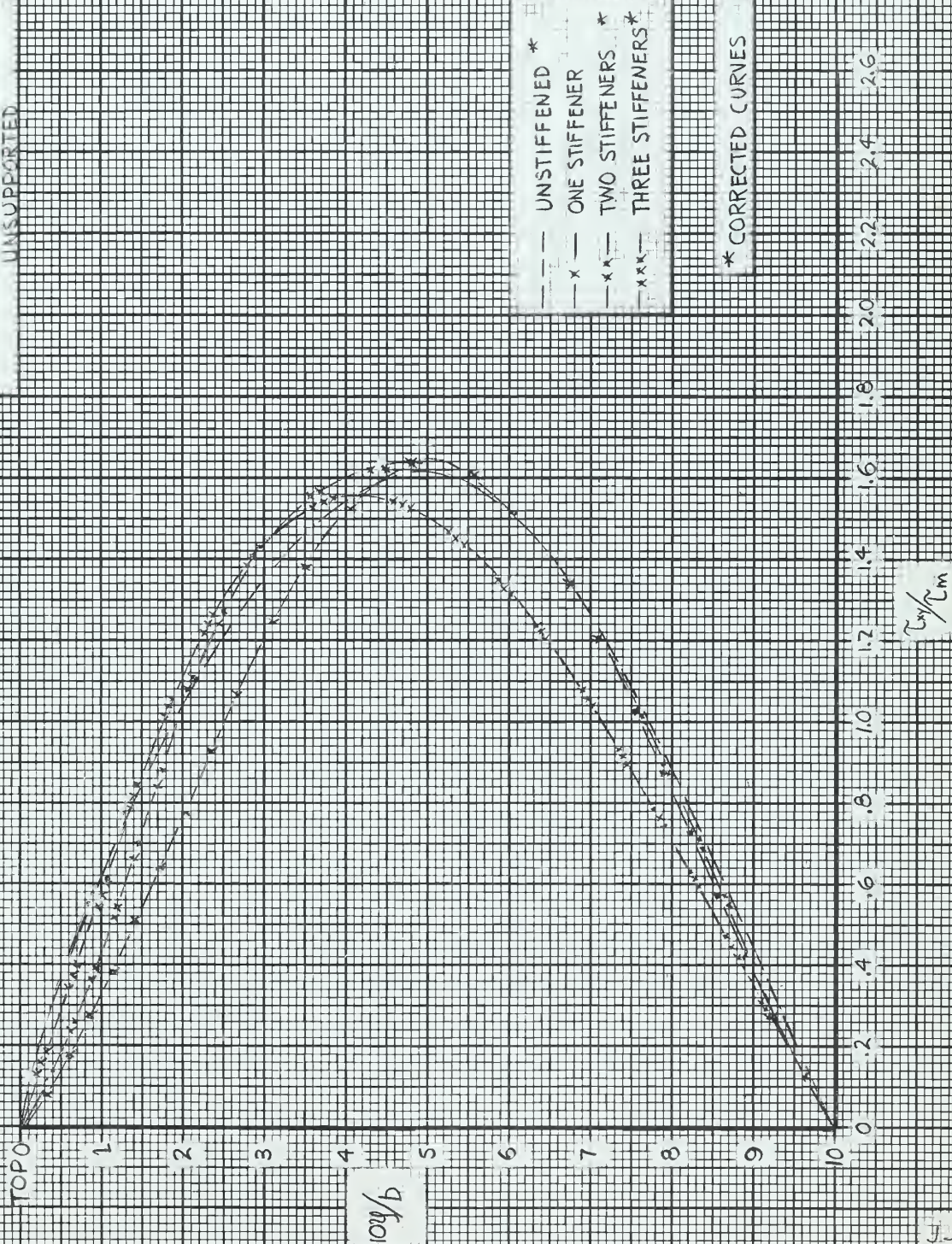
AR 2:1 UNIFORM LOAD
FOUR DEGREES OF STIFFENING
SUPPORTED



JJP
4-7-59

FIGURE XIV

AR 3:1 UNIFORM LOAD
FOUR DEGREES OF STIFFENING
UNSUPPORTED

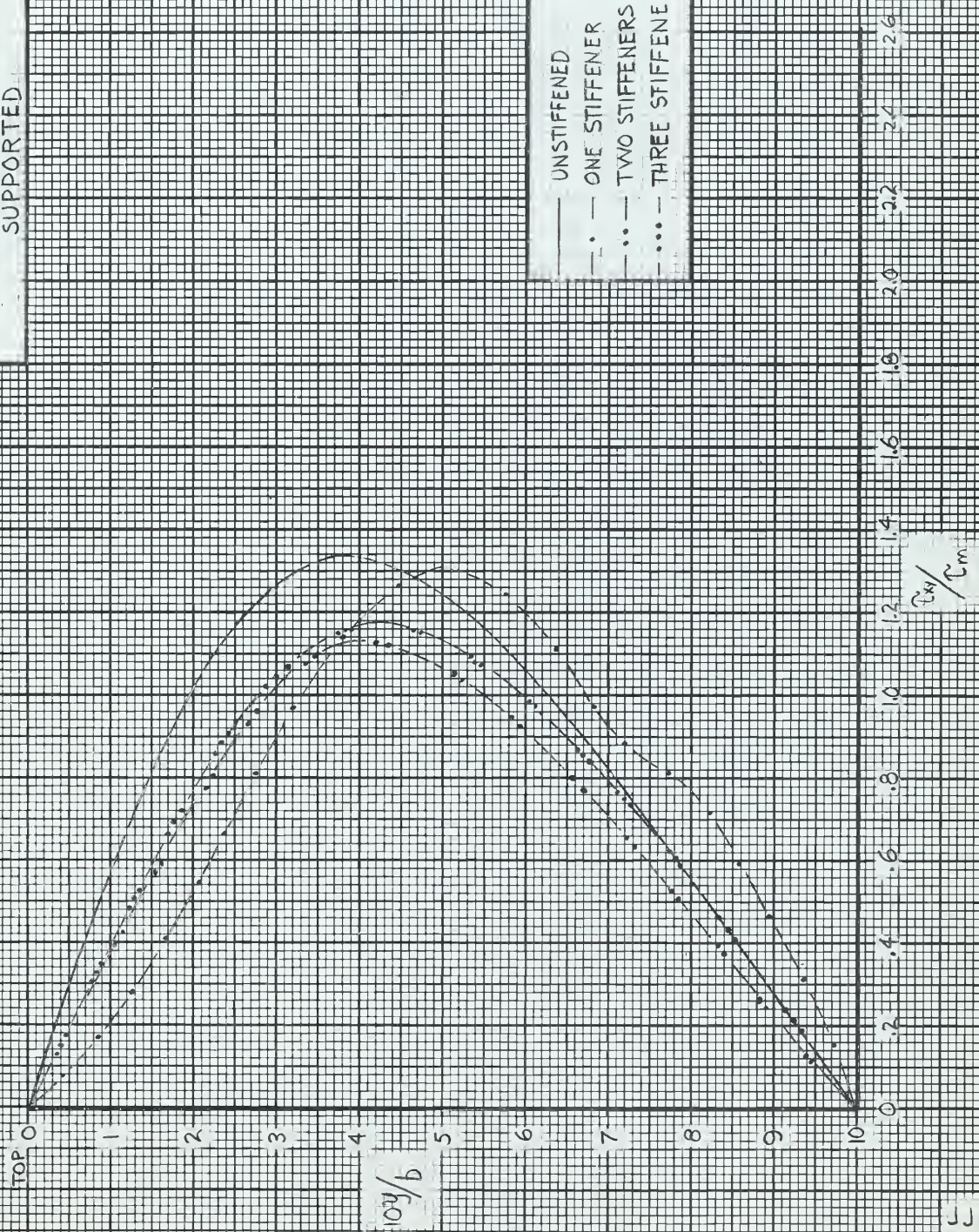


JJP
4-7-59

FIGURE XV

AR 3:1
UNIFORM LOAD
FOUR DEGREES OF STIFFENING
SUPPORTED

— UNSTIFFENED
- · - ONE STIFFENER
- · · - TWO STIFFENERS
- · · · - THREE STIFFENERS

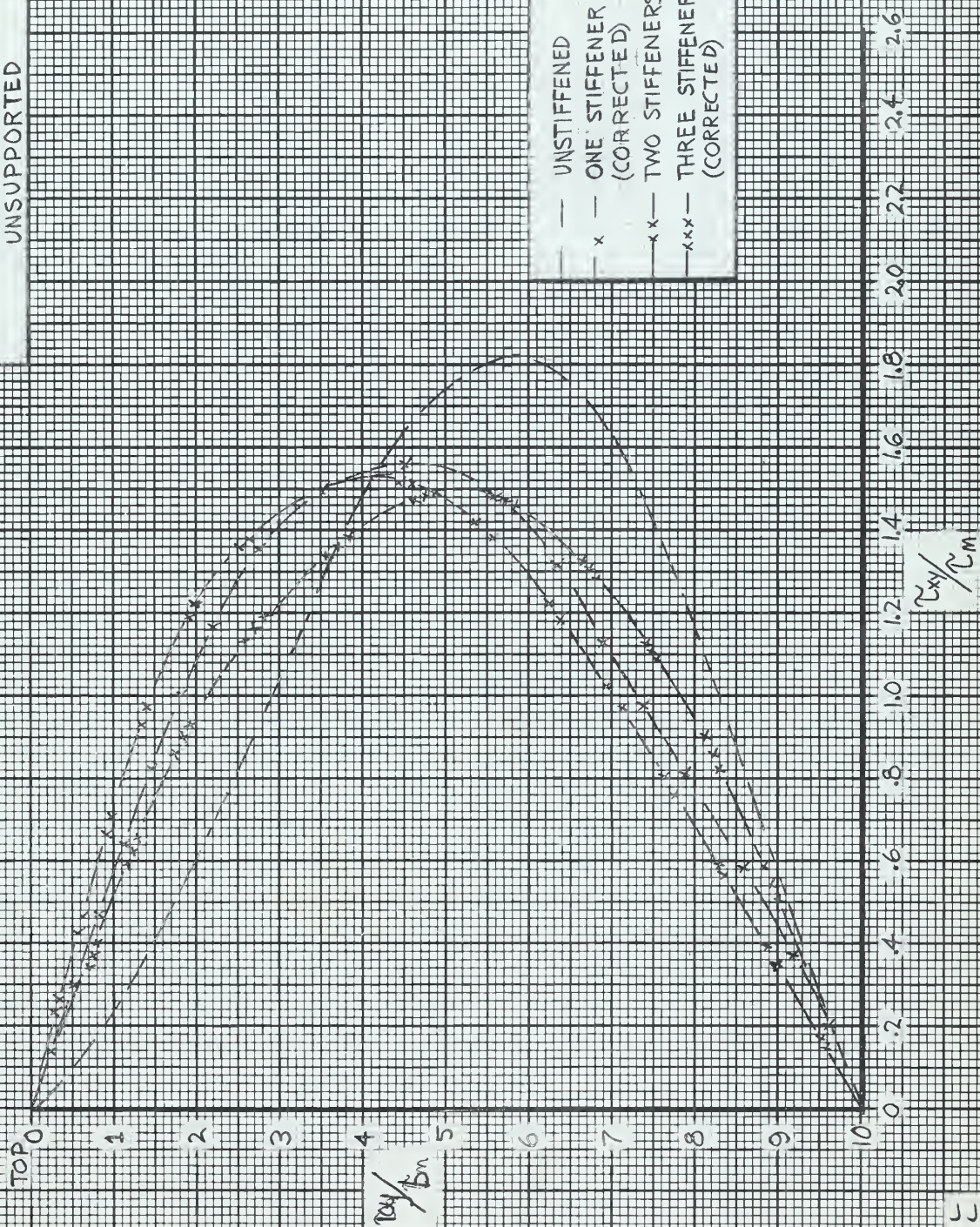


JJP
4-7-59

FIGURE XVI

AR 5:1 UNIFORM LOAD
FOUR DEGREES OF STIFFENING
UNSUPPORTED

— UNSTIFFENED
— x — ONE STIFFENER
 (CORRECTED)
— x x — TWO STIFFENERS
 (CORRECTED)
— x x x — THREE STIFFENERS
 (CORRECTED)

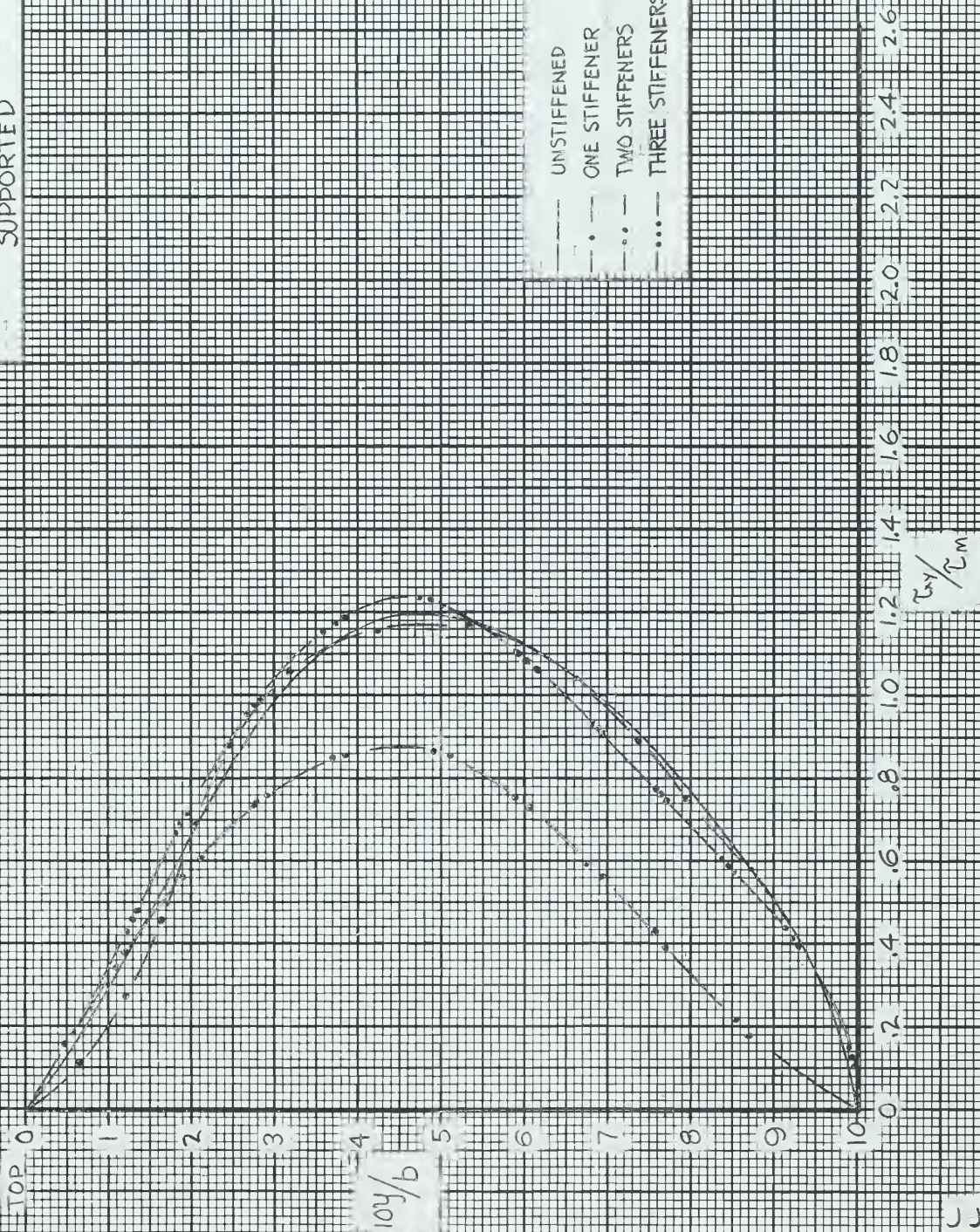


JJP
4-7-59

FIGURE XVII

AR 5:1
UNIFORM LOAD
FOUR DEGREES OF STIFFENING
SUPPORTED

UNSTIFFENED
ONE STIFFENER
TWO STIFFENERS
THREE STIFFENERS



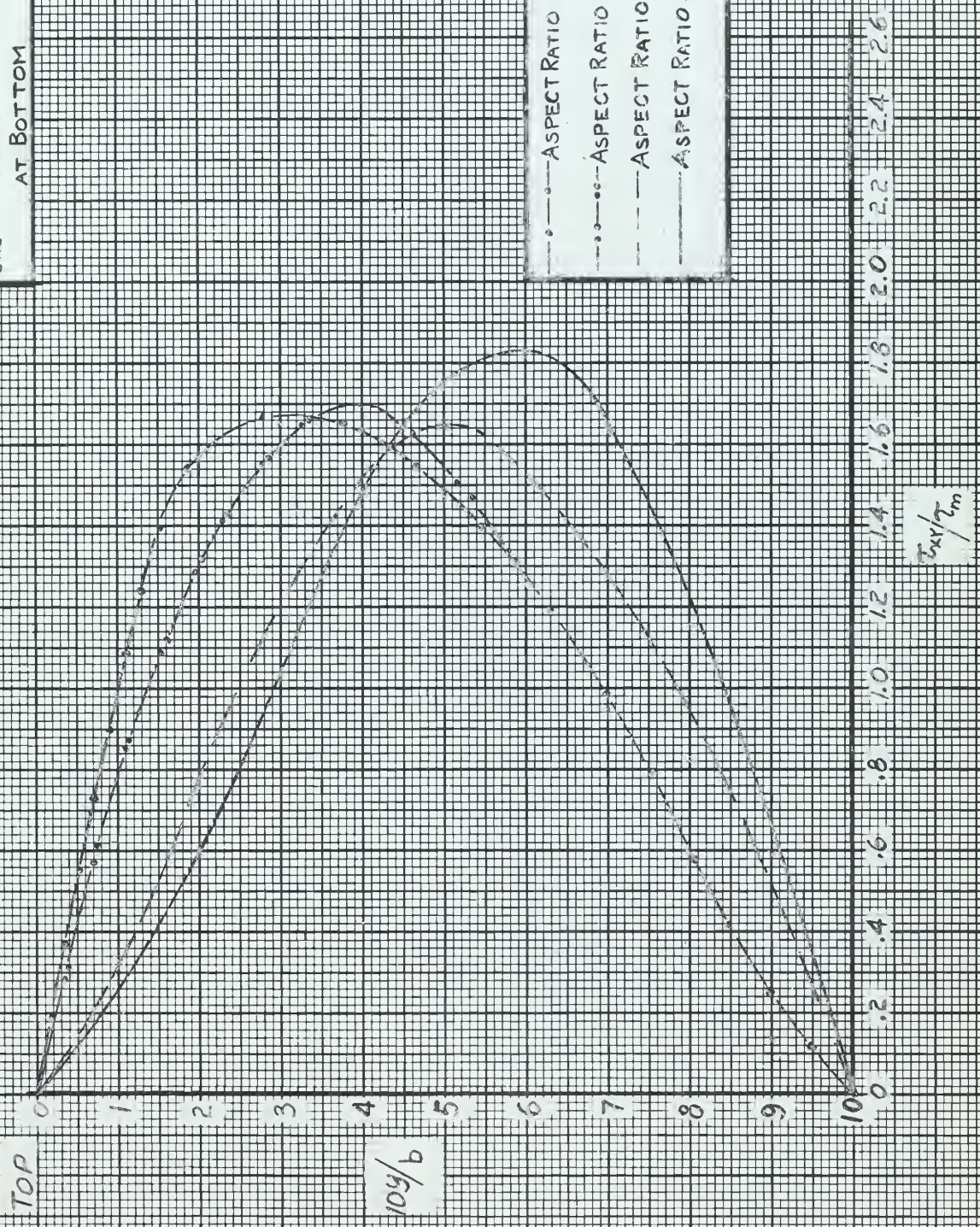
JJP
4-7-59

V.J.A.
4/8/59

FIGURE XVII

UNIFORM LOAD
UNSTIFFENED AND UNSUPPORTED
AT BOTTOM

—•— ASPECT RATIO 1:1
—••— ASPECT RATIO 2:1
--- ASPECT RATIO 3:1
- - - ASPECT RATIO 5:1

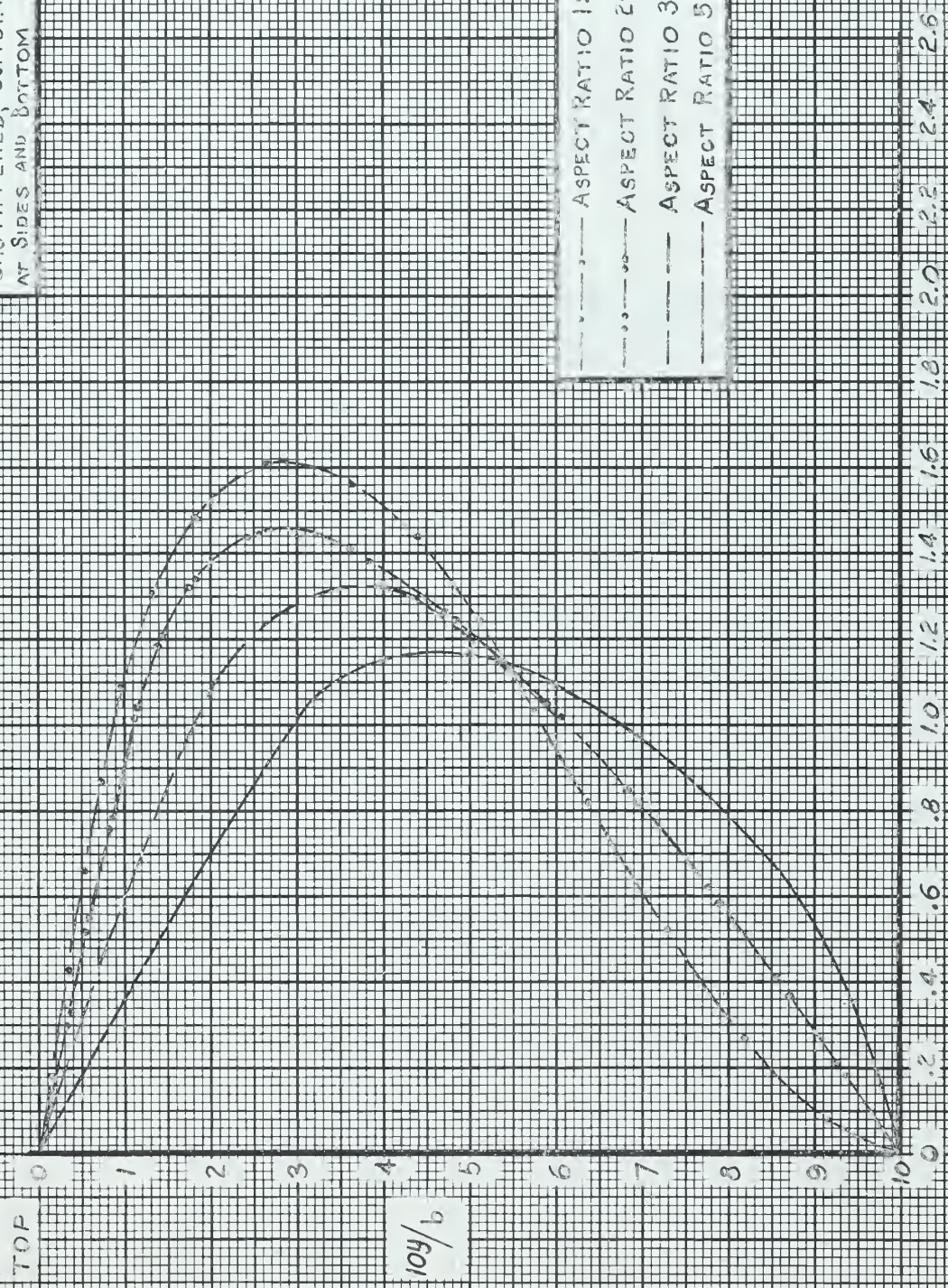


V.J.A.
A/1059

FIGURE XIX

UNIFORM LOAD
UNSTIFFENED, SUPPORTED
AT SIDES AND BOTTOM

— ASPECT RATIO 1:1
- - - ASPECT RATIO 2:1
- - - ASPECT RATIO 3:1
- - - ASPECT RATIO 5:1



x/L

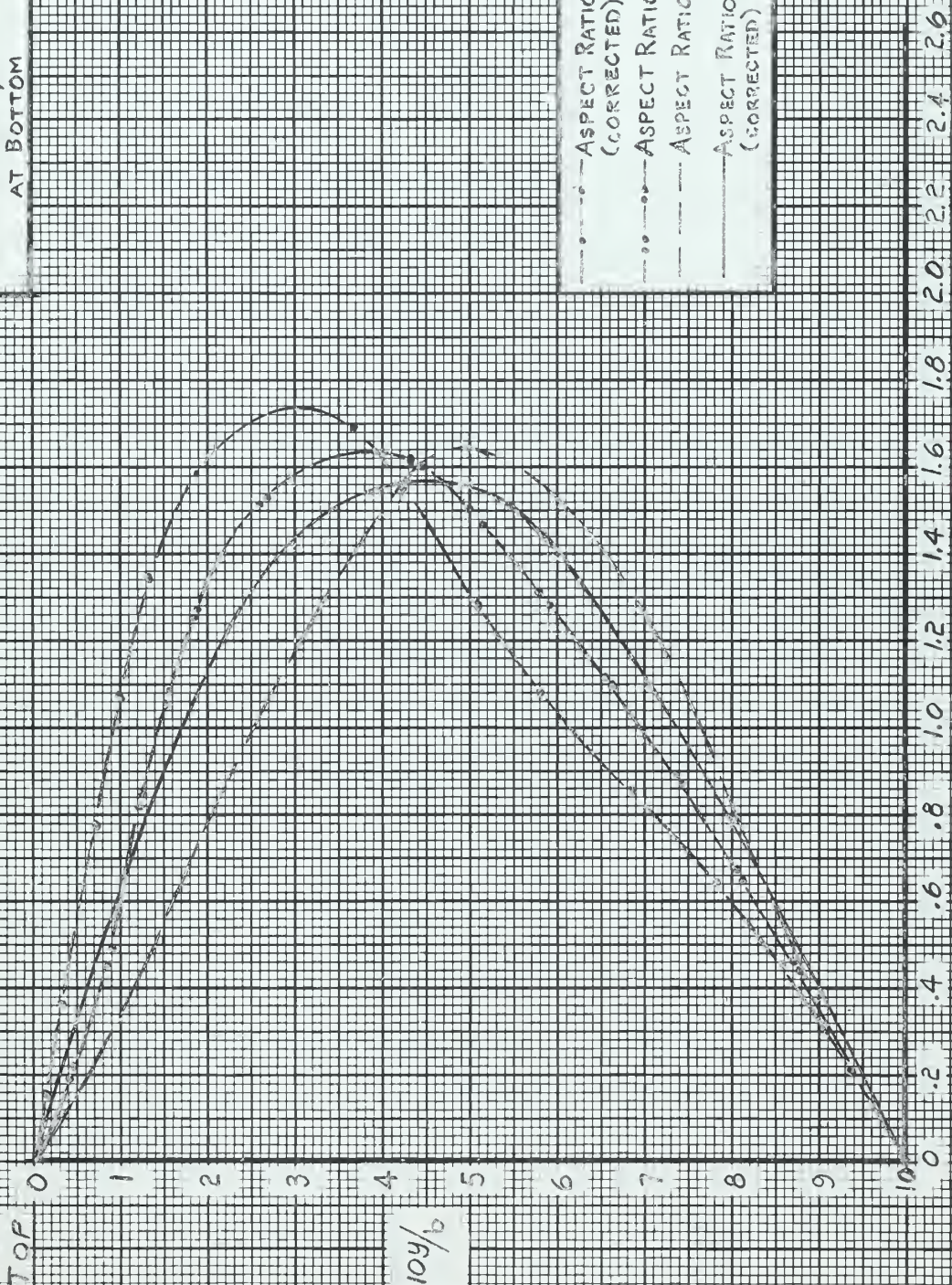
$10y/b$

VJA
4/9/59

FIGURE XX

UNIFORM LOAD
ONE STIFFENER, UNSUPPORTED
AT BOTTOM

ASPECT RATIO 1:1
(CORRECTED)
ASPECT RATIO 2:1
ASPECT RATIO 3:1
ASPECT RATIO 5:1
(CORRECTED)



x_x/x_m

$10y/b$

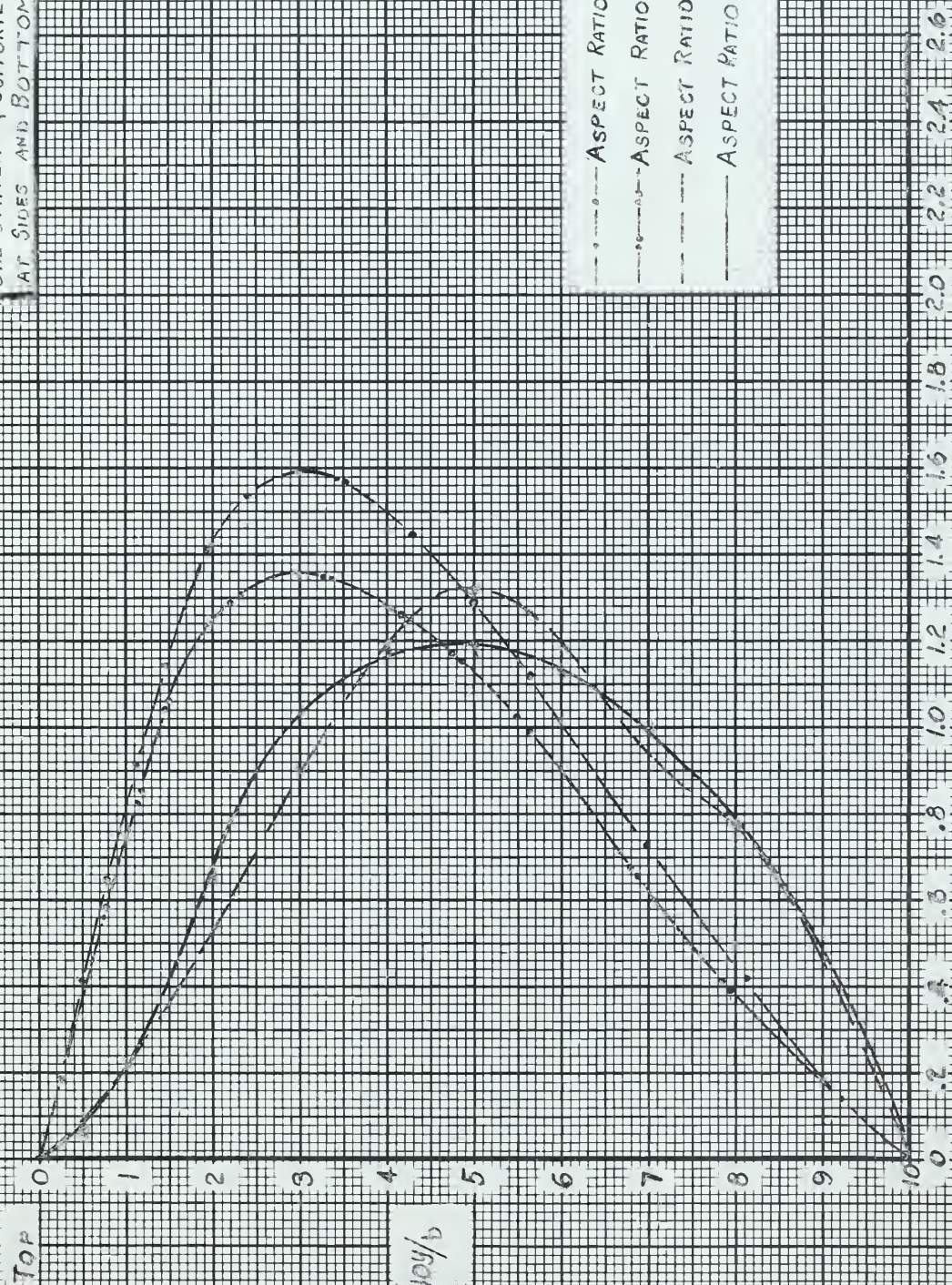
TOP

V.J.A
4/9/59

FIGURE XXI

UNIFORM LOAD
ONE STIFFENER, SUPPORTED
AT SIDES AND BOTTOM

ASPECT RATIO 1:1
ASPECT RATIO 2:1
ASPECT RATIO 3:1
ASPECT RATIO 5:1

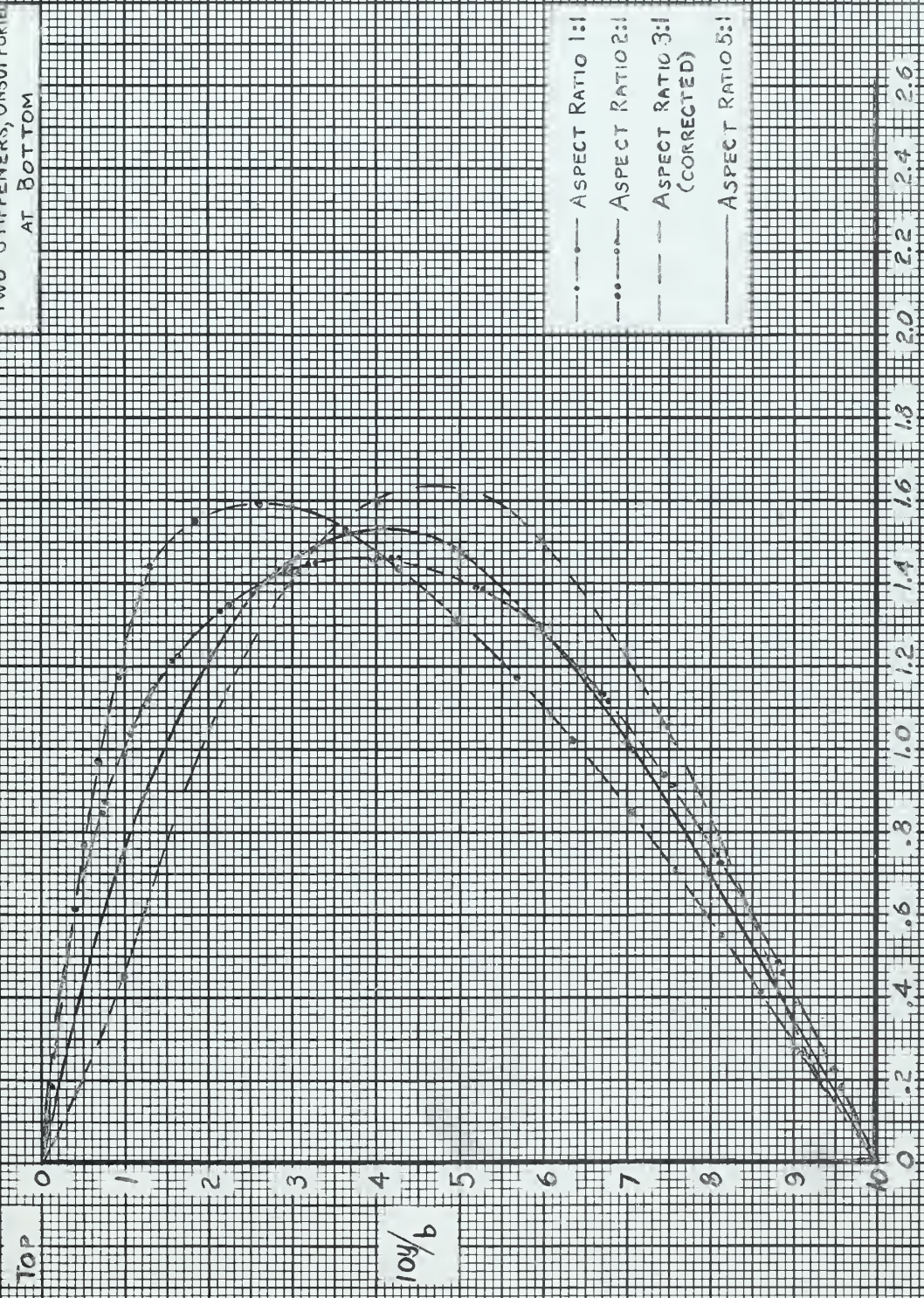


w/b

V.J.A
4/9/59

FIGURE XIII

UNIFORM LOAD
TWO STIFFENERS, UNSUPPORTED
AT BOTTOM



Top

FIGURE XXIII

UNIFORM LOAD
TWO STIFFENERS
SUPPORTED AT BOTTOM

• — ASPECT RATIO 1:1
•• — ASPECT RATIO 2:1
— ASPECT RATIO 3:1
— ASPECT RATIO 5:1

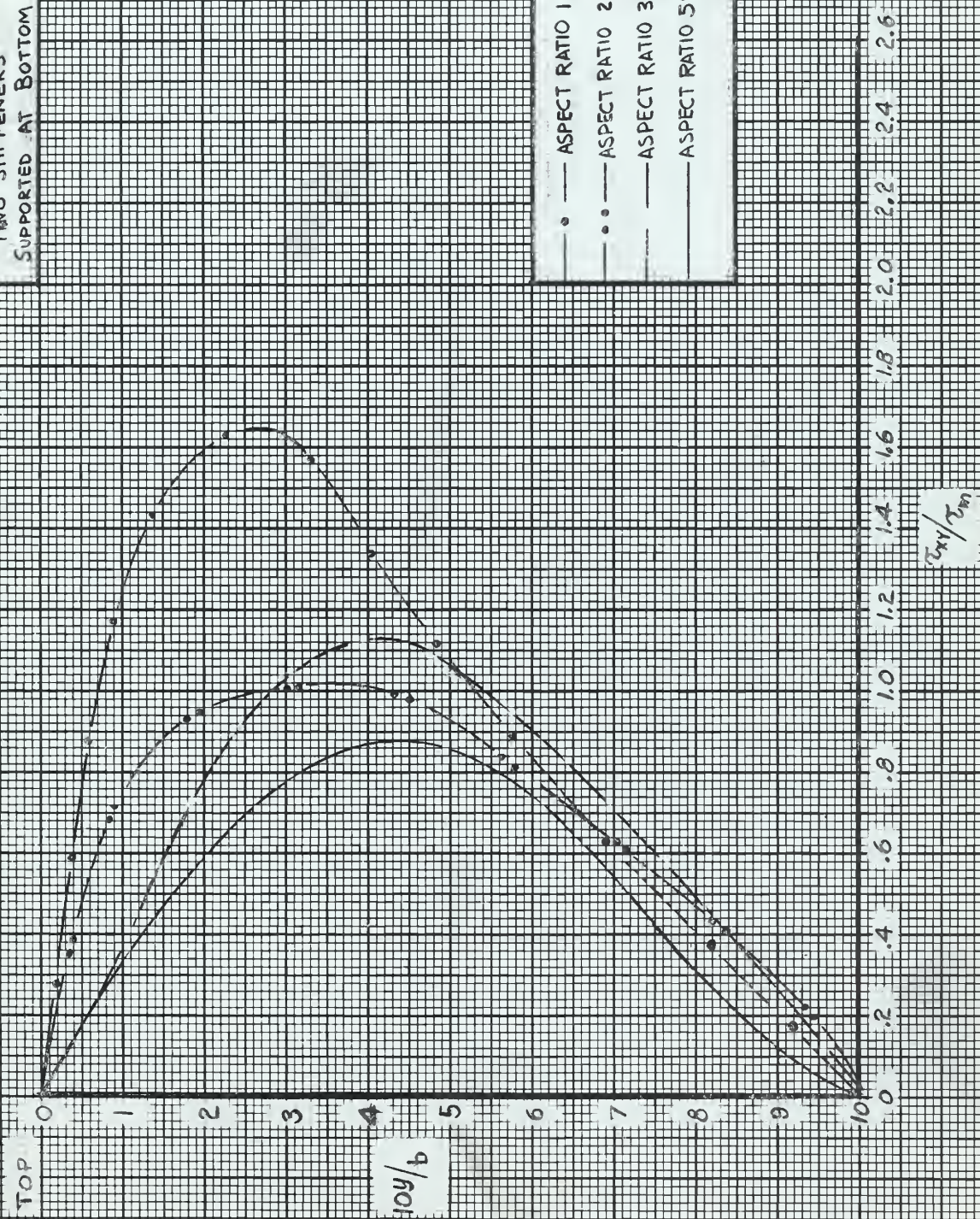
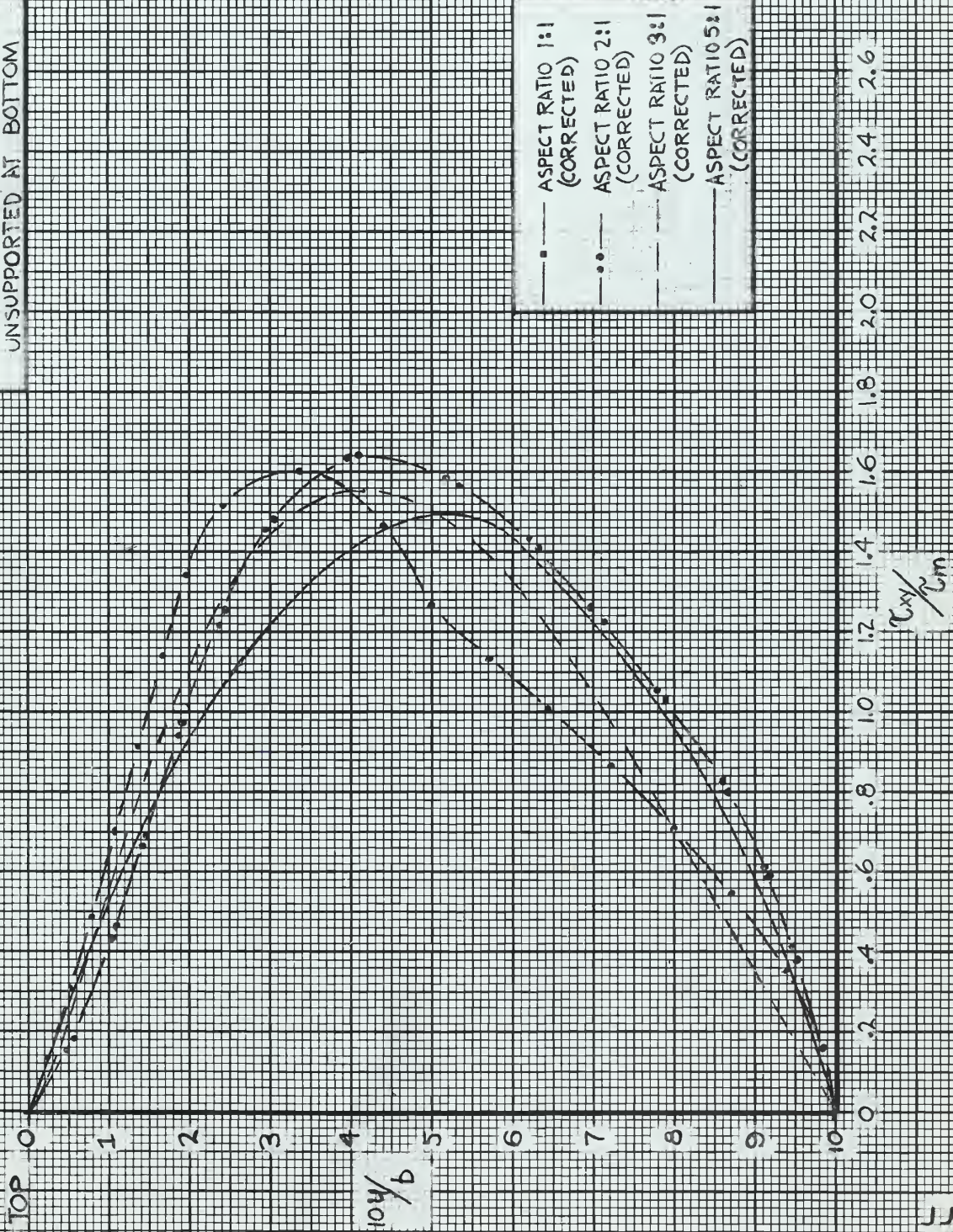


FIGURE XXIV

UNIFORM LOAD
THREE STIFFENERS
UNSUPPORTED AT BOTTOM

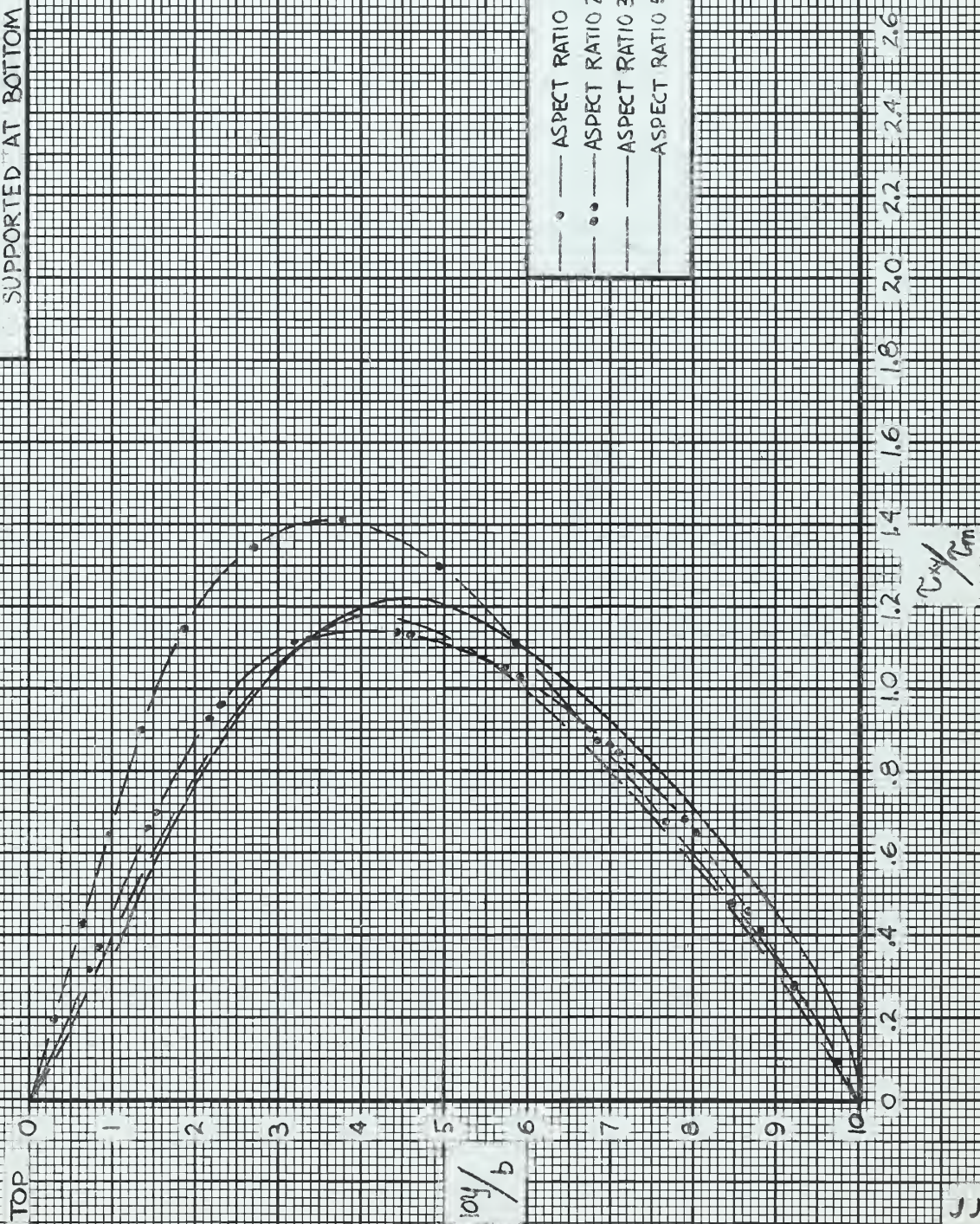


JJP
4-9-59

FIGURE XXV

UNIFORM LOAD
THREE STIFFENERS
SUPPORTED AT BOTTOM

○ ASPECT RATIO 1:1
● ASPECT RATIO 2:1
— ASPECT RATIO 3:1
— ASPECT RATIO 5:1



JJP
4-9-59

LOCATION AND MAGNITUDE OF

$$\left[\frac{\tau_{xy}}{\tau_m} \right]_{\text{MAX}}$$

BY METHOD OF LEAST SQUARES
FOR SUPPORTED AND UNSUPPORTED
UNIFORM LOAD
○ - AVERAGE POINT

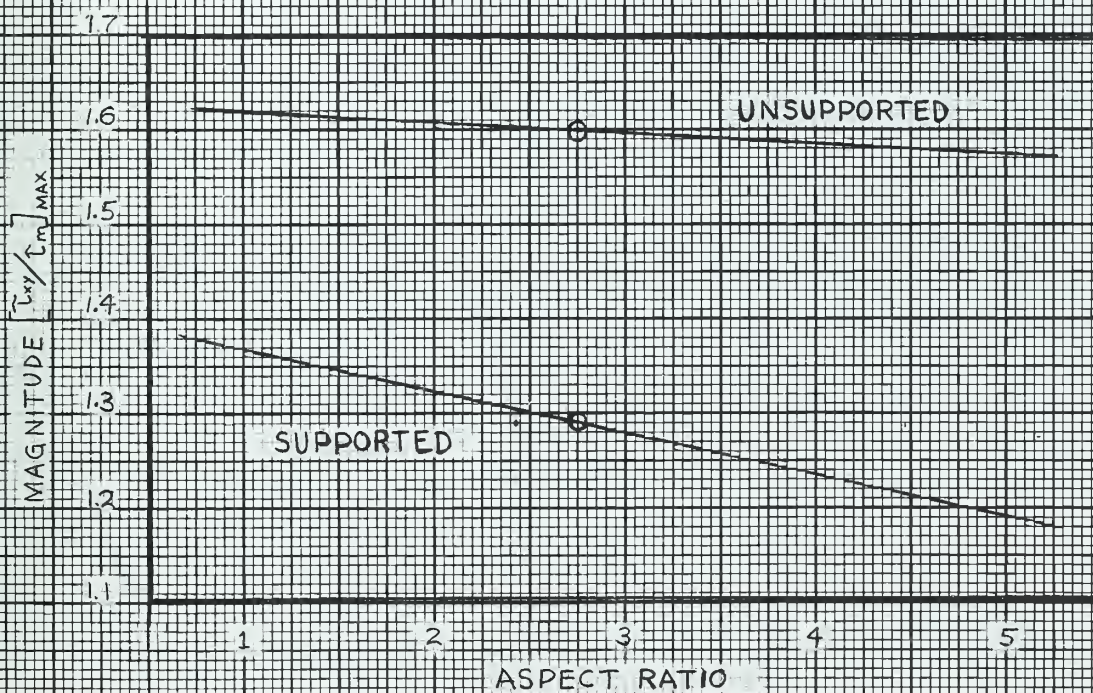
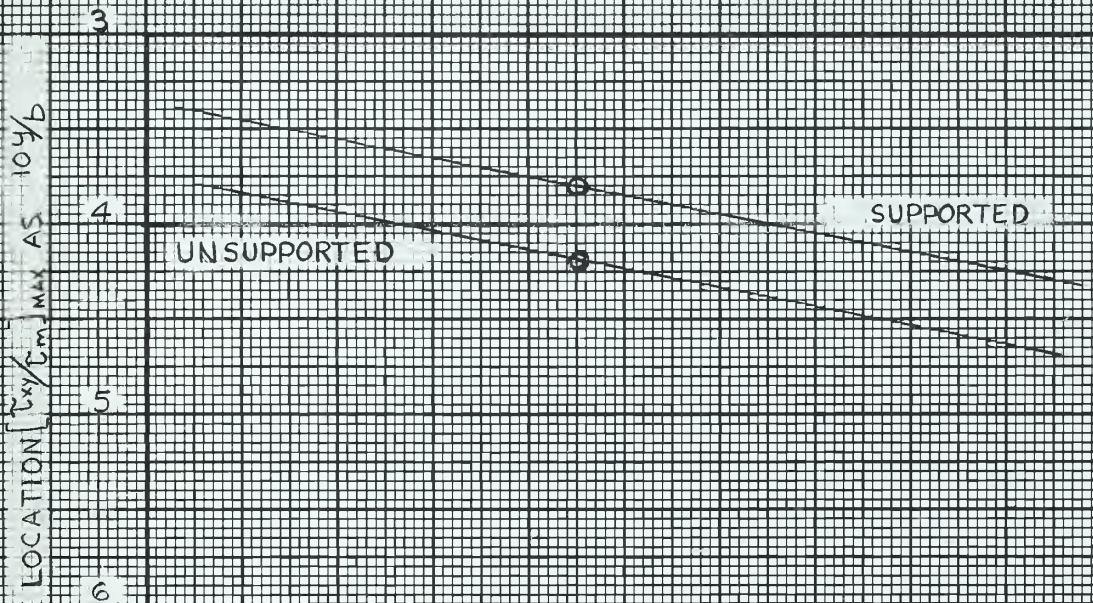


FIGURE XXVI

JJP
4-3-59

FIGURE XXVII

% REDUCTION IN $\left[\frac{C_{xy}}{C_m} \right]_{MAX}$ DUE TO SUPPORT
ASPECT RATIO
VS
PANEL WIDTH
PANEL DEPTH
UNIFORM LOAD
ASPECT RATIOS
X 1:1 O 2:1 Δ 3:1 □ 5:1

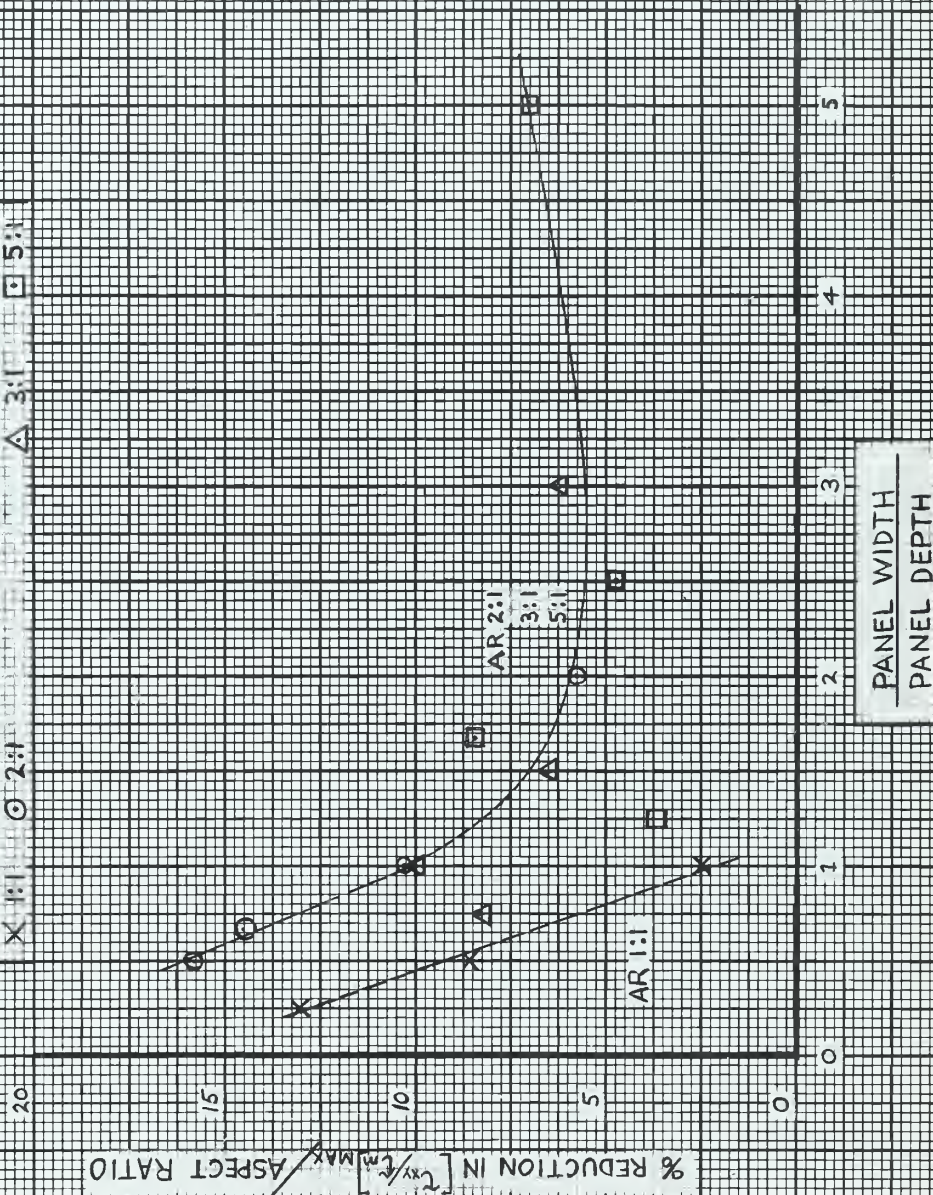


FIGURE XXVIII

% LOAD TRANSMITTED INTO BOTTOM VS

PANEL WIDTH

PANEL DEPTH

FOR UNIFORM LOAD

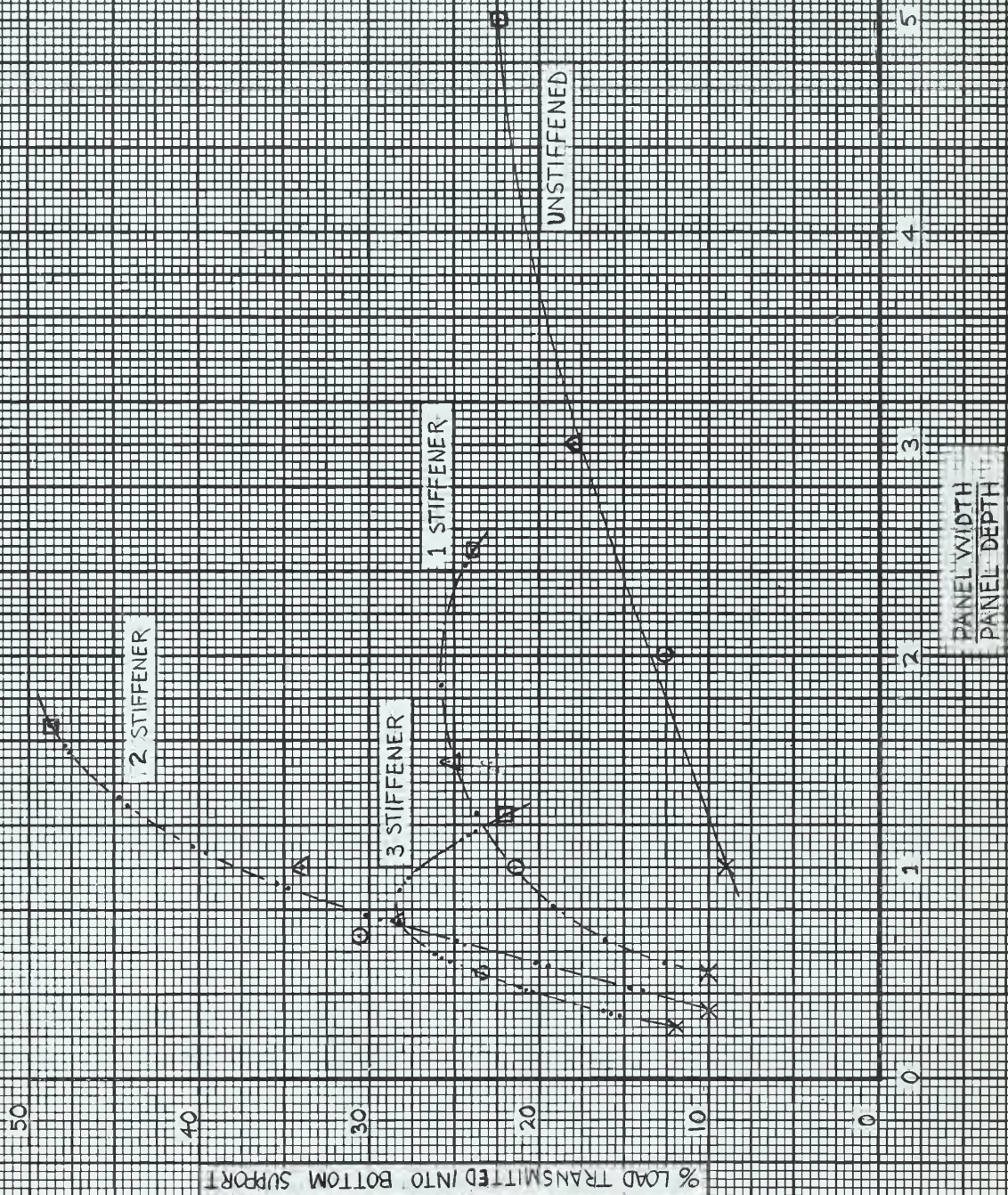
ASPECT RATIO

X 1:1

○ 2:1

△ 3:1

□ 5:1

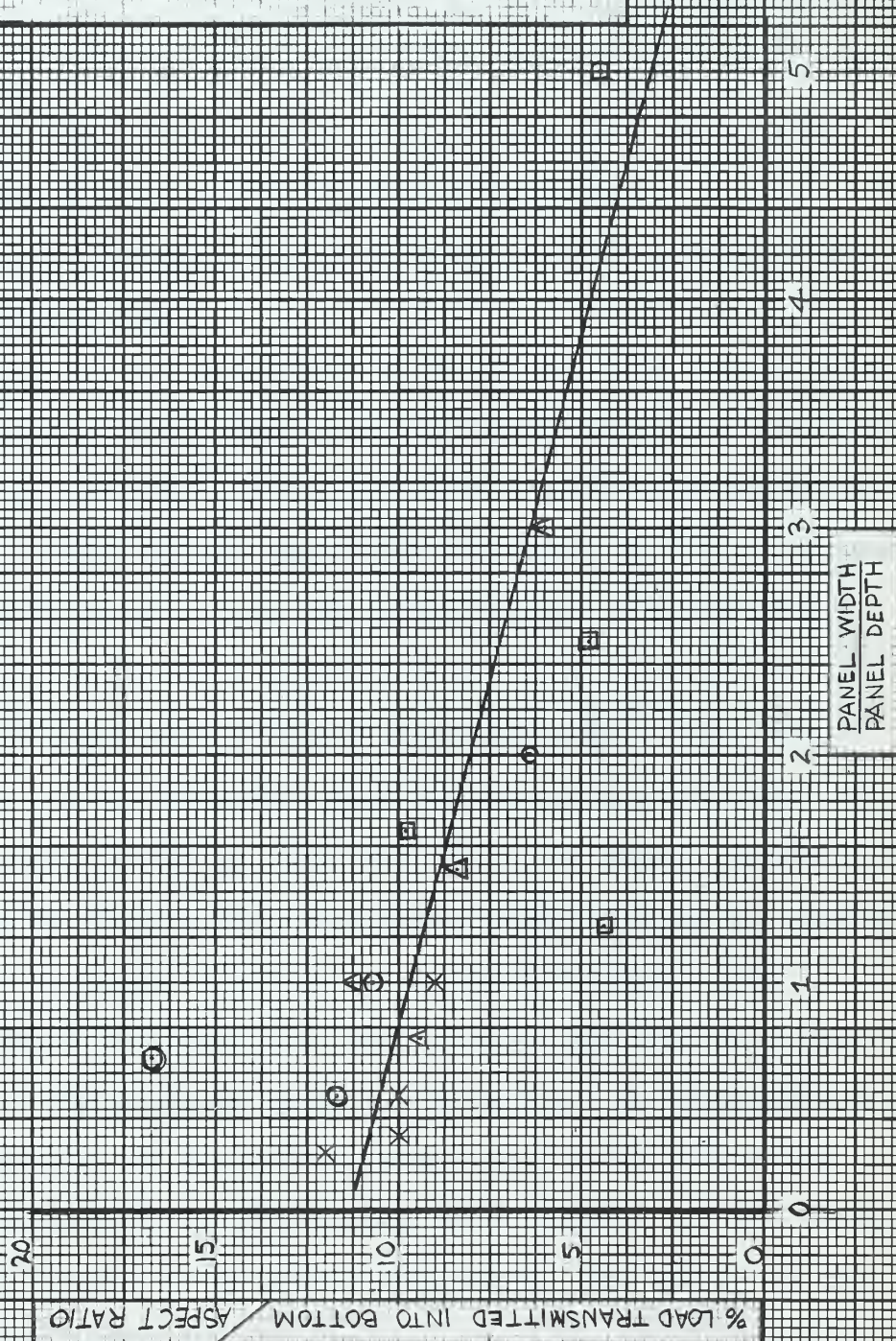


JJP
4-6-59

FIGURE XXIX

% LOAD TRANSMITTED INTO BOTTOM
ASPECT RATIO
VS
PANEL WIDTH
PANEL DEPTH
FOR UNIFORM LOAD

ASPECT RATIO
X 1:1 O 2:1 Δ 3:1 □ 5:1



JJP
4-6-59

IV DISCUSSION OF RESULTS

When using the curves presented in the Results, reference must be made to the error value which was determined by the method presented in the Procedure. The errors for all experimental cases are presented in Table I. Corrections have been made only to the uniform load cases with no bottom support. These shear distribution curves are marked "Corrected". All conclusions are based upon corrected data where such corrections were made.

A. Concentrated load cases - vertical shear stress distribution

1. Bottom unsupported

A study of the isoclinic patterns for the unstiffened and centerline stiffener cases indicate that the stiffener does not materially affect the direction of the principal stresses except in the immediate vicinity of the stiffener. This is a logical result since for cases of symmetrical loading the centerline stiffener is in a location of zero shear load (neglecting local shear effects). For this reason it may be expected that the shear distribution for the two cases would be similar. For the aspect ratio 5:1, referring to Figure III, the shear distribution is nearly parabolic in shape for the one stiffener case. The maximum point for both the unstiffened and one stiffener case occur at the same general location. As pointed out in the Details of Procedure, where the error occurring in the isoclinics is discussed, this portion of the curve is in the region of greatest accuracy. The shape of the unstiffened curve is not parabolic. However, Table I shows that the error found in this curve was -26.6%. If

the region of the curve near the maximum point is assumed to be more nearly correct, then the indication from the error found is that the rest of the curve should be fuller, or closer to a parabolic shape. Figure IV presents a comparison between the experimental and theoretical vertical shear distributions for the unstiffened case. The theoretical curves show a decrease in the maximum shear stress value with decrease in aspect ratio. There is also a lowering of the point of maximum shear stress with decrease in aspect ratio from 5:1 to 2:1. Although sufficient number of cases have not been investigated (and the accuracy of those investigated are in doubt), the experimental results appear to follow the same trends as the theoretical.

In the 5:1 case the general shape of the vertical shear distribution is parabolic. As aspect ratio decreases, the maximum shear point is lowered causing the curve to become less parabolic. It is felt that this is due primarily to the concentrated load effects since the theoretical results were developed taking this factor into account, and the experimental results are generally similar.

2. Bottom supported

The vertical shear stress distributions are more uniform over the depth of the plate than in the unsupported cases as shown in Figures VI and VII. They exhibit two distinct humps, with a definite tendency toward zero stress at the mid-depth in the 3:1 and 5:1 cases. The maximum value of shear stress is no greater

than one-half the corresponding value in the unsupported case. It is felt that the results are not complete or accurate enough to draw any quantitative or qualitative conclusions in regard to the effect of stiffeners or aspect ratio on the position of the humps or the tendency toward zero stress at mid-depth.

B. Concentrated load cases - Effect of aspect ratio and stiffening on bottom support

1. As expected, bottom support reduces the total side reaction. Referring to Figure VIII, the reduction in side reaction increases with increase in aspect ratio. The 3:1 unstiffened case with bottom support is apparently in error. The load transmitted into the bottom for this case should be nearly midway between 50% and 70% judging from the results of the 2:1, 5:1 and 3:1 stiffened cases. Whereas in other cases investigated the unstiffened and stiffened vertical shear distributions are similar, in the 3:1 case they are not (Figure II). It is believed that the amount of load distributed into the side in the lower half of the beam should be greater for the unstiffened case and less for the stiffened case. In view of the above mentioned reasons, the points for the 3:1 case were neglected in drawing the curve in Figure VIII. When these points are neglected it is interesting to note that the slope of the unstiffened line approximates that of the theoretical curve representing the concentrated load effects carried into the bottom of a semi-infinite plate.

The reason for the disparity between the theoretical and experimental curve may be explained by considering the fact that in the theoretical case the supported sides are not clamped against rotation (refer to theoretical derivation in Appendix B). This causes more load to be transmitted into the bottom support.

2. The addition of a centerline stiffener tends to reduce the part of the load taken by the bottom for aspect ratios 2:1 and 3:1, but has little effect for the 5:1 case. The conclusion arrived at in reference (4) (pg 11) appears to be in error. The statement is made that between the aspect ratios of 3:1 and 5:1 a limit is reached where in one case the stiffener tends to decrease the share of the load distributed into the bottom and in the other case tends to increase it. This is not a logical conclusion considering that for the 5:1 aspect ratio the difference in the load carried by the bottom in the two cases is only 2.3%, or about one-tenth the probable accuracy of the experimental results. Also, the share of the load taken by the bottom varies directly as the deflection that the plate would have if there were no bottom support. The stiffener increases the bending stiffness of the plate, reducing the deflection and increasing the side load. As the plate length increases, for the same depth and stiffener, this additional stiffness decreases ($K = EI/L$) and, therefore, the stiffener on the centerline should have decreasing affect with increasing aspect ratio.

3. Figure IX shows the effect of panel aspect ratio (panel width/panel depth) as well as plate aspect ratio on the percent load transmitted into the bottom. In drawing the curve for the unstiffened case, the 3:1 point was determined from Figure VIII. The significant features of the curves of equal stiffening in Figure IX are:
- a. The curves are of similar shape.
 - b. At a plate aspect ratio of 5:1 the effect of panel aspect ratio on the percent load transmitted into the bottom is negligible.

The curves of constant plate aspect ratio show the same tendency as indicated in item b above, and in addition they show that the effect of panel aspect ratio is more pronounced as plate aspect ratio decreases. While the curves shown in Figure IX are admittedly of limited value at present, due to lack of sufficient data, it is felt that as more information becomes available, the curves of constant aspect ratio would be very useful in design to predict the amount of load transmitted into the bottom.

Both figures VIII and IX point to the conclusion that in the concentrated load case the centerline stiffener did not act to transmit load to the bottom as a column. The indications are that this stiffener tended to stiffen the plate as a whole. This conclusion was reached from the fact that in all cases (except in the 5:1 case, where its effect was negligible) the stiffened plate transmitted less load into the bottom

of the plate (therefore, more into the sides). It must be borne in mind, however that the method of applying the load may have had some influence on the manner in which the stiffener acted to transmit the load.

References (4) and (5) explain that the load is applied to the model through a small aluminum bar having the same thickness as the model. Therefore, none of the load was applied directly to the stiffener.

C. Uniform load cases - Vertical shear stress distribution

1. Side Supported only, unstiffened (Figure XVIII)

For aspect ratio 5:1 the vertical shear stress distribution is generally parabolic, with the maximum vertical shear stress occurring at approximately the mid-depth of the plate. With decreasing aspect ratio (3:1 to 1:1) the deviation from a parabolic shape increases, and the location of the point of maximum shear stress intensity moves away from the mid-depth toward the loaded edge.

2. Effect of bottom support

The addition of a rigid bottom support decreases the value of maximum vertical shear stress and the total shear along the clamped side. This effect decreases with decreasing aspect ratio and becomes negligible in the 1:1 case.

3. Effect of stiffeners

The addition of stiffeners show no consistent effect in regard to the variation in vertical shear distribution with aspect ratio. In the 1:1 case the

stiffeners have little effect in both the bottom supported and unsupported conditions.

D. Uniform load cases - Location and magnitude of maximum vertical shear stress (Figure XXVI)

1. The magnitude of maximum vertical shear stress increases with decreasing aspect ratio. It should be pointed out that this conclusion is in opposition to that arrived at by Norman and Gutierrez (ref. 2, pg 17). The reason for this disagreement is that whereas in reference (2) the conclusions were based on the uncorrected data of Figure XXX, the conclusions presented here were based on the corrected data of Figure XXXI. The addition of bottom support results in a decrease in the magnitude of the maximum vertical shear stress value. This effect increases with increasing aspect ratio. While the curves obtained by the method of least squares show an appreciable difference between the magnitude of maximum shear in the 1:1 case, there is actually little difference between the supported and unsupported conditions in the experimental results (Figures XXXI and XXXIII).
2. The location of maximum vertical shear stress tends to rise toward the top of the plate as aspect ratio decreases. The curves obtained by the method of least squares have the same slope for both the supported and unsupported conditions. Once again, however, the actual experimental results show little difference in this point for the 1:1 case (Figures XXXII and XXXIV).

E. Uniform load cases - Reduction in maximum vertical shear stress due to bottom support (Figure XXVII).

1. An attempt was made to check Figure XIII of reference (3), which plots the percent reduction in maximum vertical shear stress for the stiffened and unstiffened cases as a function of aspect ratio. A linear variation was obtained for the unstiffened cases, however, the stiffened cases would not plot as either a single curve or as individual curves for each degree of stiffening. It was possible to obtain some correlation of the data by plotting it as shown in Figure XXVII. In this instance, the 2:1, 3:1 and 5:1 aspect ratios plot fairly well along a single curve whereas the 1:1 cases plot separately along a straight line. It is felt that the difference between these two curves is due to the fact that the bending effects are much less for the 1:1 aspect ratio.

F. Uniform load cases - Percent load transmitted into the bottom (Table I)

1. The number of stiffeners have very little effect on the percent load transmitted into the bottom for aspect ratio 1:1. For aspect ratio 5:1 there is little difference in the load transmitted into the bottom for the unstiffened, one, and three stiffener cases. For the aspect ratios 2:1 and 3:1 the one and three stiffener combinations cause an increase in the load transmitted into the bottom.
2. The two stiffener combination has the greatest effect in reducing vertical side shear and in transmitting load into the bottom (Figure XXVIII). This effect increases

with aspect ratio over the range investigated. The cause for this appears to be connected with the lack of a centerline stiffener. Since the variation of shear stress across the center panel is small, it is believed that the center panel may deflect as a unit as shown in Figure c below. This might result in better contact along the bottom and therefore greater transmission of the load. If the cases with centerline stiffeners deflect in a manner shown in Figures a and b, the extent of bottom contact would be less, perhaps explaining the reduction in load transmitted. It seems logical that as the number of stiffeners increase, the effect of a centerline stiffener would become increasingly less. In the limit, as the number of stiffeners increase, the condition of a homogeneous, unstiffened plate is approached. An indication of this is that the three stiffener combination more closely approaches the unstiffened condition than the two stiffener combination.

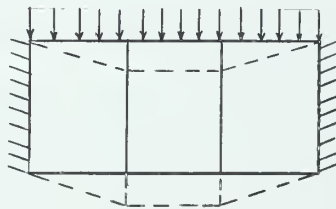


Figure c

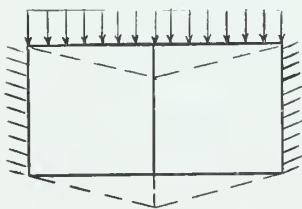


Figure a

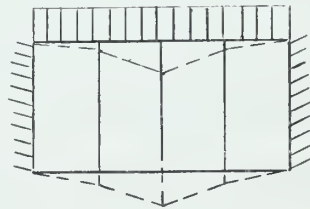


Figure b

3. Since the addition of stiffeners in general increases the load transmitted into the bottom they act as columns.
4. The validity of the experimental results pertaining to the load transmitted into the bottom are open to question because:
 - a. The actual loads transmitted into the bottom were not measured experimentally, but determined as the difference between the load applied and twice the integral of the vertical shear stress distribution across one side. As mentioned in the Details of Procedure, this method includes several experimental errors. These errors for the unsupported, uncorrected cases were $\pm 15\%$.
 - b. The distribution of the load transmitted into the bottom should be known before the results can be interpreted properly. The actual effect of stiffeners, with or without a centerline stiffener is not known. Knowledge of the distribution of the load across the bottom would also shed some light on the belief that the stiffeners act as columns.
5. The curves in Figure XXVIII all approach a peak value indicating that for a given number of stiffeners there is an optimum panel aspect ratio which will cause the maximum amount of load to be transmitted into the bottom.
6. Figure XXIX presents the percent load transmitted into the bottom as a function of plate aspect ratio and panel aspect ratio. The straight line shown was arrived at by the method of least squares. It should be pointed out that there may be some inconsistency in using panel aspect

ratio (panel width/panel depth) as a basis of comparison. For the unstiffened condition the panel width refers to the distance between the clamped supports. For the stiffened cases, it may be the distance between stiffeners, or between stiffeners and supports. In each of these cases the panel end conditions will be different and therefore the effect of the panel width on the transmission of load into the bottom will differ. Whether or not this difference is appreciable is unknown.

V CONCLUSIONS

A. Concentrated load

1. For the bottom unsupported case, the vertical shear distribution curve becomes less parabolic in shape as aspect ratio decreases.
2. For the bottom supported case, the vertical shear distribution is more uniform than in the unsupported case and exhibits two distinct humps with a tendency toward zero stress at the mid-depth of the beam.
3. Bottom support reduces the total side reaction. The reduction increases with increase in aspect ratio.
4. The addition of a centerline stiffener tends to reduce the part of the load taken by the bottom. This tendency decreases with aspect ratio.
5. The centerline stiffener increases the bending stiffness of the beam and does not act as a column to transmit load into the bottom support.

B. Uniform load

1. With decreasing aspect ratio the deviation from a parabolic vertical shear distribution increases, and the location of the point of maximum vertical shear stress intensity moves away from the mid-depth of the plate toward the loaded edge.
2. The addition of a rigid bottom support decreases the value of maximum vertical shear stress and the total shear along the clamped side. This effect decreases with decreasing aspect ratio and becomes negligible in the 1:1 case.



3. The addition of stiffeners show no consistent effect in regard to the variation of vertical shear distribution with aspect ratio. In the 1:1 case the stiffeners have little effect in both the bottom supported and unsupported conditions.
4. In both the unsupported and supported cases the magnitude of maximum vertical shear stress increases with decreasing aspect ratio. The addition of bottom support decreases the magnitude of maximum vertical shear stress and this effect increases with increasing aspect ratio.
5. The location of maximum vertical shear stress tends to rise toward the top of the plate as aspect ratio decreases. The maximum points for the supported cases are higher than the unsupported cases.
6. For the unstiffened cases, the percent load transmitted into the bottom increases with increasing aspect ratio.
7. The addition of stiffeners in general increases the load transmitted into the bottom. The stiffeners tend to act as columns in transmitting load into the bottom.
8. The two stiffener combination has the greatest effect in reducing side shear. This effect increases with increasing aspect ratio.
9. The validity of the experimental results pertaining to the load transmitted into the bottom are open to question.
10. It appears that the load transmitted into the bottom support is a function of both plate aspect ratio and panel aspect ratio.
11. There is an indication that for a given number of stiffeners there is an optimum panel aspect ratio which

will cause the maximum amount of load to be transmitted into the bottom.

VI RECOMMENDATIONS

1. Any further experimental work should be confined to the uniform load case as this is more representative of the true loading conditions on an actual ship bulkhead.
2. For the bottom supported cases it is necessary to spot-check the accuracy of previous experimental results since the load transmitted into the bottom was not measured. It is also necessary to determine the distribution of the load transmitted into the bottom in order to properly analyze the column effect of the stiffeners. This may be accomplished by:
 - a. Measure the load transmitted into the bottom by using a load cell, strain gages, or photoelasticity methods.
 - b. Qualitatively determine the stress distribution along the bottom using stresscoat or photoelasticity techniques.
3. It would be desirable to test models having a greater number of stiffeners (4, 5, and perhaps 6 stiffener cases.) This will eliminate the significance of the centerline stiffener on the experimental results and, therefore, more closely approach actual bulkhead conditions.
4. Consideration should be given to the investigation of a model having an aspect ratio of 4:1 in order to more clearly determine the effect of stiffeners. Apparently there is some reduction in the influence of stiffeners between the 3:1 and 5:1 cases.
5. The fact that load corrections had to be made to the experimental results points out the necessity for using a more accurate loading device.

6. Further investigation should be conducted into the possibility of arriving at an analytical solution for the stress distribution. A modification of McHenry's method (ref. 12) in conjunction with the 704 computer seems to be most promising in this respect.
7. A determination of the actual conditions of side and bottom support existing on a ship bulkhead must be made before the results of experimental investigations can be applied with any confidence.

VII APPENDICES

APPENDIX A

SUPPLEMENTARY INTRODUCTION

In the preparation of this paper the survey of available literature failed to yield any material related specifically to the problem of shear distribution along the edges of a deep beam. In instances where studies have been made, the boundary conditions differed from those existing in the transverse bulkhead of a ship. In spite of this, it is felt that the presentation of information, even remotely related to the present problem, will contribute to the understanding of the factors involved. If for no other reason, the technique and general approach used in the cases investigated, should be of interest. With this purpose in mind the following summary of the more pertinent literature is presented.

1. Two-dimensional Elasticity Solutions

a. Polynomial Stress Functions

If a load is continuously distributed along the length of a rectangular beam of narrow cross-section, a stress function in the form of a polynomial, may be used to represent the boundary forces in certain simple cases. Solutions can be obtained which satisfy all the equations of elasticity, but the solutions are exact only if the surface forces are distributed in the manner given. For example, in the case of a beam which is either completely or partially fixed at the ends (Figure a) a solution can be obtained by the proper superposition of elementary solutions for pure bending, pure shear and a uniform

lateral loading. For pure bending the bending

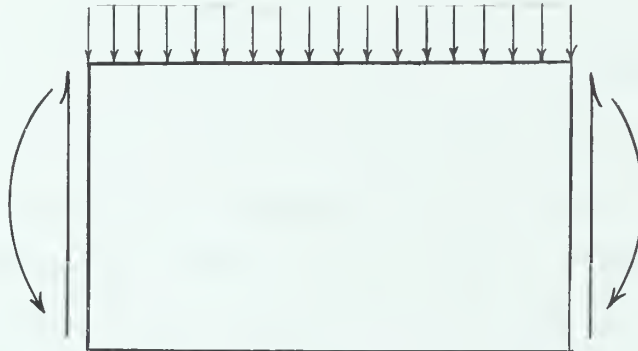


Figure a

moment is produced by tensions and compressions at the ends, proportional to the distance from the neutral axis. The fastening of the end must not interfere with the distortion of the plane end, otherwise the bending moment will be applied in a different manner or the constraint will impose other forces on the end section. If this happens the final solution, which includes the supposition of pure bending, is no longer exact. Similarly, the shear at the side boundaries must be distributed in some known manner, for example, uniformly or parabolically.

Application of the specialized solution obtained in the preceding manner may be extended to many practical problems by utilizing the Principle of Saint-Venant, which states that "if the forces acting on a small portion of the surface of an elastic body are replaced by another statically

equivalent system of forces acting on the same portion of the surface, this redistribution of loading produces substantial changes in the stresses locally but has negligible effect on stresses at distances which are large in comparison with the linear dimensions of the surface on which the forces are changed." (ref. 8, pg. 33). In short, deep beams, because the dimensions of depth and span are of nearly equal magnitude, there is no region which satisfies Saint-Venant's requirement for "distances which are large in comparison with linear dimensions". Therefore, as applied to short, deep beams this procedure has the same limitations as the elementary beam theory. (For solutions of the above type, see ref. 8, pages 29-45).

b. Trigonometric Stress Functions

A stress function in the form of a trigonometric series may be used to represent a discontinuous type of loading. Timoshenko and Goodier (ref. 8, pg. 46) develop a solution for the beam illustrated in Figure b by using a trigonometric series that satisfies the conditions on the two discontinuously loaded sides. This solution may be applied to a beam whose depth is small in comparison with its length because it does not consider the conditions over the short ends of the beam.

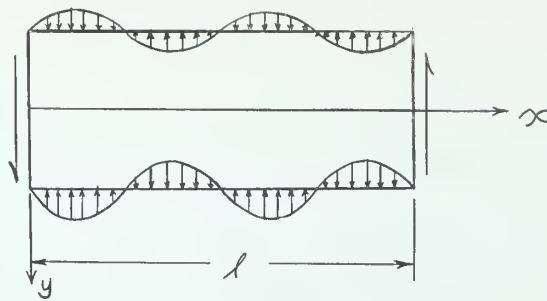


Figure b

c. Hyperbolic Stress Functions

Dischinger has solved a great number of cases for a deep beam with infinite span under periodic loading by means of a stress function in the form of an infinite series of hyperbolic functions. The results of his mathematical analysis have been presented in the form of bending stress curves by the Portland Cement Association (ref. 9). One conclusion of his work, which has subsequently been verified by independent solutions, is that beams of infinite length, with a depth greater than their span, have stress distributions similar to those obtained in simply supported beams of depth equal to span (ref. 10, pg. 163).

d. Other Methods

Conway, Chew, and Morgan, (ref. 10) have presented a method of analyzing the stress distribution in a simply supported deep beam of finite length by superimposing two stress functions. The first stress function is a Fourier series for the continuous beam, which satisfies all but one boundary condition; that of zero normal stress on the free ends of the beam. To neutralize these

stress components a second stress function is obtained by strain-energy methods giving the same stress distribution on the free ends as that which is left by the first stress function. Then, by superimposing the two solutions all the boundary conditions are satisfied.

Archer and Kitchen (ref. 11) have obtained solutions for simply supported beams by a direct strain energy method which does not depend upon the solution of a continuous beam. An interesting feature of their method is that the expressions derived for (σ_x) and (τ_{xy}) appear in two parts. The first part is equivalent to the expressions derived from elementary beam theory, while the second part represents the corrections to be made to the elementary beam theory stresses.

The general failing of all these procedures as applied to the present problem is that the boundary conditions must be completely defined over the edges of the beam. This is not possible in the case of a transverse bulkhead of a ship, nor is it possible for the photoelastic representation of the bulkhead used in the experimental studies. The stress distribution across the ends, which is required in these elasticity solutions, is in fact the very information sought.

2. Approximate Solutions

It has been pointed out that an exact solution to the equations developed from elasticity theory has not been

possible due to the difficulty in finding the correct stress function which satisfies the boundary conditions. However, there have been a number of methods proposed which approximate the true solution. Of those investigated, the method developed by McHenry (ref. 12) appears to be most promising. McHenry uses a two dimensional lattice analogy for the approximate solution of the stress problem. The concept of the lattice analogy is that of replacing the plate prototype (representing the bulk-head) with a pin-connected lattice having the same boundary conditions, loading, and deformations as the plate. The bar strains produced by the load deformations must be such that they satisfy the equations of equilibrium and compatibility.

The load is applied to the lattice network and the resulting deflections are allowed to occur. The condition of clamped edges in the prototype is equivalent to zero horizontal and vertical displacements in the lattice. The second order partial differential equations are approximated by second finite differences. In this manner the resulting displacements and boundary forces may be computed either by a relaxation method or by solving a large number of simultaneous linear equations. Further discussion of this method, examples of its use, and degree of accuracy achieved may be found in reference (13).

3. Related Experimental Solutions

Takeda and Suatengo (ref. 14) evaluated the elastic behavior of simply supported structural I-beams of spans

from two to four times the depth, under various load conditions. They present graphs of the stress distribution at mid-span and one-third points with variation of applied load. The relation of applied load to observed deflection and the trajectories of the principal stresses are also shown. The conclusions arrived at as a result of this study are:

- a. Stresses vary linearly with load and superposition is valid up to the proportional limit.
- b. The elementary beam theory gives an erroneous indication of the stress distribution in short, deep beams. The Stoke's Formula (ref. 15) modified for I-beam sections adequately represents the section at the load point for a short, centrally loaded beam with a concentrated load.
- c. Deflections vary linearly with load.
Deflections computed by elementary beam theory are 51-58% of the corrected deflection for loading at mid-span and 32-45% of the corrected deflection for loading at the one-third points.

P. H. Kaar (ref. 1) investigated the non-linear stress situation in tests conducted on centrally loaded, simply supported deep beams. Plots of the centerline stresses (σ_x and σ_y) for various aspect ratios are shown. The effect of normal forces, of little significance in beams of normal dimensions, is clearly indicated by non-linear stress behavior showing considerable σ_x tension above, and compression below, the beam mid-depth.

Some other conclusions arrived at in this paper are:

- a. The σ_x stresses (horizontal) in beams of height-to-span ratios 2.00, 2.33, 2.67 and 3.00 show little effect of depth change. Apparently, after a certain height is reached in a deep beam (height-to-span of approximately 2.00), for a given loading, the σ_x stresses are so dependent upon the normal forces that the effects of increases in beam height on the σ_x pattern are negligible.
- b. The horizontal compressive stress near a beam support will substantially reduce the tensile stresses at the bottom mid-span region, if the span is small.
- c. The stresses in centrally loaded, simply supported, deep beams computed by ordinary flexure formulas are seriously in error for height-to-span ratios above 0.67.

As further studies are made and sufficient information becomes available so that present design procedures may be evaluated more intelligently, a thesis written by R. N. Crawford and J. R. Wales (ref. 16) should prove useful. In this paper a summary of design procedures used for structural design of naval vessels is presented.

APPENDIX B

DETAILS OF PROCEDURE

CORRECTIONS TO UNIFORM LOAD DATA

The Procedure describes the method used to determine an error value for the experimentally determined side shear distributions of the bottom unsupported cases. The error may be the result of any one or combination of five items:

(1) Error in calculation of τ_{xy}

The values of τ_{xy} presented in the original theses were used without recalculation. An error of the type that effects all the results for one model condition would become obvious when the area under the (τ_{xy}/τ_m) curve was compared with $(\tau_{xy}/\tau_m \approx 1.0)$. Any important isolated error would be obvious from an unfairness in the generally fair shear distribution curves. Nothing was discovered during the analysis to suggest any error in the calculation of τ_{xy} .

(2) Unsymmetrical loading

The shear distributions were determined for one edge of the plate only. If the load was not applied symmetrically the distribution over one side will not represent one-half of the load. This error is considered negligible as the photographed isochromatic patterns are all approximately symmetrical about the model centerlines.

(3) Condition of side support

The actual condition of clamping over the side supports is one of the more important experimental unknowns. Through the application of the experience of previous theses and the development of modified procedures

it is believed that references (2) and (3) have approached the condition of uniform clamping. Isolated instances of extreme non-uniformity in edge clamping should be apparent as discontinuities in the shear distribution curves.

(4) Error in determination of isoclinics

All the investigators agree that the most inaccurate part of the experiments was the determination of the isoclinic patterns. In many cases the patterns at the clamped edges were barely distinct. Generally an error of $\pm 5\%$ has been given for the accuracy of measurement of the principal stress angle at the boundary.

From the two-dimensional photoelasticity procedure the vertical shear stress is determined by;

$$\tau_{xy} = \frac{Fh}{2h} \sin 2\theta \quad (3)$$

In the region where the direction of the principal stress (θ) is between $40^\circ - 50^\circ$ a 5° error will cause a maximum error in τ_{xy} of 4%. As points along the boundary become more removed from this region the accuracy of the shear stress intensity decreases. At $\theta = 15^\circ$ a 5° error will result in a 30% error in τ_{xy} . All but two points of maximum τ_{xy} lie in the $40^\circ - 50^\circ$ region. The exceptions lie within a $\pm 5^\circ$ range of this region. Therefore, the points of maximum τ_{xy} are considered to be the most accurately determined values of vertical shear stress.

(5) Error in magnitude of applied load

References (2) and (3) both experienced difficulties with the uniform loading device. In reference (3), the investigators could not accurately measure the pressure

applied because there was a pressure gage installed on only one side of the model. There were also tendencies for the pressure to vary during the tests as a result of leakage and for the pressure tube to seal itself off. These factors led the authors to remark, on page 16, that, "there was doubt at times as to the exact pressure in the tube". There was, therefore, doubt as to the exact load applied. Page 31 of the same reference notes that while some tests were conducted at a pressure of 500 psi the uniform loading device could only be calibrated up to 350 psi. The calibration curve followed a straight line variation of load with pressure and was extrapolated linearly to 500 psi.

The investigators of reference (2) installed pressure gages on both sides of the model. A check valve between the model and the gage at the pump prevented a drop in pressure at the model from being readily observable. Also, as indicated on page 46, the uniform loading device was calibrated to 400 psi and it was necessary to extrapolate the calibration curve to 500 psi at which pressure some tests were conducted. The investigators reported no sealing off of the pressure tube and apparently had little trouble with leakage. The fact that they obtained better operation of the uniform loading device is the probable reason for their greater experimental accuracy. (See Table I).

Since the values of maximum τ_{xy} are considered to be the most accurate experimental values they were investigated as to the effect of aspect ratio and degree of

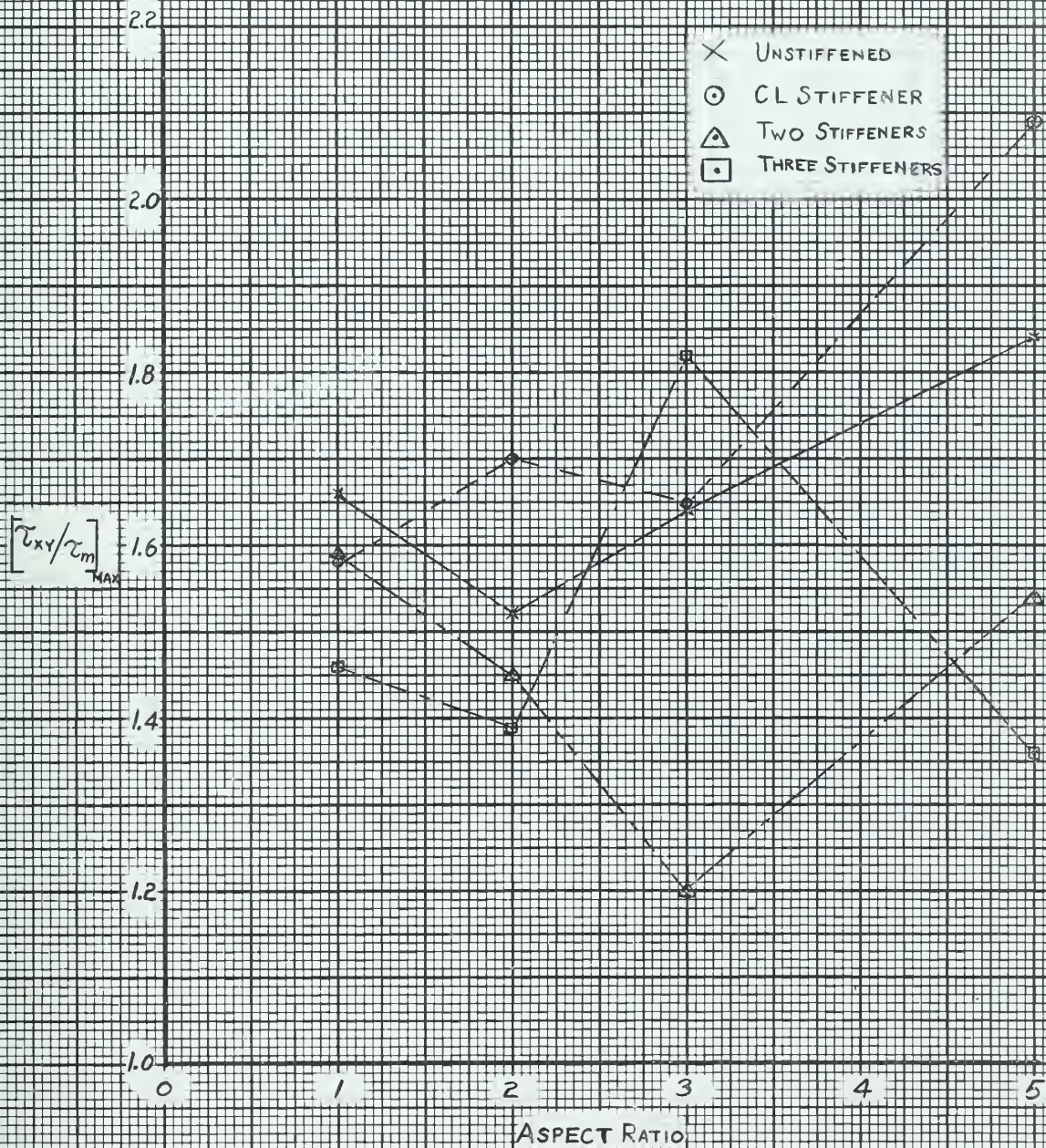
stiffening. The location and magnitude of the maximum τ_{xy} are presented in a non-dimensional form in Figures XXX - XXXIV. For the bottom unsupported case the shear magnitudes plot in an erratic pattern (Figure XXX) which indicates both an increase and decrease of the maximum τ_{xy} with decrease in aspect ratio, depending upon which stiffener line is followed. If the error is not in the value of maximum τ_{xy} then it must be in the value of τ_m . (i.e. in the magnitude of the applied load). Corrections were made to each bottom unsupported case where the experimental error was $\pm 5\%$ and where the shear distribution curve was not irregular over some region of the edge, by assuming that the experimental error was actually an error in the magnitude of the applied load. Table I summarizes the experimental and corrected errors obtained from the data presented in Appendix C. Figure XXXI presents the corrected magnitudes of maximum τ_{xy} for the unsupported cases. The corrected results are more uniform and generally indicate a small increase in the maximum shear magnitude with decrease in aspect ratio.

No correction was made to the 5:1 unstiffened case because the experimental error was only - 1.0%. It would be expected that this case because of its high aspect ratio and freedom from stiffening should approach the parabolic shape of elementary beam theory with a maximum value of 1.5. Actually as illustrated in Figure XVI it is further from the elementary beam condition than are the stiffened cases. The curve should

FIGURE XXX

$\left[\tau_{xy} / \tau_m \right]_{\text{MAX.}}$ vs. ASPECT RATIO

FOR CONDITION OF SIDE SUPPORT ONLY (UNCORRECTED)

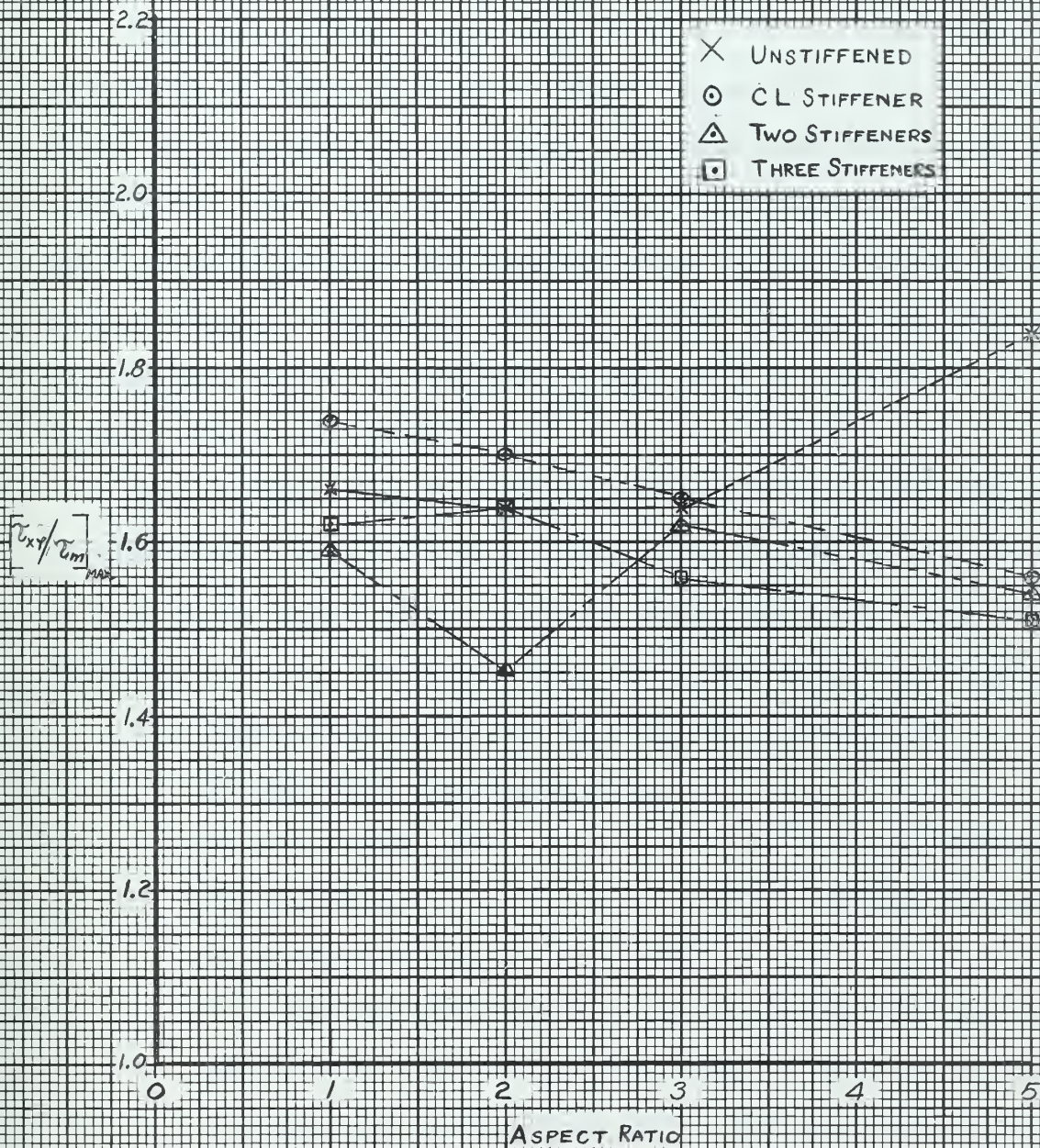


V.J.A.
4/20/58

FIGURE XXX

$\left[\frac{\tau_{xy}}{\tau_m} \right]_{\text{MAX.}}$ vs. ASPECT RATIO

FOR CONDITION OF SIDE SUPPORT ONLY (CORRECTED)



V.J.A.
4/20/59

probably be fuller over the upper portion of the plate. This would increase the area under the (τ_{xy}/τ_m) curve and require a correction to τ_m which would reduce the maximum value of (τ_{xy}/τ_m) . Since this case was believed in error and was not corrected it was neglected in determining the results of Figure XXVI.

The corrections applied to the bottom unsupported cases could not be applied to the bottom supported cases because there is no assurance that the same load was applied in both instances. The results for the bottom supported cases are more uniform (Figure XXXIII) and display the same trend as the bottom unsupported cases. The corrections have no effect on the locations of the maximum values of τ_{xy} presented in Figures XXXII and XXXIV.

Corrections cannot be made without observing their effect on the shear distribution curves. The following are examples of the three types of corrections made and their effects. All experimental and corrected data are presented in Appendix C.

- (1) Example of a faired correction. (Refer to Figure XXXV and Table XXI).

Aspect Ratio 3:1

Uniform Load

Unstiffened

Bottom Unsupported

Experimental Error = + 19.5%

The original data displays a hump in the lower portion of the curve. The hump is in the region where the angle θ varies from 20° ~ 40° and therefore a region of less accuracy than the point of maximum τ_{xy} . The

FIGURE XXXII

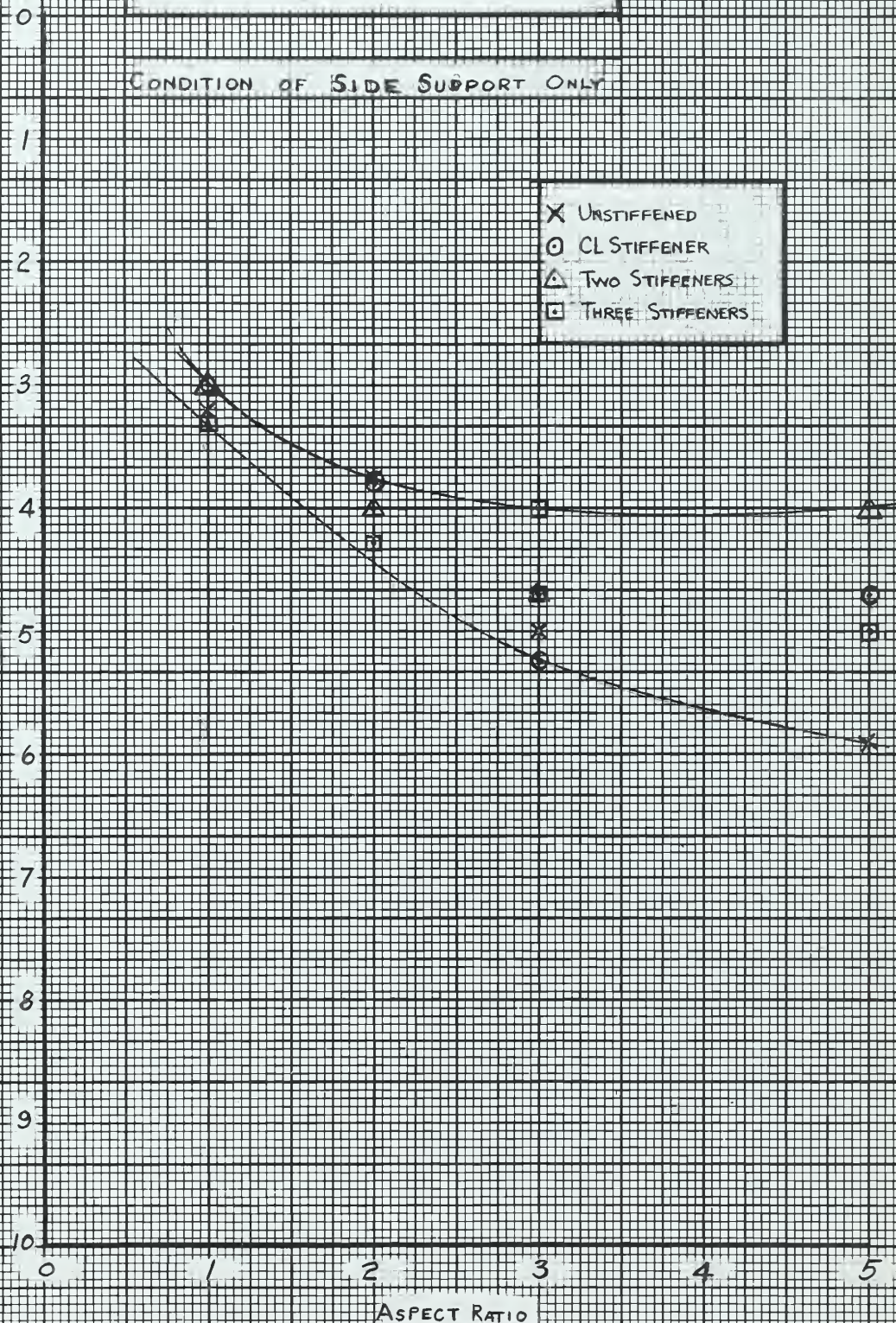
LOCATION OF MAX. SHEAR VS. ASPECT RATIO

TOP

CONDITION OF SIDE SUPPORT ONLY

- X UNSTIFFENED
- CL STIFFENER
- △ TWO STIFFENERS
- THREE STIFFENERS

$(10y/b)$ MAX. SHEAR POINT



JJP

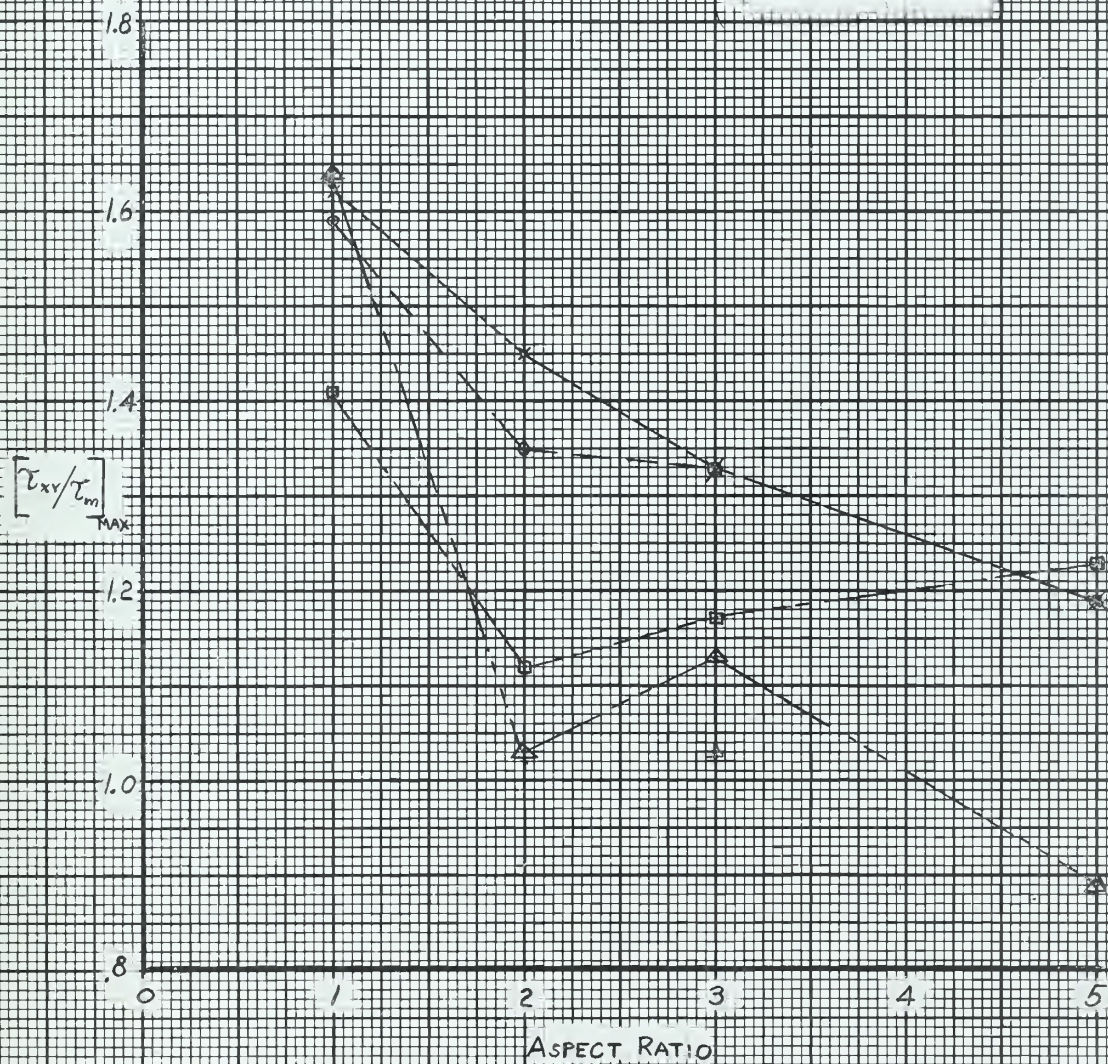
4-17-59

FIGURE XXXIII

$\left[\frac{\tau_{xy}}{\tau_m} \right]_{\text{MAX.}}$ vs. ASPECT RATIO

FOR CONDITION OF SIDE AND BOTTOM SUPPORT

- X UNSTIFFENED
- CL STIFFENER
- △ TWO STIFFENERS
- THREE STIFFENERS



V.J.A
4/20/59

FIGURE XXXIV

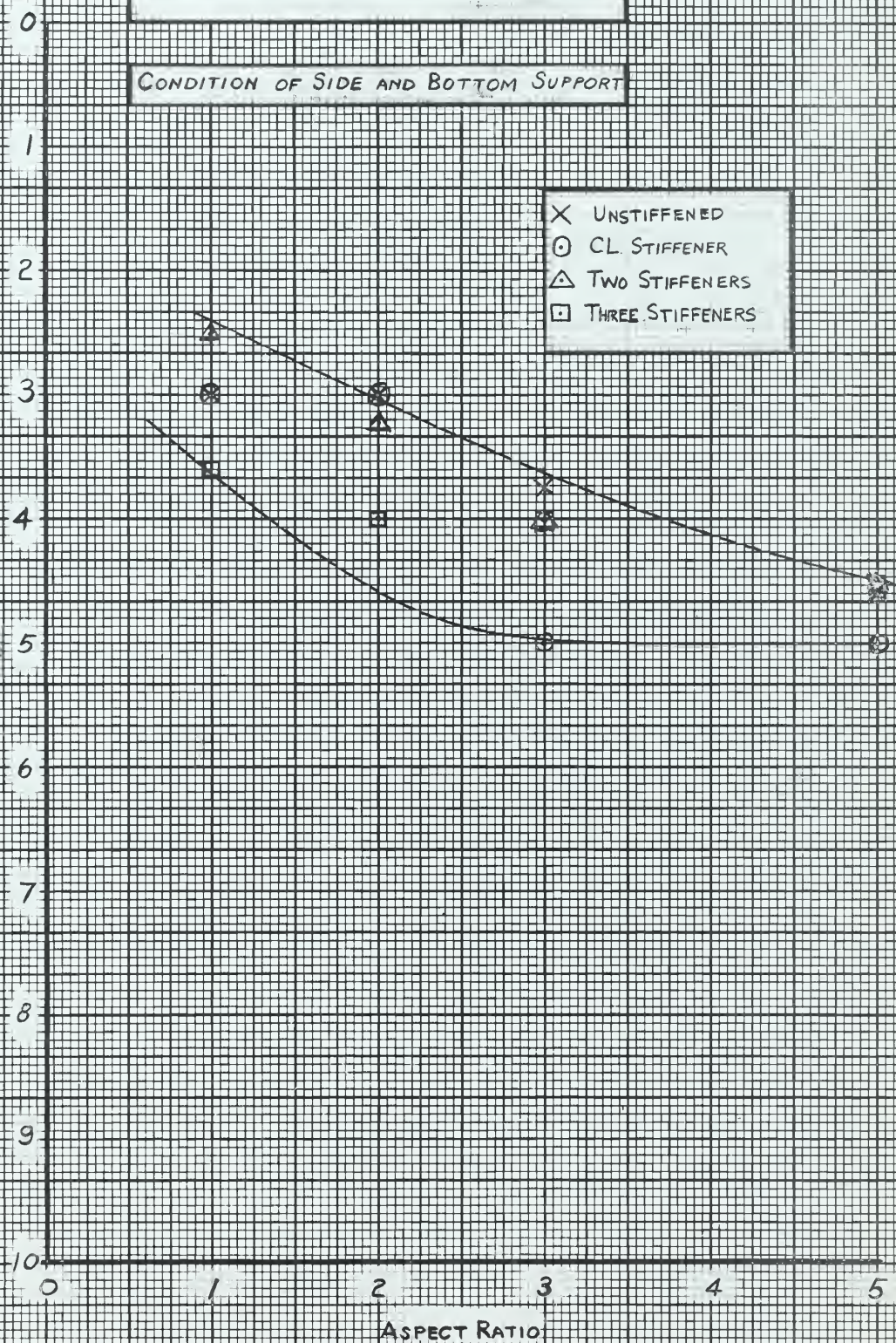
LOCATION OF MAX. SHEAR VS. ASPECT RATIO

CONDITION OF SIDE AND BOTTOM SUPPORT

TOP

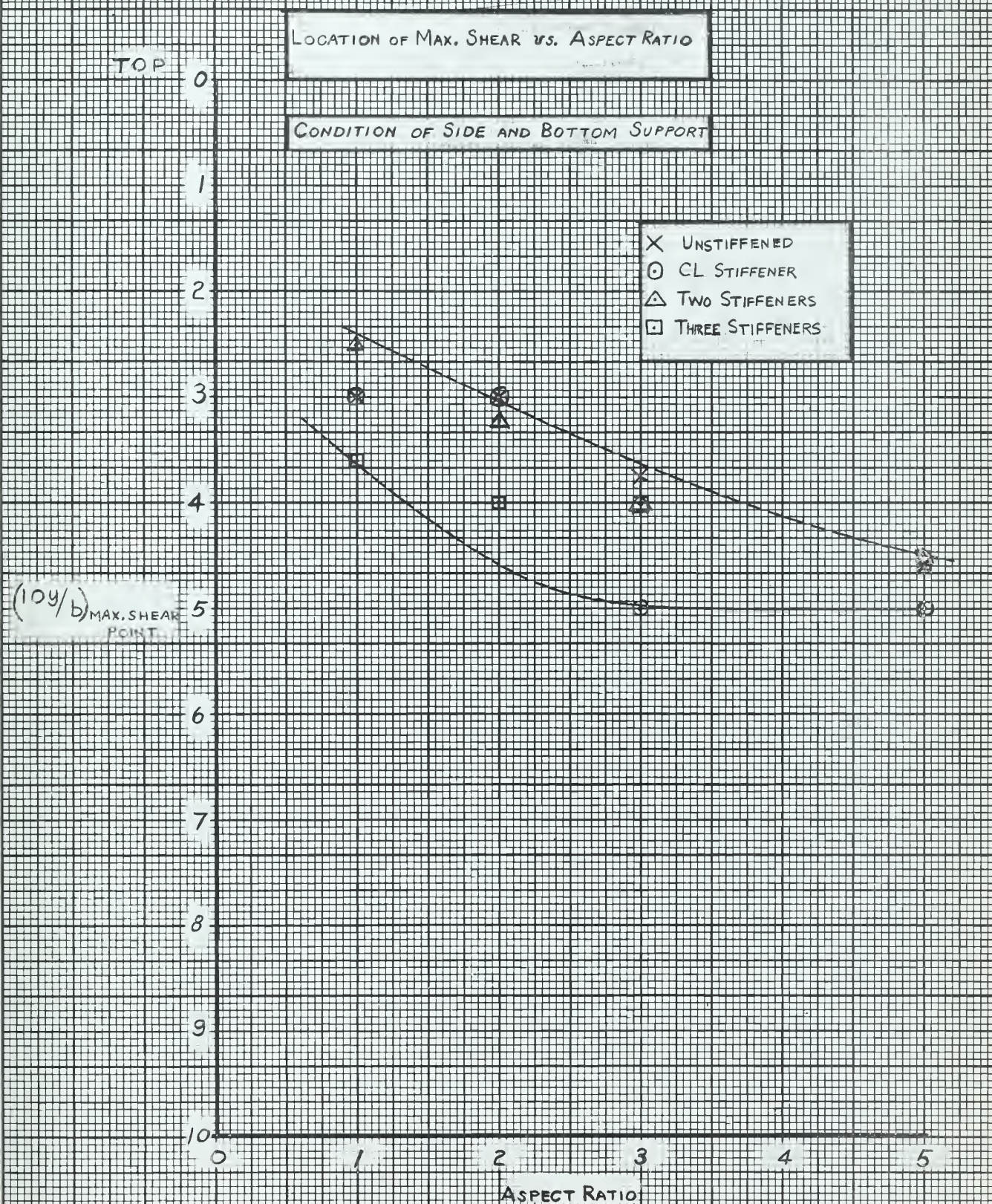
- X UNSTIFFENED
- CL. STIFFENER
- △ TWO STIFFENERS
- THREE STIFFENERS

$(10y/b)$ MAX. SHEAR
POINT



JJP
4-17-59

FIGURE XXXIV

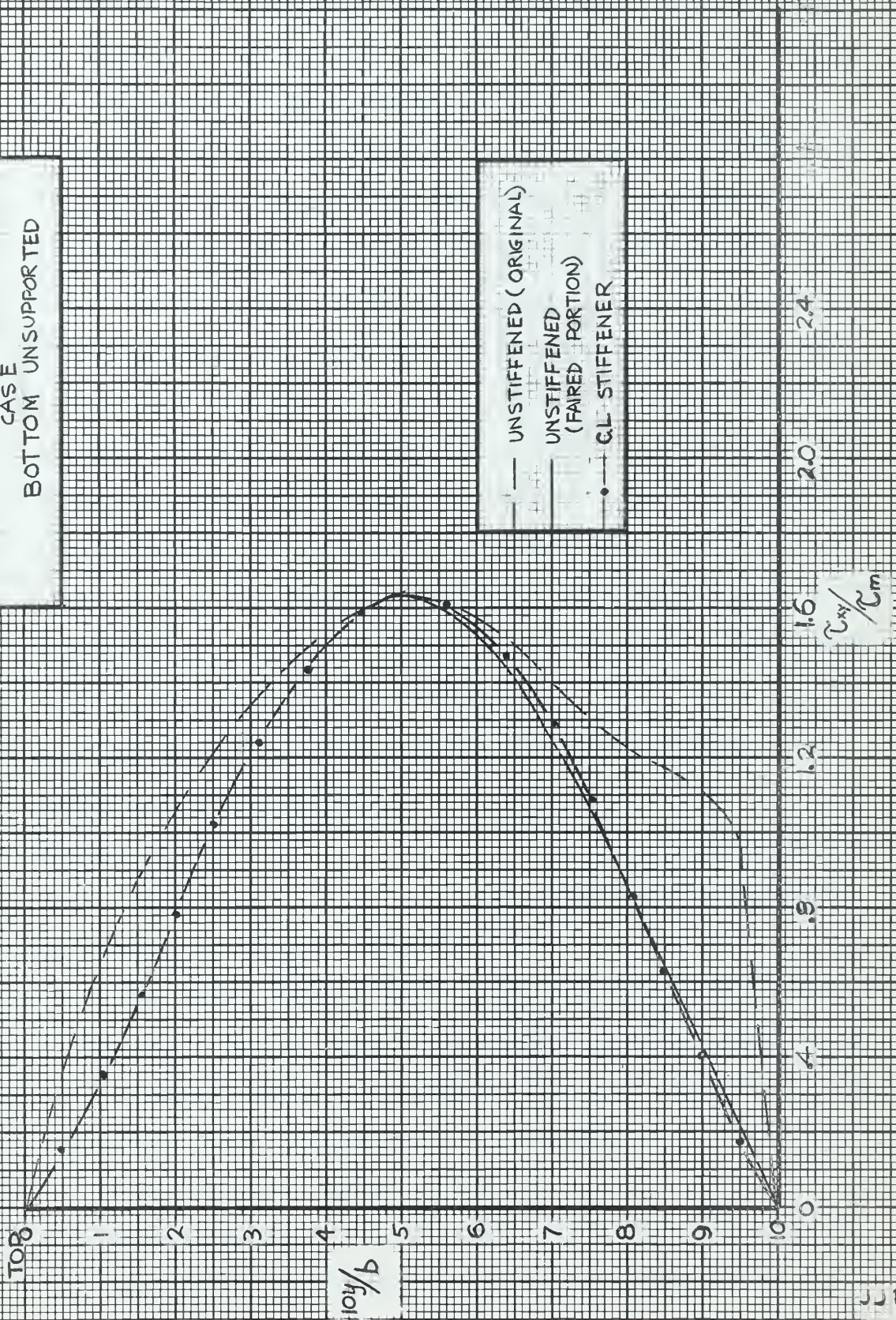


JJP
4-17-59

FIGURE XXXV

AR 3:1 UNIFORM LOAD
FAIRED CORRECTION TO UNSTIFFENED
CASE
BOTTOM UNSUPPORTED

— UNSTIFFENED (ORIGINAL)
— UNSTIFFENED
(FAIRED PORTION)
••• CL STIFFENER



JJP
4-17-59

curve for the case of a centerline stiffener approaches a parabolic distribution and has an experimental error of -1.9%.

The results of references (2, 3, 4, 5, 6) all indicate that for the plates examined the addition of a centerline stiffener does not materially affect the direction of the principal stresses except in the immediate vicinity of the stiffener. This is to be expected since for the case of symmetrical loading the centerline stiffener is in a location of zero shear force except for local shear effects. Thus assuming that the unstiffened and centerline stiffener shear distribution curves should be similar, as in fact they are over the upper 60% of the beam, a faired correction is made to the unstiffened curve in the region of the hump. The error of the faired curve is - 3.0%.

(2) Example of a load correction. (Refer to Figure XXXVI and Table XXIII).

Aspect Ratio 3:1

Uniform Load

Two Stiffeners

Bottom Unsupported

Experimental Error = -25.8%

The shear distribution curve is smooth and approaches a parabolic shape, therefore the error is assumed to be in the magnitude of the applied load. A corrected τ_m , known as τ_{mc} , is computed as follows:

$$\tau_{mc} = \tau_m (1 - \text{Error}) = 732 (1 - .258) = 542 \text{ psi}$$

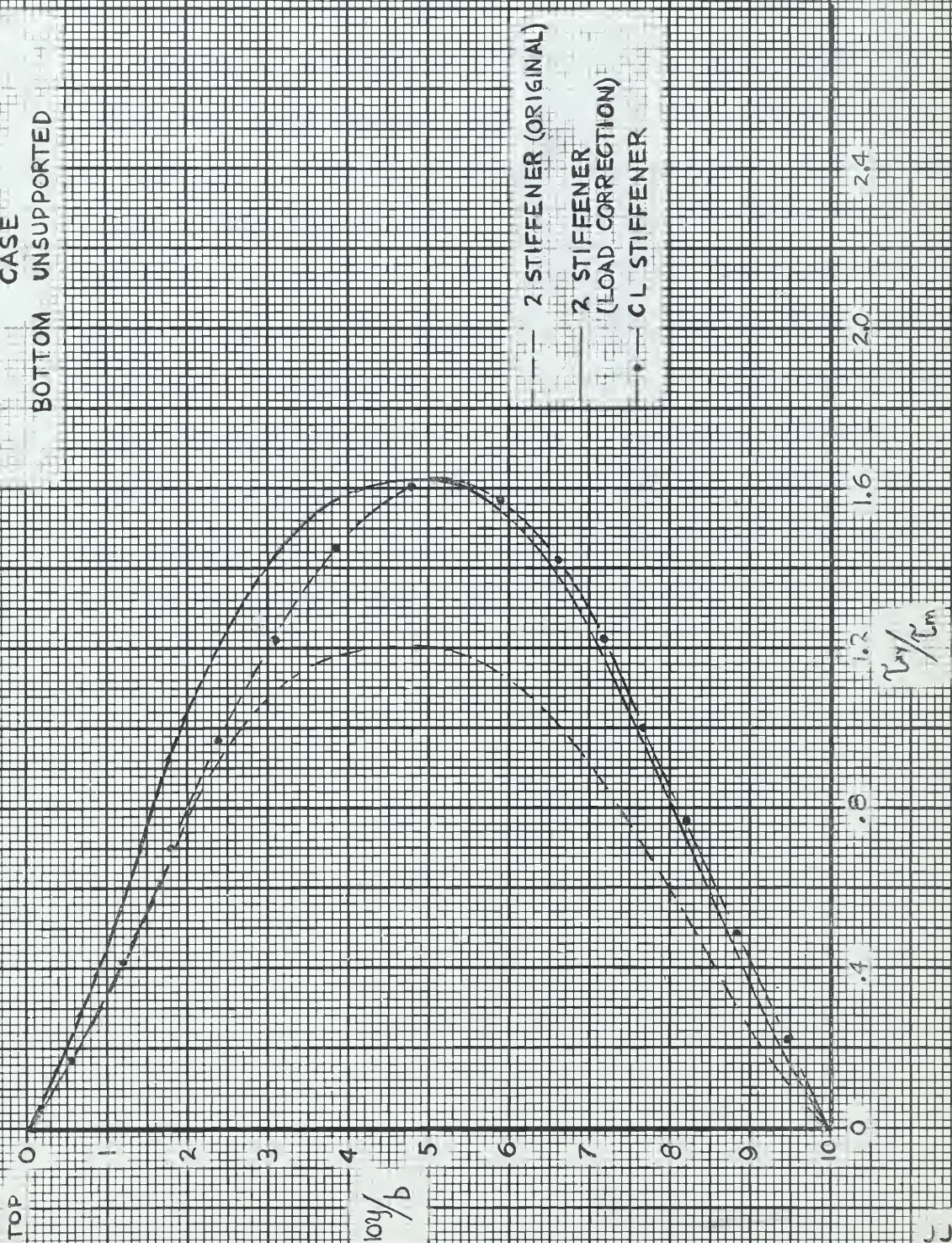
The corrected curve has an error of 1.0%. The case of the centerline stiffener is shown for comparison.



FIGURE XXXVI

AR 3:1
UNIFORM LOAD
LOAD CORRECTION TO 2 STIFFENER
CASE
BOTTOM UNSUPPORTED

--- 2 STIFFENER (ORIGINAL)
— 2 STIFFENER
(LOAD CORRECTION)
••• CL STIFFENER



JJP
4-18-59

- (3) Example of a faired plus load correction. (Refer to Figure XXXVII and Table XVII).

Aspect Ratio 2:1

Uniform Load

Unstiffened

Bottom Unsupported

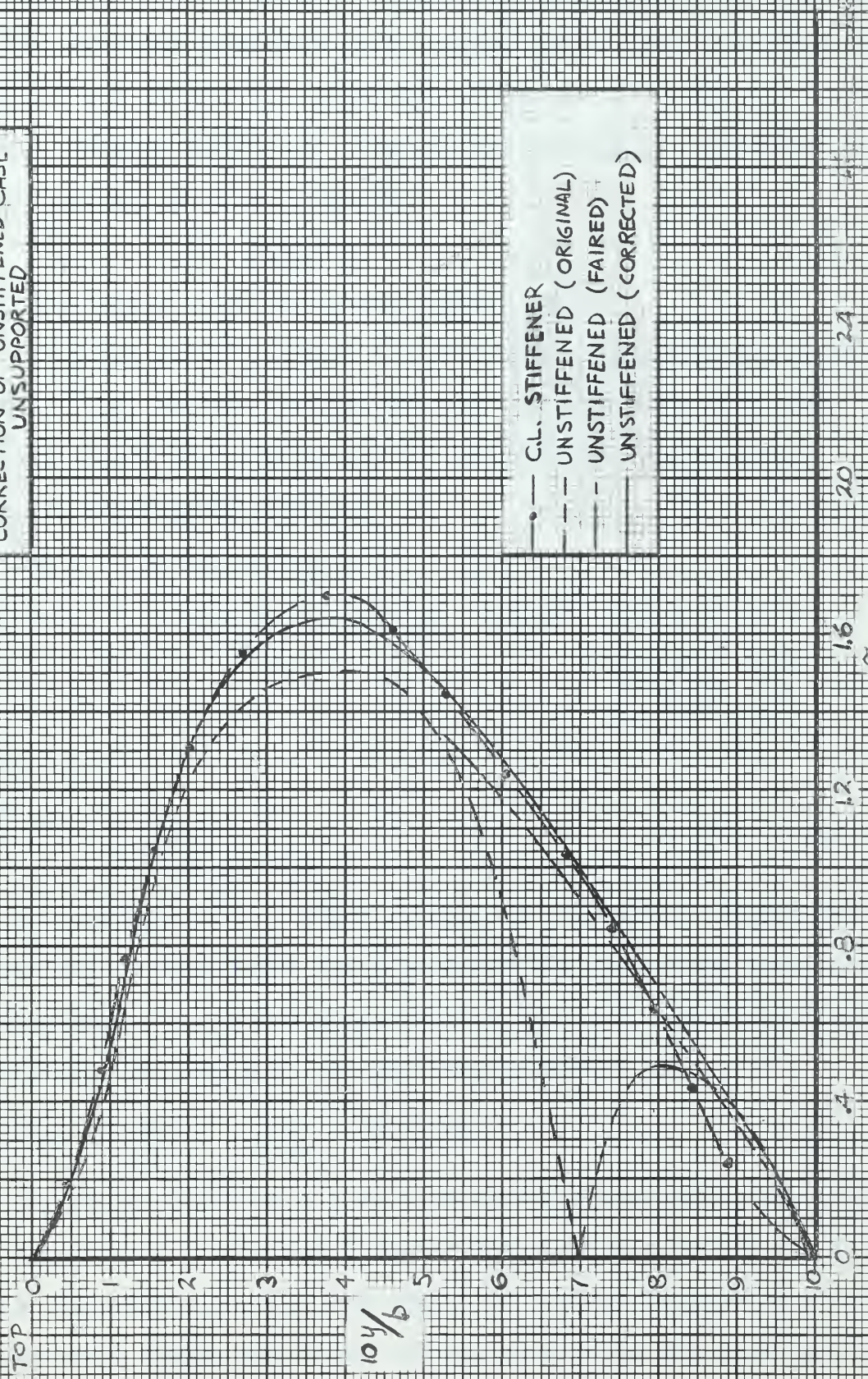
Experimental Error = -18.1%

The shear distribution curve has a zero value at 70% of the beam depth. The cause of the discontinuity is probably a result of non-uniform clamping and/or an error in the determination of the isoclinic pattern. The investigators (ref. 3) report that the isoclinic patterns for the 2:1 cases were just barely distinct. A faired correction is plotted across the discontinuity approximating the shape of the centerline stiffener curve. The error of the faired curve is - 8.0%. It is further corrected by a load correction. The error of the final corrected curve is - 2.0%.

FIGURE XXXVII

AR 2:1 UNIFORM LOAD
CORRECTION OF UNSTIFFENED CASE
UNSUPPORTED

— C.L. STIFFENER
— UNSTIFFENED (ORIGINAL)
— UNSTIFFENED (FAIRED)
— UNSTIFFENED (CORRECTED)



JJP
4-16-59

THEORETICAL APPROXIMATION FOR CONCENTRATED LOADING

Frecht in reference (17) presents the solution by Flamant for the stresses produced by a concentrated load P acting vertically upon a horizontal straight boundary of a semi-infinite plate (Figure XXXVIII). The resulting stress distribution is purely radial, and is given by

$$\sigma_r = - \frac{2P}{\pi h} \frac{\cos \theta}{r} \quad (4)$$

where the minus sign indicates compression.

From the radial stress distribution the vertical shear stress (τ_{xy}) can be determined for any point in the semi-infinite plate and expressed in rectangular coordinates.

Referring to Figure XXXVIII;

$$\tau_{xy} = \sigma_r \sin \theta \cos \theta$$

$$\tau_{xy} = - \frac{2P \sin \theta \cos^2 \theta}{\pi h r} \quad \text{where} \quad \begin{aligned} \cos \theta &= y/r \\ \sin \theta &= x/r \\ r &= \sqrt{x^2 + y^2} \end{aligned}$$

therefore,

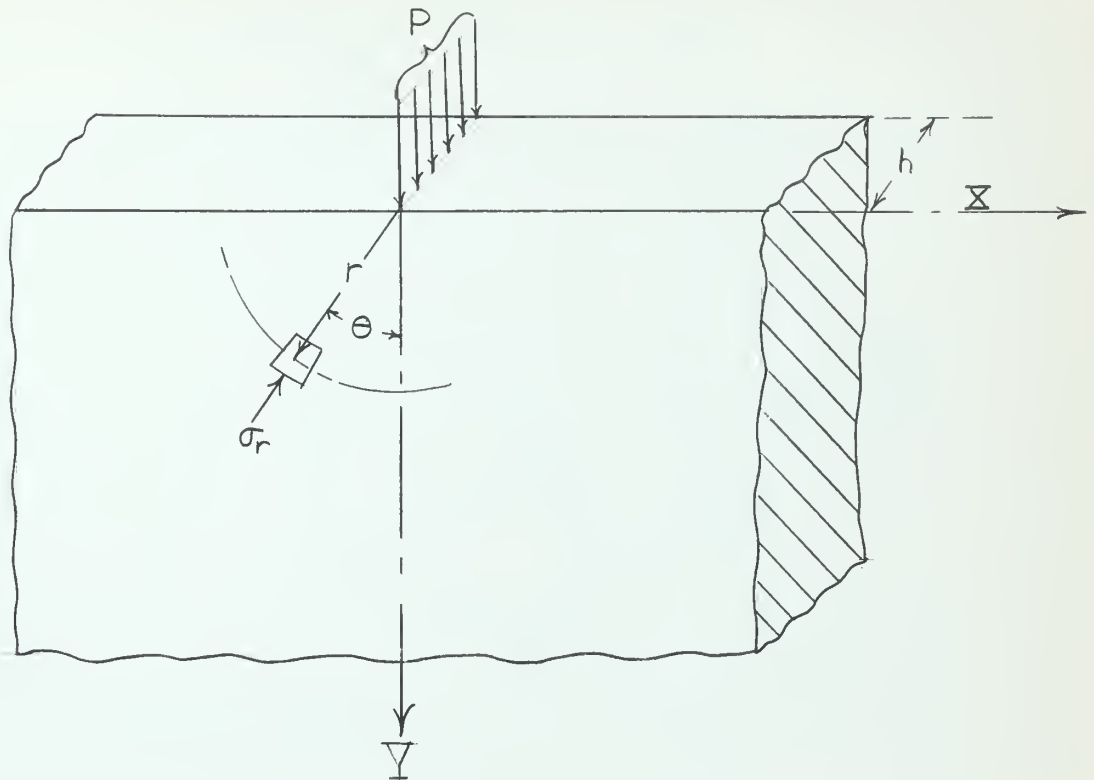
$$\tau_{xy} = - \frac{2Pxy^2}{\pi h(x^2 + y^2)^2} \quad (5)$$

In the Benoulli - Euler theory of elementary beams the effects of concentrated loads and end restraint are neglected. The elementary vertical shear stress for the side supported, unstiffened rectangular beam of Figure XXXIX is;

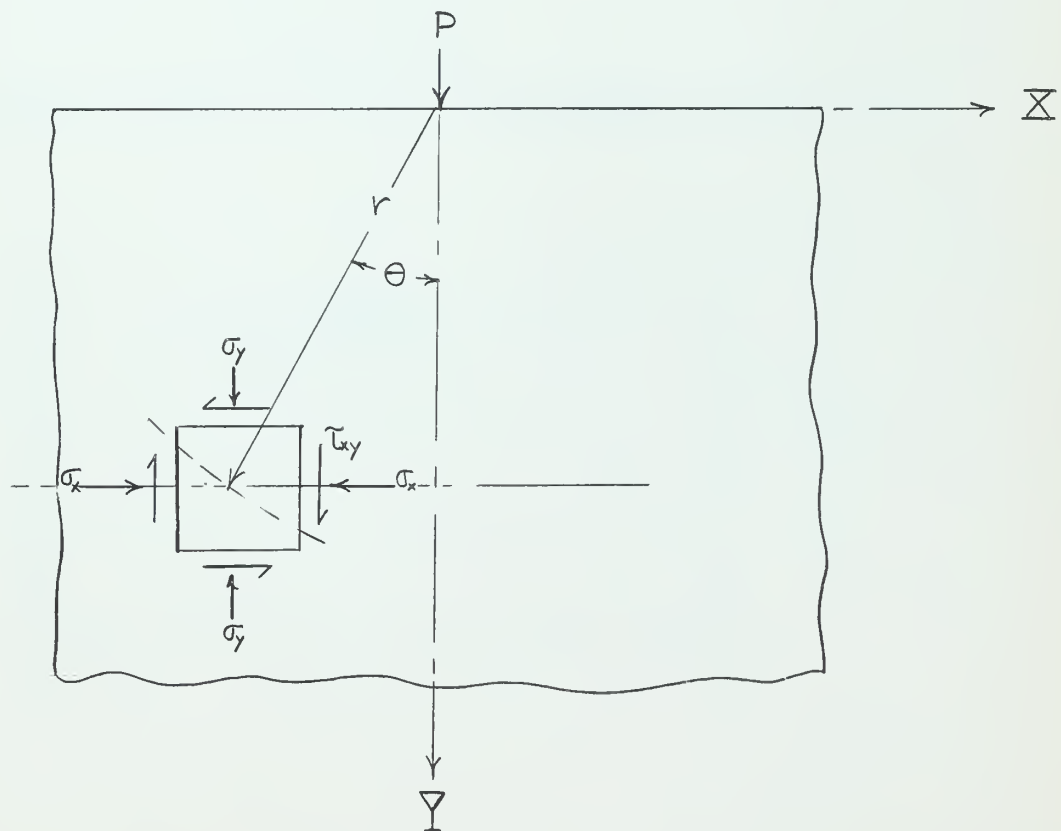
$$\tau_{xy} = \frac{VA\bar{y}}{hI} = - \frac{3P}{8hc^3} (2c - y)y \quad (6)$$

Hendry in reference (15) has demonstrated experimentally that for simply supported I-beams the radial compressive stresses from a concentrated load are small at points further than one and one-half times the depth of the beam from the load point,

FIGURE XXXVIII



RADIAL STRESSES IN A SEMI-INFINITE PLATE



RECTANGULAR STRESS COMPONENTS IN A SEMI-INFINITE PLATE

irrespective of the span of the beam. The relative magnitude of the elementary bending and radial stresses is dependent upon the beam span, the ratio of radial to bending stress increasing with decrease in beam aspect ratio. There is no reason to believe that the range of concentrated load effects should differ in the side supported beam. Therefore, of the beams investigated at M.I.T., only the one of aspect ratio 5:1 would by Hendry's definition have "small" concentrated load effects over the side supports.

The concentrated load effects on the side supported beam can be considered by superimposing the radial system of stress of the semi-infinite plate (Equation 5) over the elementary bending stress system (Equation 6).

$$\tau_{xy} = \frac{-2P}{h} \left[\frac{3}{16c^3} (2cy - y^2) + \frac{1}{\pi} \left(\frac{xy^2}{x^2 + y^2} \right)^2 \right] \quad (7)$$

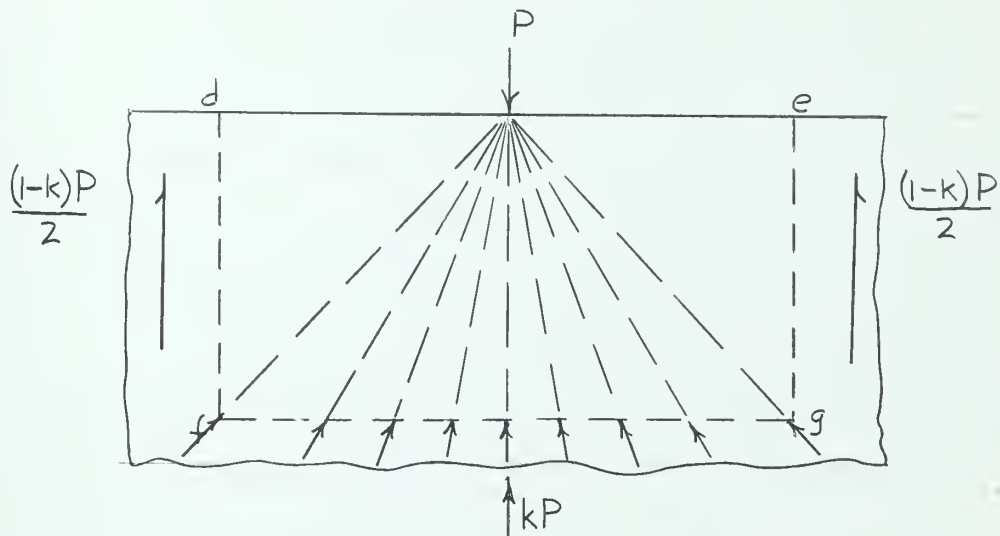
This solution is presented in Figure XL. For equilibrium it requires the presence of radial compressive loads along the free boundary f-g, which in fact cannot exist. This radial compressive load may be eliminated by a radial tensile load along the boundary. However, whereas the stress system produced by the radial compressive boundary load is represented exactly by Equation (4), the stresses produced by the radial tensile boundary load cannot be represented by any simple stress function and must be approximated. In this procedure it will be approximated by the statically equivalent resultant vertical tensile load.

The resulting approximate procedure of superposition is presented in Figure XLI. The factor k is the fraction of the concentrated load P which is transmitted into the bottom boundary

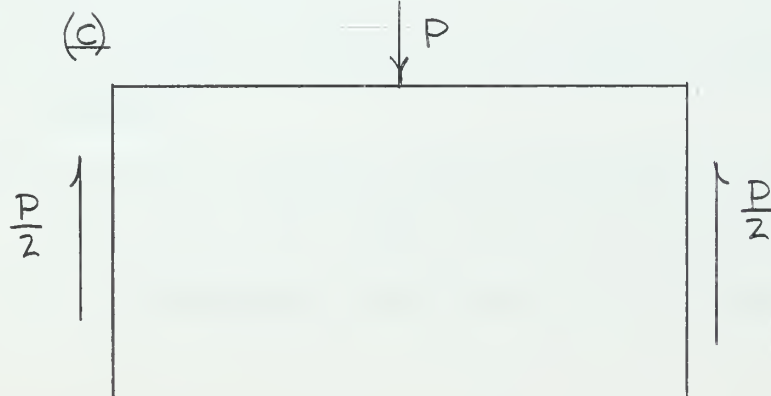
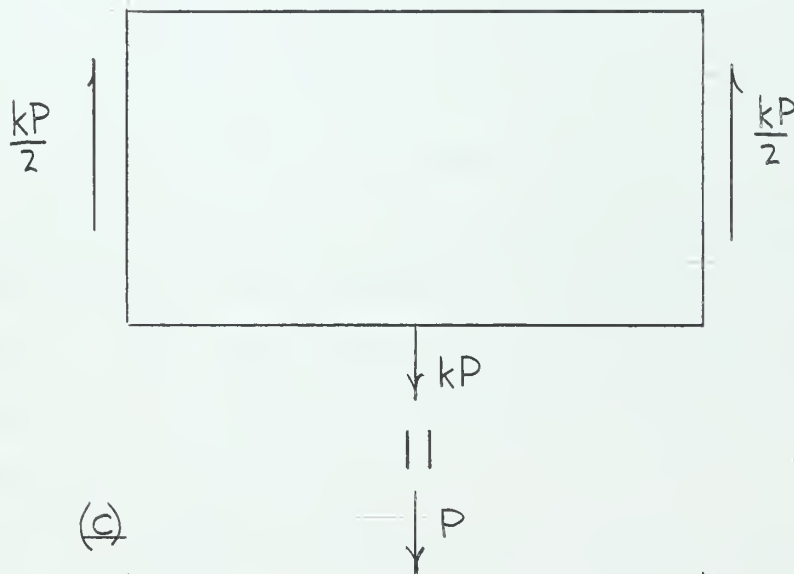
FIGURE XLI

APPROXIMATE SUPERPOSITION OF RADIAL AND ELEM. BENDING STRESS SYSTEMS

(a) SEMI-INFINITE PLATE THEORY



(b) ELEMENTARY BENDING THEORY



of the beam $f=g$ by the radial compressive stresses. For the case of no bottom support kP is the part of the load which, because it is not distributed into the side supports as concentrated load effect, is assumed to be the applied bending load of elementary beam theory. For the case of side and bottom support k is assumed to be the fraction of the load which is transmitted into the bottom support. The factor $(1-k)$ is the fraction of the load P that is distributed into the side supports by the radial concentrated load stress system of the semi-infinite plate. This superposition procedure is represented by the equation

$$\tau_{xy} = -\frac{2P}{h} \left[\frac{3k}{16c^3} (2cy - y^2) + \frac{1}{\pi} \frac{xy^2}{(x^2 + y^2)^2} \right] \quad (8)$$

The procedure of Figure XLI and Equation (8) was utilized to analyze the shear distributions and fractions of load transmitted into the bottom supports for aspect ratios 1:1, 2:1, 3:1, and 5:1. A sample calculation of this procedure is presented in Appendix D and summaries of calculations for all aspect ratios are presented in Appendix C (Tables II, III, VII and X). When analyzing the results of this procedure it is important to remember the following restrictive assumptions implied in its derivation;

- (1) The supported ends are not rigidly clamped against rotation.
- (2) The radial tensile forces necessary to eliminate stress over the bottom free boundary are approximated by a statically equivalent vertical tensile loading.

Another method of solution attempted by the authors was that of J. Boussinesq as presented on page 98 of reference (18). This method utilizes Flamant's solution for the semi-infinite plate and through a corrective procedure annuls the stresses over the bottom free boundary by distributing the loading into the side supports. Referring to Figure XL, to annul the stresses over the boundary f-g an equal and opposite system of stresses are superimposed and Flamant's solution is used again considering the beam as a semi-infinite plate extending above line f-g. This corrective system distributes some stress into the sides and the remainder as additional stresses over the top boundary d-e which again can be removed by Flamant's solution. A satisfactory solution was not obtained because each correction attempts to nullify distributed radial stresses over a free boundary with statically equivalent concentrated boundary loads.

APPENDIX C
ORIGINAL DATA AND CALCULATIONS

TABLE II

Aspect 1:1
Theoretical Calculation
Bottom Unsupported
Load Transmitted into Bottom Free Boundary = 55.1%

Concentrated Load
Error = 0%
Unstiffened

(10y/b) Station	$(\tau_{xy}/\tau_m)_\theta$	+	$(\tau_{xy}/\tau_m)_\phi$	=	τ_{xy}/τ_m
0 (Top)	0		0		0
1	.2976		.0944		.392
2	.5280		.3024		.830
3	.6940		.4960		1.19
4	.7920		.6040		1.40
5	.8320		.5868		1.42
6	.7920		.6160		1.41
7	.6940		.5696		1.26
8	.5280		.5160		1.04
9	.2976		.4592		0.757
10 (Bottom)	0		.4080		0.408

TABLE III

Aspect Ratio 2:1

Concentrated Load

Theoretical Calculation

Error = + 0.2%

Bottom Unsupported

Unstiffened

Load Transmitted into Bottom Free Boundary = 81.8%

(10y/b)

Station	$(\tau_{xy}/\tau_m)_\beta$	$(\tau_{xy}/\tau_m)_{\beta^*}$	τ_{xy}/τ_m
0 (Top)	0	0	0
1	0.4420	0.0120	0.454
2	0.7860	0.0472	0.833
3	1.032	0.0964	1.13
4	1.178	0.1516	1.33
5	1.236	0.2036	1.44
6	1.178	0.2480	1.43
7	1.032	0.2812	1.31
8	0.7860	0.3036	1.09
9	0.4420	0.3152	0.757
10 (Bottom)	0	0.3188	0.319

TABLE IV

Aspect Ratio 2:1

Concentrated Load at Centerline

Bottom Unsupported

Load = 1650#

Unstiffened

 $\tau_m = 550 \text{ psi}$ Dimensions 12" x 6" x $\frac{1}{4}$ "

Error = -18.7%

Reference (5)

<u>Original Station</u>	<u>(10y/b) Station</u>	<u>τ_{xy}</u>	<u>τ_{xy}/τ_m</u>
0 (Top)	0	0	0
$\frac{1}{2}$	0.84	179	0.33
1	1.67	287	0.52
$1\frac{1}{2}$	2.50	430	0.78
2	3.34	508	0.92
$2\frac{1}{2}$	4.16	566	1.03
3	5.00	612	1.11
$3\frac{1}{2}$	5.83	650	1.18
4	6.65	654	1.19
$4\frac{1}{2}$	7.50	587	1.07
5	8.35	483	0.88
$5\frac{1}{2}$	9.15	298	0.54
6 (Bottom)	10.00	0	0



TABLE V

Aspect Ratio 2:1

Concentrated Load at Centerline

Dimensions 12" x 6" x $\frac{1}{4}$ "Load = 1650[#]

Reference (5)

 $\tau_m = 550$ psi

Bottom Supported

Unstiffened

Load Carried by Bottom Support = 58.1%

<u>Original Station</u>	<u>Station</u>	<u>τ_{xy}</u>	<u>τ_{xy}/τ_m</u>
0 (Top)	0	0	0
$\frac{1}{2}$	0.84	158.5	0.29
1	1.67	262	0.48
$1\frac{1}{2}$	2.50	298	0.54
2	3.34	294	0.53
$2\frac{1}{2}$	4.16	286	0.52
3	5.00	303	0.55
$3\frac{1}{2}$	5.83	306.5	0.56
4	6.65	280	0.51
$4\frac{1}{2}$	7.50	233.5	0.42
5	8.35	177	0.32
$5\frac{1}{2}$	9.15	101.8	0.185
6 (Bottom)	10.00	27.7	0.05

TABLE VI

Aspect Ratio 2:1

Concentrated Load at Centerline

Dimensions 12" x 6" x $\frac{1}{4}$ "

Load = 1650#

Reference (5)

 $\tau_m = 550$ psi

Bottom Supported

One Stiffener at Centerline

Load Carried by Bottom Support = 50.2%

<u>Original Station</u>	<u>(10y/b) Station</u>	<u>τ_{xy}</u>	<u>τ_{xy}/τ_m</u>
0 (Top)	0	0	0
$\frac{1}{2}$	0.84	272	0.49
1	1.67	379	0.69
$1\frac{1}{2}$	2.50	370	0.67
2	3.34	340	0.62
$2\frac{1}{2}$	4.16	322	0.59
3	5.00	320	0.58
$3\frac{1}{2}$	5.83	351	0.64
4	6.65	319	0.58
$4\frac{1}{2}$	7.50	236	0.43
5	8.35	173	0.31
$5\frac{1}{2}$	9.15	98	0.18
6 (Bottom)	10.00	0	0

TABLE VII

Aspect Ratio 3:1

Concentrated Load

Theoretical Calculation

Error = -0.8%

Bottom Unsupported

Unstiffened

Load Transmitted into Bottom Free Boundary = 91.0%

$(10y/b)$	$(\tau_{xy}/\tau_m)_\beta$	$+$	$(\tau_{xy}/\tau_m)_\rho$	$=$	(τ_{xy}/τ_m)
0 (Top)	0		0		0
1	.492		.0036		.496
2	.872		.0148		.887
3	1.148		.0316		1.18
4	1.312		.0528		1.37
5	1.372		.0764		1.45
6	1.312		.1008		1.41
7	1.148		.1248		1.27
8	.872		.1460		1.02
9	.492		.1684		.660
10 (Bottom)	0		.1808		.181

TABLE VIII

Aspect Ratio 3:1

Concentrated Load at Centerline

Bottom Supported

Load = 540#

Unstiffened

 $\tau_m = 270$ psiDimensions 12" x 4" x $\frac{1}{4}$ "

Load Carried by Bottom = 80.2%

Reference (4)

<u>Original Station</u>	($10y/b$) <u>Station</u>	<u>τ_{xy}</u>	<u>τ_{xy}/τ_m</u>
0 (Top)	0	0	0
$\frac{1}{2}$	1.25	53.3	0.20
1	2.50	113	0.42
$1\frac{1}{2}$	3.75	111	0.41
2	5.00	0	0
$2\frac{1}{2}$	6.25	47.6	0.18
3	7.50	28.4	0.11
$3\frac{1}{2}$	8.75	16.9	0.06
4 (Bottom)	10.0	35.4	0.13

TABLE IX

Aspect Ratio 3:1

Concentrated Load at Centerline

Bottom Supported

Load = 850#

One Stiffener at Centerline

 $\tau_m = 425$ psiDimensions 12" x 4" x $\frac{1}{4}$ "

Load Carried by Bottom = 50.3%

Reference (4)

<u>Original Station</u>	<u>(10y/b) Station</u>	<u>τ_m</u>	<u>τ_{xy}/τ_m</u>
0 (Top)	0	0	0
$\frac{1}{2}$	1.25	156	0.37
1	2.50	213	0.50
$1\frac{1}{2}$	3.75	175	0.41
2	5.00	79.2	0.19
$2\frac{1}{2}$	6.25	222	0.52
3	7.50	281	0.66
$3\frac{1}{2}$	8.75	330	0.78
4 (Bottom)	10.0	352	0.83

TABLE X

Aspect Ratio 5:1

Concentrated Load

Theoretical Calculation

Error = + 0.4%

Bottom Unsupported

Unstiffened

Load Transmitted Into Bottom Free Boundary = 97.7%

$(10y/b)$	$(\tau_{xy}/\tau_m)_\theta$	$+$	$(\tau_{xy}/\tau_m)_\phi$	$=$	$(\tilde{\tau}_{xy}/\tilde{\tau}_m)$
0 (Top)	0		0		0
1	.528		0		.528
2	.936		0		.936
3	1.232		.00642		1.24
4	1.408		.01232		1.42
5	1.476		.0188		1.50
6	1.408		.0264		1.43
7	1.232		.0344		1.27
8	.936		.0428		.979
9	.528		.0516		.580
10 (Bottom)	0		.0604		.060

TABLE XI

Aspect Ratio 5:1

Concentrated Load at Centerline

Dimensions 12" x 2.4" x $\frac{1}{4}$ "Load = 540[#]

Reference (4)

 $\tau_m = 450$ psi

Bottom Unsupported

Unstiffened

Error = - 26.6%

<u>Original Station</u>	<u>($10y/b$) Station</u>	<u>τ_{xy}</u>	<u>τ_{xy}/τ_m</u>
0 (Top)	0	0	0
$\frac{1}{2}$	2.08	180	0.40
1	4.16	576	1.28
$1\frac{1}{2}$	6.24	624	1.39
2	8.32	203	0.45
2.4 (Bottom)	10.00	0	0

Bottom Unsupported

One Stiffener at Centerline

Error = + 13.9%

0 (Top)	0	0	0
$\frac{1}{2}$	2.08	463	1.03
1	4.16	701	1.56
$1\frac{1}{2}$	6.24	725	1.61
2	8.32	529	1.17
2.4 (Bottom)	10.00	0	0

TABLE XII

Aspect Ratio 5:1

Concentrated Load at Centerline

Dimensions 12" x 2.4" x $\frac{1}{4}$ "

Load = 540#

Reference (4)

 $\tau_m = 450$ psi

Bottom Supported

Unstiffened

Load Carried by Bottom Support = 70.7%

<u>Original Station</u>	<u>(10y/b) Station</u>	<u>τ_{xy}</u>	<u>τ_{xy}/τ_m</u>
0 (Top)	0	0	0
$\frac{1}{2}$	2.08	230	0.51
1	4.16	165.5	0.37
$1\frac{1}{2}$	6.24	152	0.34
2	8.32	69.5	0.15
2.4 (Bottom)	10.00	104	0.23

Bottom Supported

One Stiffener at Centerline

Load Carried by Bottom Support = 73.0%

0 (Top)	0	0	0
$\frac{1}{2}$	2.08	218	0.48
1	4.16	194	0.43
$1\frac{1}{2}$	6.24	67.6	0.15
2	8.32	63	0.14
2.4 (Bottom)	10.00	13.8	0.03

TABLE XIII

Aspect Ratio 1:1

 $h = 0.250$ in.

Reference (2)

Uniform Load

Load = $139\#/in.$ $\tau_m = 278$ psi

Bottom Unsupported

Unstiffened

Error = + 3.4%

(10y/b) Station	τ_{xy}	τ_{xy}/τ_m
0 (Top)	0	0
1	299	1.07
2	443	1.58
3	461	1.65
4	458	1.64
5	413	1.48
6	348	1.245
7	266	0.95
8	168	0.60
9	35	0.13
10 (Bottom)	0	0

Bottom Supported

Unstiffened

Load Carried by Bottom Support = 9.1%

0 (Top)	0	0
1	315	1.13
2	424	1.52
3	449	1.62
4	405	1.46
5	343	1.23
6	266	0.95
7	172	0.61
8	85	0.31
9	23	0.08
10 (Bottom)	0	0

TABLE XIV

Aspect Ratio 1:1

 $h = 0.250$ in.

Reference (2)

Uniform Load

Load = $139\frac{\#}{\text{in.}}$ $\tau_m = 278$ psi

Bottom Unsupported

Error = -9.0%

One Stiffener at Centerline

Error (Corrected) = + 1.0%

 τ_m (Corrected) = 253 psi

$(10^4/b)$	Station	τ_{xy}	τ_{xy}/τ_m	τ_{xy}/τ_{mc}
	0 (Top)	0	0	0
	1	255	0.92	1.01
	2	412	1.48	1.63
	3	440	1.58	1.74
	4	407.4	1.46	1.61
	5	330	1.19	1.30
	6	251	0.90	0.99
	7	206	0.74	0.82
	8	157	0.57	0.625
	9	74	0.27	0.29
	10 (Bottom)	0	0	0

Bottom Supported

One Stiffener at Centerline

Load Carried by Bottom Support = 10.2%

	0 (Top)	0	0
	1	209	0.75
	2	395	1.42
	3	443	1.59
	4	406	1.46
	5	364	1.31
	6	287	1.02
	7	186	0.67
	8	138	0.50
	9	54	0.19
	10 (Bottom)	0	0

TABLE XV

Aspect Ratio 1:1

 $h = 0.250$ in.

Reference (2)

Uniform Load

Load = $139\#/in.$ $\tau_m = 278$ psi

Bottom Unsupported

Two Stiffeners

Error = $\pm 1.3\%$ $(104/b)$ Station τ_{xy} τ_{xy}/τ_m

0 (Top)

0

0

1

332

1.19

2

437

1.57

3

443

1.59

4

406

1.46

5

364

1.31

6

286

1.03

7

236

0.85

8

176

0.63

9

77

0.28

10 (Bottom)

0

0

Bottom Supported

Two Stiffeners

Load Carried by Bottom Support = 10.1%

0 (Top)

0

0

1

338

1.22

2

444

1.60

3

456

1.63

4

377

1.36

5

299

1.07

6

220

0.79

7

160

0.58

8

116

0.42

9

60

0.22

10 (Bottom)

0

0

TABLE XVI

Aspect Ratio 1:1

Uniform Load

 $h = 0.250$ in.

Load = 139#/in.

Reference (2)

 $\tau_m = 278$ psi

Bottom Unsupported

Three Stiffeners

Error = -10.0%

Error (Corrected) = -3.0%

 τ_m (Corrected) = 251 psi

$(\frac{10y}{b})$ Station	τ_{xy}	τ_{xy}/τ_m	τ_{xy}/τ_{mc}
0 (Top)	0	0	0
1	154	0.55	0.61
2	338	1.22	1.35
3	401	1.45	1.60
4	390	1.40	1.55
5	314	1.13	1.25
6	277	0.99	1.10
7	235	0.85	0.94
8	183	0.66	0.73
9	119	0.43	0.47
10 (Bottom)	0	0	0

Bottom Supported

Three Stiffeners

Load Carried by Bottom Support = 12.1%

0 (Top)	0	0
1	185	0.66
2	343	1.24
3	384	1.38
4	388	1.40
5	346	1.25
6	299	1.08
7	224	0.80
8	160	0.58
9	87	0.31
10 (Bottom)	0	0

TABLE XVII

Aspect Ratio 2:1

 $h = 0.249$ in.

Reference (3)

Uniform Load

Load = $97.5^{\#}$ / in. $\tau_m = 392$ psi

Bottom Unsupported

Unstiffened

Error = -18.1%

Error (Corrected) = 0%

Error (Faired Correction) = -8.0%

 τ_m (Corrected) = 363 psi

Original Station	(104/b) Station	τ_{xy}	τ_w/τ_m	$[\tau_w/\tau_m]$ Faired	τ_{xy}/τ_m
10 (Top)	0	0	0	0	0
$9\frac{1}{2}$	$\frac{1}{2}$	65	0.17	0.17	0.18
9	1	215	0.55	0.55	0.59
8	2	482	1.23	1.23	1.33
7	3	570	1.45	1.45	1.57
6	4	597	1.52	1.52	1.64
5	5	538	1.37	1.37	1.48
4	6	347	0.88	1.14	1.23
3	7	0	0	0.90	0.97
2	8	197	0.50	0.64	0.69
1	9	155	0.40	0.36	0.39
$\frac{1}{2}$	$9\frac{1}{2}$	70	0.18	0.18	0.19
0 (Bottom)	10	0	0	0	0

Bottom Supported

Unstiffened

Load Carried by Bottom Support = 12.7%

10 (Top)	0	0	0
$9\frac{1}{2}$	$\frac{1}{2}$	120	0.31
9	1	349	0.89
8	2	543	1.38
7	3	568	1.45
6	4	520	1.33
5	5	451	1.15
4	6	376	0.96
3	7	316	0.81
2	8	222	0.57
1	9	95.2	0.24
$\frac{1}{2}$	$9\frac{1}{2}$	47.8	0.12
0 (Bottom)	10	0	0

TABLE XVIII

Aspect Ratio 2:1

 $h = 0.249$ in

Reference (3)

Uniform Load

Load = 97.5#/in.

 $\tau_m = 392$ psi

Bottom Unsupported

One Stiffener at Centerline

Error = + 2.0 %

<u>Original Station</u>	<u>Station</u>	<u>τ_{xy}</u>	<u>τ_{xy}/τ_m</u>
10 (Top)	0	0	0
$9\frac{1}{2}$	$\frac{1}{2}$	90.8	0.23
9	1	243	0.62
8	2	529	1.35
7	3	620	1.58
6	4	667	1.70
5	5	576	1.47
4	6	490	1.25
3	7	375	0.96
2	8	226	0.58
1	9	82.6	0.21
$\frac{1}{2}$	$9\frac{1}{2}$	17.8	0.045
0 (Bottom)	10	0	0

Bottom Supported

One Stiffener at Centerline

Load Carried by Bottom Support = 21.4%

10 (Top)	0	0	0
$9\frac{1}{2}$	$\frac{1}{2}$	129	0.33
9	1	296	0.76
8	2	490	1.25
7	3	529	1.35
6	4	502	1.28
5	5	427	1.09
4	6	362	0.92
3	7	242	0.62
2	8	139	0.35
1	9	68.4	0.175
$\frac{1}{2}$	$9\frac{1}{2}$	33.9	0.087
0 (Bottom)	10	0	0

TABLE XIX

Aspect Ratio 2:1

 $h = 0.250$ in.

Reference (2)

Uniform Load

Load = 139 #/ in.

 $\tau_m = 556$ psi

Bottom Unsupported

Two Stiffeners

Error = + 3.1%

$(10y/b)$ Station	τ_{xy}	τ_{xy}/τ_m
0 (Top)	0	0
1	557	1.00
2	702	1.25
3	796	1.43
4	812	1.45
5	807	1.44
6	724	1.29
7	613	1.10
8	425	0.77
9	214	0.38
10 (Bottom)	0	0

Bottom Supported

Two Stiffeners

Load Carried by Bottom Support = 30.6%

0 (Top)	0	0
1	427	0.77
2	536	0.96
3	572	1.03
4	568	1.02
5	521	0.94
6	435	0.78
7	355	0.64
8	267	0.48
9	154	0.28
10 (Bottom)	0	0

TABLE XIX

Aspect Ratio 2:1

 $h = 0.250$ in.

Reference (2)

Uniform Load

Load = 139 #/ in.

 $\tau_m = 556$ psi

Bottom Unsupported

Two Stiffeners

Error = + 3.1%

$(10y/b)$ Station	τ_{xy}	τ_{xy}/τ_m
0 (Top)	0	0
1	557	1.00
2	702	1.25
3	796	1.43
4	812	1.45
5	807	1.44
6	724	1.29
7	613	1.10
8	425	0.77
9	214	0.38
10 (Bottom)	0	0

Bottom Supported

Two Stiffeners

Load Carried by Bottom Support = 30.6%

0 (Top)	0	0
1	427	0.77
2	536	0.96
3	572	1.03
4	568	1.02
5	521	0.94
6	435	0.78
7	355	0.64
8	267	0.48
9	154	0.28
10 (Bottom)	0	0

TABLE XX

Aspect Ratio 2:1

 $h = 0.250$ in.

Reference (2)

Uniform Load

Load = 139#/ in.

 $\tau_m = 556$ psi

Bottom Unsupported

Three Stiffeners

Error = -15.2%

Error (Corrected) = 0%

 τ_m (Corrected) = 473 psi.

$(10y/b)$ Station	τ_{xy}	τ_{xy}/τ_m	τ_{xy}/τ_{mc}
0 (Top)	0	0	0
1	193	0.345	0.41
2	499	0.89	1.05
3	711	1.27	1.49
4	776	1.39	1.64
5	757	1.35	1.59
6	729	1.30	1.53
7	581	1.04	1.22
8	401	0.72	0.85
9	120	0.215	0.25
10 (Bottom)	0	0	0

Bottom Supported

Three Stiffeners

Load Carried by Bottom Support = 23.3%

0 (Top)	0	0
1	250	0.45
2	487	0.87
3	616	1.10
4	629	1.12
5	620	1.11
6	577	1.03
7	490	0.88
8	374	0.67
9	196	0.35
10 (Bottom)	0	0

TABLE XXI

Aspect Ratio 3:1

 $h = 0.249$ in.

Reference (3)

Uniform Load

Load = 97.5# /in.

 $\tau_m = 586$ psi

Bottom Unsupported

Error = + 19.5%

Unstiffened

Error (Faired Correction) = +3.0%

Original Station	(10y/b) Station	τ_{xy}	τ_{xy}/τ_m	$[\tau_{xy}/\tau_m]_{\text{Faired}}$
10 (Top)	0	0	0	0
9 $\frac{1}{2}$	$\frac{1}{2}$	216	0.37	0.37
9	1	371	0.63	0.63
8	2	617	1.05	1.05
7	3	792	1.35	1.35
6	4	884	1.51	1.51
5	5	960	1.64	1.64
4	6	884	1.51	1.51
3	7	818	1.40	1.22
2	8	723	1.23	0.86
1	9	683	1.16	0.45
$\frac{1}{2}$	9 $\frac{1}{2}$	568	0.97	0.23
0 (Bottom)	10	0	0	0

Bottom Supported

Load Carried by Bottom Support = 17.9%

Unstiffened

10 (Top)	0	0	0
9 $\frac{1}{2}$	$\frac{1}{2}$	173	0.29
9	1	349	0.59
8	2	634	1.08
7	3	729	1.24
6	4	779	1.33
5	5	691	1.18
4	6	614	1.05
3	7	478	0.81
2	8	327	0.56
1	9	168	0.29
$\frac{1}{2}$	9 $\frac{1}{2}$	91.2	0.16
0 (Bottom)	10	0	0

TABLE XXII

Aspect Ratio 3:1

 $h = 0.249$ in.

Reference (3)

Uniform Load

Load = $97.5\frac{\text{lb}}{\text{in.}}$ $\tau_m = 586$ psi

Bottom Unsupported

One Stiffener at Centerline

Error = -1.9%

<u>Original Station</u>	<u>$(10y/b)$ Station</u>	<u>τ_{xy}</u>	<u>τ_{xy}/τ_m</u>
10 (Top)	0	0	0
$9\frac{1}{2}$	$\frac{1}{2}$	90.8	0.155
9	1	194	0.33
8	2	446	0.76
7	3	707	1.20
6	4	871	1.49
5	5	965	1.65
4	6	887	1.51
3	7	750	1.28
2	8	485	0.83
1	9	231	0.39
$\frac{1}{2}$	$9\frac{1}{2}$	114	0.195
0 (Bottom)	10	0	0

Bottom Supported

One Stiffener at Centerline

Load Carried by Bottom Support = 25.3 %

10 (Top)	0	0	0
$9\frac{1}{2}$	$\frac{1}{2}$	62.2	0.11
9	1	130	0.22
8	2	312	0.53
7	3	530	0.90
6	4	695	1.19
5	5	776	1.32
4	6	693	1.18
3	7	521	0.89
2	8	459	0.78
1	9	240	0.41
$\frac{1}{2}$	$9\frac{1}{2}$	155	0.26
0 (Bottom)	10	0	0

TABLE XXIII

Aspect Ratio 3:1

Uniform Load

 $h = 0.250$ in.

Load = 122 #/ in.

Reference (2)

 $\tau_m = 732$ psi

Bottom Unsupported

Two Stiffeners

Error = -25.8 %

Error (Corrected) = + 1.0 %

$(10y/b)$ Station	τ_{xy}	τ_m (Corrected) = 542 psi	
		τ_{xy}/τ_m	τ_{xy}/τ_{mc}
0 (Top)	0	0	0
1	243	0.33	0.45
2	568.3	0.78	1.05
3	756.6	1.03	1.39
4	867	1.185	1.60
5	879	1.20	1.62
6	820	1.12	1.51
7	673	0.92	1.24
8	450	0.615	0.83
9	178	0.24	0.33
10 (Bottom)	0	0	0

Bottom Supported

Two Stiffeners

Load Carried by Bottom Support = 34.0 %

0 (Top)	0	0
1	267	0.355
2	557	0.76
3	752	1.03
4	826	1.13
5	769	1.05
6	650	0.89
7	516	0.71
8	340	0.465
9	171	0.23
10 (Bottom)	0	0

TABLE XXIV

Aspect Ratio 3:1

 $h = 0.249$ in.

Reference (3)

Uniform Load

Load = 97.5# / in.

 $\tau_m = 586$ psi

Bottom Unsupported

Error = + 14.8 %

Three Stiffeners

Error (Corrected) = -2.0 %

 τ_m (Corrected) = 690 psiOriginal
Station(104/b)
Station τ_{xy} τ_{xy}/τ_m τ_{xy}/τ_{mc}

10 (Top)

0

0

0

0

 $9\frac{1}{2}$ $\frac{1}{2}$

166

0.28

0.24

9

1

372

0.63

0.54

8

2

764

1.30

1.11

7

3

1005

1.71

1.46

6

4

1070

1.82

1.56

5

5

1040

1.77

1.51

4

6

913

1.55

1.32

3

7

725

1.24

1.05

2

8

490

0.84

0.71

1

9

234

0.40

0.34

 $\frac{1}{2}$ $9\frac{1}{2}$

123.4

0.21

0.18

0 (Bottom)

10

0

0

0

Bottom Supported

Three Stiffeners

Load Carried by Bottom Support = 28.3 %

10 (Top)

0

0

0

 $9\frac{1}{2}$ $\frac{1}{2}$

97.2

0.165

9

1

220

0.37

8

2

450

0.77

7

3

626

1.07

6

4

689

1.17

5

5

658

1.12

4

6

565

0.96

3

7

487

0.83

2

8

342

0.58

1

9

164

0.28

 $\frac{1}{2}$ $9\frac{1}{2}$

73

0.125

0 (Bottom)

10

0

0

TABLE XXV

Aspect Ratio 5:1

 $h = 0.249$ in.

Reference (3)

Uniform Load

Load = 59.5#/in.

 $\tau_m = 596$ psi

Bottom Unsupported

Unstiffened

Error = ± 1.0 %

Original Station	($10y/b$) Station	τ_{xy}	τ_{xy}/τ_m
10 (Top)	0	0	0
9 $\frac{1}{2}$	$\frac{1}{2}$	60.2	0.10
9	1	125	0.21
8	2	345	0.60
7	3	615	1.03
6	4	865	1.45
5	5	1040	1.75
4	6	1090	1.83
3	7	975	1.64
2	8	690	1.16
1	9	350	0.59
$\frac{1}{2}$	9 $\frac{1}{2}$	166	0.28
0 (Bottom)	10	0	0

Bottom Supported

Unstiffened

Load Carried by Bottom Support = 22.4 %

10 (Top)	0	0	0
9 $\frac{1}{2}$	$\frac{1}{2}$	83.9	0.14
9	1	182	0.30
8	2	399	0.67
7	3	601	1.01
6	4	691	1.16
5	5	700	1.18
4	6	659	1.10
3	7	582	0.98
2	8	465	0.78
1	9	301	0.50
$\frac{1}{2}$	9 $\frac{1}{2}$	214	0.36
0 (Bottom)	10	0	0

TABLE XXV

Aspect Ratio 5:1

 $h = 0.249$ in.

Reference (3)

Uniform Load

Load = 59.5#/in.

 $\tau_m = 596$ psi

Bottom Unsupported

Unstiffened

Error = + 1.0 %

Original Station	($10y/b$) Station	τ_{xy}	τ_{xy}/τ_m
10 (Top)	0	0	0
9 $\frac{1}{2}$	$\frac{1}{2}$	60.2	0.10
9	1	125	0.21
8	2	345	0.60
7	3	615	1.03
6	4	865	1.45
5	5	1040	1.75
4	6	1090	1.83
3	7	975	1.64
2	8	690	1.16
1	9	350	0.59
$\frac{1}{2}$	9 $\frac{1}{2}$	166	0.28
0 (Bottom)	10	0	0

Bottom Supported

Unstiffened

Load Carried by Bottom Support = 22.4 %

10 (Top)	0	0	0
9 $\frac{1}{2}$	$\frac{1}{2}$	83.9	0.14
9	1	182	0.30
8	2	399	0.67
7	3	601	1.01
6	4	691	1.16
5	5	700	1.18
4	6	659	1.10
3	7	582	0.98
2	8	465	0.78
1	9	301	0.50
$\frac{1}{2}$	9 $\frac{1}{2}$	214	0.36
0 (Bottom)	10	0	0

TABLE XXVI

Aspect Ratio 5:1

 $h = 0.249$ in.

Reference (3)

Uniform Load

Load = 59.5# / in.

 $\tau_m = 596$ psi

Bottom Unsupported

Error = + 33.7 %

One Stiffener at Centerline

Error (Corrected) = -1.0 %

 τ_m (Corrected) = 798 psi

Original Station	(10y/b) Station	τ_{xy}	τ_{xy}/τ_m	τ_{xy}/τ_{mc}
10 (Top)	0	0	0	0
9½	½	260	0.43	0.33
9	1	451	0.76	0.57
8	2	856	1.44	1.07
7	3	1130	1.90	1.42
6	4	1230	2.06	1.54
5	5	1240	2.08	1.56
4	6	1110	1.86	1.39
3	7	870	1.46	1.09
2	8	625	1.05	0.78
1	9	360	0.60	0.45
½	9½	189	0.32	0.24
0 (Bottom)	10	0	0	0

Bottom Supported

One Stiffener at Centerline

Load Carried by Bottom Support = 23.9 %

10 (Top)	0	0	0
9½	½	36	0.06
9	1	129	0.22
8	2	384	0.66
7	3	617	1.04
6	4	688	1.15
5	5	707	1.19
4	6	674	1.13
3	7	594	1.00
2	8	438	0.73
1	9	312	0.52
½	9½	190	0.32
0 (Bottom)	10	0	0

TABLE XXVII

Aspect Ratio 5:1

 $h = 0.250$ in.

Reference (2)

Uniform Load

Load = $71.5\# / \text{in.}$ $\tau_m = 715$ psi

Bottom Unsupported

Two Stiffeners

Error = -1.0 %

 $(10^4/b)$ Station τ_{xy} τ_{xy}/τ_m

0 (Top)

0

0

1

538

0.75

2

878

1.23

3

1020

1.43

4

1100

1.54

5

1050

1.47

6

915

1.28

7

715

1.00

8

494

0.69

9

254

0.355

10 (Bottom)

0

0

Bottom Supported

Two Stiffeners

Load Carried by Bottom Support = 48.8 %

0 (Top)

0

0

1

219.5

0.31

2

418.9

0.59

3

564.1

0.79

4

621.4

0.87

5

622.3

0.87

6

512.0

0.72

7

369.5

0.52

8

226.9

0.32

9

100.2

0.14

10 (Bottom)

0

0

TABLE XXVIII

Aspect Ratio 5:1

 $h = 0.250$ in.

Reference (2)

Uniform Load

Load = 71.5# / in.

 $\tau_m = 715$ psi

Bottom Unsupported

Error = -10.1 %

Three Stiffeners

Error (Corrected) = 0 %

 τ_m (Corrected) = 643 psi

$(10y/b)$ Station	τ_{xy}	τ_{xy}/τ_m	τ_{xy}/τ_{mc}
0 (Top)	0	0	0
1	348.9	0.49	0.54
2	608.7	0.85	0.95
3	769.8	1.08	1.20
4	907.5	1.27	1.41
5	973.1	1.36	1.51
6	926.9	1.295	1.44
7	786.2	1.10	1.22
8	624.8	0.87	0.97
9	345.2	0.48	0.54
10 (Bottom)	0	0	0

Bottom Supported

Three Stiffeners

Load Carried by Bottom Support = 22.1 %

0 (Top)	0	0
1	245.3	0.34
2	531.3	0.74
3	744.1	1.04
4	862.8	1.21
5	863.0	1.21
6	776.6	1.09
7	636.4	0.89
8	502.4	0.705
9	338.4	0.47
10 (Bottom)	0	0

APPENDIX D

SAMPLE CALCULATIONS

SAMPLE THEORETICAL CALCULATION

Aspect Ratio 2:1
Bottom Unsupported

Concentrated Load
Unstiffened

Referring to Equation (8) and Figure XXXIX of Appendix B

$$\tau_{xy} = -\frac{2P}{h} \left[\frac{3k}{16c^3} (2cy - y^2) + \frac{1}{\pi} \frac{xy^2}{(x^2 + y^2)^2} \right] \quad (8)$$

At the ends of the beam

$$x = l$$

$$y = 0 \rightarrow 2c \text{ where } c = 0.5$$

Therefore (8) becomes

$$\tau_{xy} = \frac{-2P}{h} \left[\frac{3}{2} k (y - y^2) + \frac{1}{\pi} \frac{l y^2}{(l^2 + y^2)^2} \right] \quad (8a)$$

$$\text{Now } \tau_m = \frac{1}{2} \cdot \frac{P}{2ch} = \frac{P}{2h}$$

$$\text{Therefore } (\tau_{xy}/\tau_m) = -4 \left[\frac{3}{2} k (y - y^2) + \frac{1}{\pi} \frac{l y^2}{(l^2 + y^2)^2} \right] \quad (8b)$$

For AR = 2:1 $l = 2c = 1.0$ Therefore (8b) becomes

$$(\tau_{xy}/\tau_m) = -4 \left[\frac{3}{2} k (y - y^2) + \frac{1}{\pi} \frac{y^2}{(1 + y^2)^2} \right] \quad (8c)$$

The factor k is the resultant of the vertical components of stress acting on the bottom free boundary $f-g$ of Figure (XLla) expressed as a fraction of the applied load P . It is determined as follows:

$$k = \frac{1}{P} \int_f^g \frac{2P}{\pi rh} \cos \theta \cdot \cos \theta \, r d\theta h \quad (9)$$

$$k = \int_0^g \frac{4}{\pi} \cos^2 \theta \, d\theta \quad \text{Then from } 0-g, \theta = 0 \rightarrow 45^\circ$$

$$k = \frac{4}{\pi} \left[\frac{\theta}{2} + \frac{\sin 2\theta}{4} \right]_0^{\pi/4}$$

$$k = 0.818$$

The remaining calculations for the shear distribution

(τ_{xy}/τ_m) are presented in Table XXIX.

TABLE XXIX

Summary of Data for Calculation of
Theoretical Shear Stress Distribution

Aspect Ratio 2:1

①	②	③	④	⑤	⑥	⑦	⑧
10y/b							
<u>Station</u>	<u>y</u>	<u>y²</u>	<u>y-y²</u>	<u>3/2k(y-y²)</u>	<u>(1+y²)²</u>	<u>$\frac{1}{\pi} \frac{y^2}{(1+y^2)^2}$</u>	<u>4x ⑤+⑦</u>
0	0	0	0	0	0	0	0
1	0.1	0.01	0.09	0.1105	1.026	0.0030	0.454
2	0.2	0.04	0.16	0.1965	1.080	0.0118	0.833
3	0.3	0.09	0.21	0.2580	1.187	0.0241	1.13
4	0.4	0.16	0.24	0.2945	1.344	0.0379	1.33
5	0.5	0.25	0.25	0.3090	1.563	0.0509	1.44
6	0.6	0.36	0.24	0.2945	1.850	0.0620	1.43
7	0.7	0.49	0.21	0.2580	2.219	0.0703	1.31
8	0.8	0.64	0.16	0.1965	2.694	0.0759	1.09
9	0.9	0.81	0.09	0.1105	3.273	0.0788	0.757
10	1.0	1.0	0	0	4.000	0.0797	0.319

APPENDIX E

LITERATURE SURVEY

- (1) Kaar, P. H. "Stresses in Centrally Loaded Deep Beams", Proc. Society for Experimental Stress Analysis, Vol. XV, No. 1, 1957.
- (2) Norman, T. V.,
Rodriguez Gutierrez, G. A. "Stress Distribution in Ship Bulkheads with Various Stiffening and Bottom Support - A Photoelastic Study", Thesis-Dept. of Naval Arch. and Marine Eng., M.I.T., 1958.
- (3) Miller, E. A.,
Metcalf, J. T. "A Photoelastic Study of the Stress Distribution in Flat Plate Panels Simulating Ship Bulkheads", Thesis-Dept. of Naval Arch. and Marine Eng., M.I.T., 1957.
- (4) Freire, T. D.,
DaSilva Sa, R. O.,
Serrao, J.B.W. "A Photoelastic Study of the Stress Distribution in Flat Plating Panels", Thesis-Dept. of Naval Arch. and Marine Eng., M.I.T., 1957.
- (5) Figueiredo, A. R.,
Marangiello, D. A.,
Guerra, W. V. "A Photoelastic Study of the Stress Distribution in Ship Transverse Bulkheads", Thesis-Dept. of Naval Arch. and Marine Eng., M.I.T., 1956.
- (6) Holman, R. "A Photoelastic Study of the Stress Distribution in Stiffened Plating", Thesis-Dept. of Naval Arch. and Marine Eng., M.I.T., 1955.
- (7) Frocht, M. M. "Photo-Elasticity", Vol. I, New York, John Wiley and Sons, 1941.
- (8) Timoshenko, S.,
Goodier, J. N. "Theory of Elasticity", New York, McGraw-Hill, 1951.
- (9) Portland Cement Assn. "Design of Deep Girders", Structural Bureau, Portland Cement Assn., Concrete Information No. ST 66.
- (10) Conway, H. D.,
Chou, Li,
Morgan, A. "Analysis of Deep Beams", Journal ASME (Applied Mechanics), Vol. 18, No. 2, June 1951.

- (11) Archer, F. E.,
Kitchen, E. M. "Stresses in Single Span Deep Beams", Australian Journal of Applied Science, Vol. 7, No. 4, Dec. 1956, pp 314-26.
- (12) McHenry, D. "A Lattice Analogy for the Solution of Stress Problems", Journal Inst. of Civil Engineers, Vol. 21, Dec. 1943.
- (13) Grinter, L. E. Numerical Methods of Analysis in Engineering, New York, MacMillan Company, 1949.
- (14) Suatengco, E. T.,
Takeda, T. "Stresses and Deflections of Short Deep Beams", Thesis-Dept. of Civil Eng., M.I.T., 1950.
- (15) Hendry, A. W. "The Stress Distribution in a Simply Supported Beam of I-Section Carrying a Centrally Concentrated Load", Proc. Society for Experimental Stress Analysis, Vol. VIII, No. 2, 1950.
- (16) Crawford, R. N.,
Wales, J. R. "A Summary of Current Design Methods in the Structural Design of Naval Ships", Thesis-Webb Institute of Naval Architecture, 1957.
- (17) Frecht, M. M. Photo-Elasticity, Vol. II, New York, John Wiley and Sons, 1948, pp 104-17.
- (18) Timoshenko, S. Theory of Elasticity, New York, McGraw-Hill, 1934.

thesP145

Shear distribution and its relation to b



3 2768 001 97151 8

DUDLEY KNOX LIBRARY